Dynamics of a Spur Gear Pair under Stochastic Internal and External Excitations

by

Yining Fang

A thesis submitted in partial fulfillment of the requirements for the degree of

Doctor of Philosophy

Department of Mechanical Engineering

University of Alberta

Abstract

Gear systems, which are one of the most widely adopted mechanical parts, receive lots of research attention. The dynamic modeling of gear systems under deterministic excitations has been widely investigated in existing studies. However, due to the diversity in both manufacturing processes and working environments, gear systems face stochastic internal and external excitations in reality, which result in the gear modeling to be complicated. In practical situations, the stochastic internal and external excitations should be considered when modeling gear systems. Besides the modeling complexity, stochastic excitations also lead to a large increase of time complexity when obtaining the statistic features of gear responses by numerical methods. Therefore, this thesis focuses on two aspects, including the modeling and the solving of gear dynamic models under stochastic excitations.

The objective of this thesis is to investigate the dynamics of a spur gear pair, including analyzing the effects on dynamic characteristics from the stochastic excitations and investigating the solving techniques to stochastic dynamic models. First, a spur gear dynamic model considering one more internal stochastic excitation, friction, is proposed. The effects of friction are investigated in gear dynamic models under stochastic load for the first time. Then, one more external excitation factor (i.e., driving speed) is taken into account in gear models and its effects on the dynamic characteristics are also studied. The results of our work show that some excitations that have not yet been modeled cannot be ignored when modeling gear systems. After that, considering the large time complexity of numerical methods for solving gear models under stochastic excitations, an efficient method is proposed to obtain an approximate analytical solution of a

spur gear pair model under stochastic load with one additional stochastic internal factor. Compared to the numerical methods, the proposed method can achieve similar accuracy responses but with much smaller time complexity.

In summary, this thesis helps us understand the mechanism of a spur gear pair and gives insights into developing more realistic gear models for gear design and condition monitoring. Future works will explore other possible internal and external excitations in gear modeling. The gear models under different working conditions are also worthy to study.

Preface

The material presented in this thesis is based on original work by Yining Fang. As detailed in the following, material from some chapters of this thesis has been published or submitted in conference proceedings, and as journal articles under the supervision of Dr. Ming J. Zuo in concept formation and by providing comments and corrections to the article manuscript.

Chapter 2 includes the results published in the following papers:

- Y. Fang, X. Liang, and M. J. Zuo, "Effect of sliding friction on transient characteristics of a gear transmission under random loading," in *Proceedings of 2017 IEEE International Conference on Systems, Man, and Cybernetics (SMC)*. IEEE, Banff, Canada, Oct. 5-8, 2017, pp. 2551–2555.

- Y. Fang, X. Liang, and M. J. Zuo, "Effects of friction and stochastic load on transient characteristics of a spur gear pair," *Nonlinear Dynamics*, vol. 93, no. 2, pp. 599–609, Jul. 2018.

The work presented in Chapter 3 has been accepted or submitted for peer review as follows:

- Y. Fang, M. J. Zuo, and Y. Li, "Investigation of gear dynamic characteristics under stochastic external excitations," in *Proceedings of 2019 International Conference on Advances in Materials, Mechanical and Manufacturing (AMMM)*, Beijing, China, Mar. 22-24, 2019. Accepted on Jan. 3, 2019.

- Y. Fang, X. Liang, and M. J. Zuo, "Effects of driving speed variation on gear dynamic characteristics under stochastic loading," *Mechanism and Machine Theory*. Submitted on Oct. 8, 2018.

The work presented in Chapter 4 has been accepted or submitted for peer review as follows:

- Y. Fang, M. J. Zuo, and Y. Li, "Efficient analytical method to obtain the responses of a gear model with stochastic load and stochastic friction," in *Proceeding of the 6th International Conference on Mechanical Engineering, Materials Science and Civil Engineering (ICMEMSCE)*, Xiamen, China, Dec. 21-22, 2018. 7 pages (USB).

- Y. Fang, X. Liang, and M. J. Zuo, "Approximate analytical solution to a spur gear model with stochastic excitations," *Journal of Mechanical Science and Technology*. Submitted on Oct. 28, 2018.

Acknowledgements

I would like to express my deepest appreciation to my supervisor *Prof. Ming J. Zuo* for his supportive attitude, encouragement, and guidance through my research at the University of Alberta. Undoubtedly, without his constant help and supervision, this dissertation would not have been possible. His research attitude and standard will continue encouraging and influencing me in my future career.

It is a honor for me to extend my gratitude to all my Ph.D. defense committee members *Dr. Zhigang Tian*, *Dr. Ben Jar*, *Dr. Samer Adeeb*, and *Dr. Liming Dai* from University of Regina for reviewing my thesis and providing thoughtful comments to improve it. My special thanks go to my colleagues and friends at the Reliability Research Lab with whom I had a wonderful time during my Ph.D. program.

I would like to thank my parents and my fiance Ziling Wei for their great understanding and support throughout my research.

Table of Contents

List of Tables

List of Figures

List of Symbols

b	Backlash
C_1	Tangent point between action line and base circle 1
C_2	Tangent point between action line and base circle 2
d	Center distance
E	Young's modulus
c	Damping coefficient
f_0	Mean of torque
f_j	Amplitude of jth harmonic term in torque
F	Elastic force between contact teeth
G	Hertzian damping force between contact teeth
I_g	Moment of inertia of gear
I_p	Moment of inertia of pinion
$k_{1,2}$	Segmented stiffness
K	Effective stiffness
l	Length of action line
L	Equivalent length of force arm
r	Variance of Gaussian white noise
r_1	Variance of Gaussian white noise for driving speed
r_2	Variance of Gaussian white noise for load
R_g	Base circle radius of gear
R_p	Base circle radius of pinion
T	Equivalent torque to gear system
$\mathrm{T_g}$	Torque to gear
$\mathrm{T_p}$	Input torque to pinion
t	Time
$W(t)$	A standard Wiener process
X_1	Tangent distance in the action line
α_0	Gear pressure angle
β_j	Initial phase angle of jth harmonic term in torque
δ	Relative angular displacement of gear pair
$\dot{\delta}$	Relative angular velocity of gear pair
$\ddot{\delta}$	Relative angular acceleration of gear pair
η_1	Sensitivity index of driving speed
η_2	Sensitivity index of load

θ_g	Angle of gear
θ_p	Angle of pinion
$\dot{\theta}_g$	Angular velocity of gear
$\dot{\theta}_p$	Angular velocity of pinion
$\ddot{\theta}_g$	Angular acceleration of gear
$\ddot{\theta}_p$	Angular acceleration of pinion
κ_1	Increasing rate by driving speed
κ_1	Increasing rate by load
λ	Drift coefficient
μ	Friction coefficient
ν_j	Angular frequency of jth harmonic term in torque
$\xi_1(t)$	Gaussian white noise in driving speed
$\xi_2(t)$	Gaussian white noise in torque
ρ_n	Angular frequency of nth harmonic term in driving speed
σ	Diffusion coefficient
$\tau,\ \Delta t$	Time increment
ϕ_n	Mesh period of gear teeth
ϕ_m	Double pairs of teeth mesh duration in a mesh period
χ_0	Mean of driving speed
χ_n	Initial phase angle of nth harmonic term in driving speed
ψ_n	Initial phase angle of nth harmonic term in driving speed
$\Phi(t)$	External load process
Ω_m	Load coefficient

List of Acronyms

FEM	Finite element modelling
LPM	Lumped parameter modelling
LTI	Linear time-invariant
LTV	Linear time-varying
MC	Monte Carlo
NTI	Nonlinear time-invariant
NTV	Nonlinear time-varying
ODE	Ordinary differential equation
PDF	Probability density function
PI	Path integration
RK4	Fourth-order Runge-Kutta method
st.d	Standard deviation
SDOF	Single degree of freedom
SDE	Stochastic differential equation
TVMS	Time-varying mesh stiffness

1 Introduction

This chapter is divided into three sections. The background of this thesis is introduced in Section 1.1. Section 1.2 provides a detailed literature review of the research challenges around gear dynamics considering stochastic internal and external excitations. Section 1.3 provides the research objectives and the organizational structure of this whole thesis.

1.1 Background

Geared systems are widely used in modern power transmission systems. Geared systems can change the speed, torque, and direction of a power source and create a mechanical advantage. They play an important role in wind turbines, helicopters, milling machines, and other equipment. A real gearbox with the casing removed is shown in Fig. 1.1, which is an example of geared systems. In this figure, a group of components are combined to form a gearbox, such as bearing, shaft, and clutch. A bearing is a component that constrains the relative motion to the desired motion only, and reduces friction between moving parts. A shaft is used to hold the other components and transmit power. A clutch engages and disengages power transmission from different shafts. Since gears are the key components in a geared system, this study focuses on the gear system. Gear system refers to the system considering gears only, which means the effects of bearings, shafts, and other components are ignored.

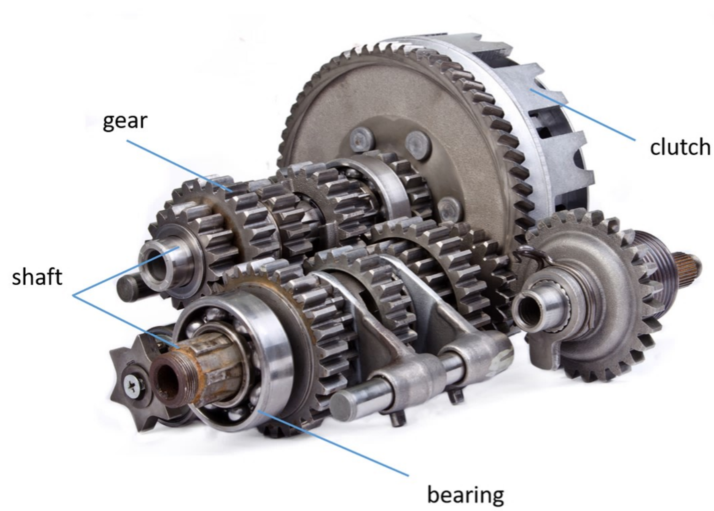

Fig. 1.1: An example of geared systems

In Section 1.1.1, the fundamentals of gear systems are introduced. Section 1.1.2 includes basic concepts of gear dynamics and generation of dynamic responses. Section 1.1.3 and Section 1.1.4 discuss different kinds of dynamic characteristics and how factors affect them, respectively. In Section 1.1.5, modelling of deterministic and stochastic excitations is explained. Section 1.1.6 and Section 1.1.7 introduce basic ideas and give examples of numerical and analytical approaches, respectively.

1.1.1 Fundamentals of Gear systems

This section introduces the fundamental concepts of gear systems, including classification of gear system and involute profile basic theory.

There are many different classification methods of gear systems. This section introduces three classification methods of gear systems based on positions of axis, transmission train, and tooth type, respectively. Gear systems can be broadly classified by looking at the positions of axis such as parallel shafts, intersecting shafts, and non-intersecting shafts. Fig. 1.2 (a) gives an example of parallel shaft gear systems and Fig. 1.2 (b) shows an example of intersecting shaft gear systems. A case of non-intersecting shaft gear systems is described in Fig. 1.2 (c).

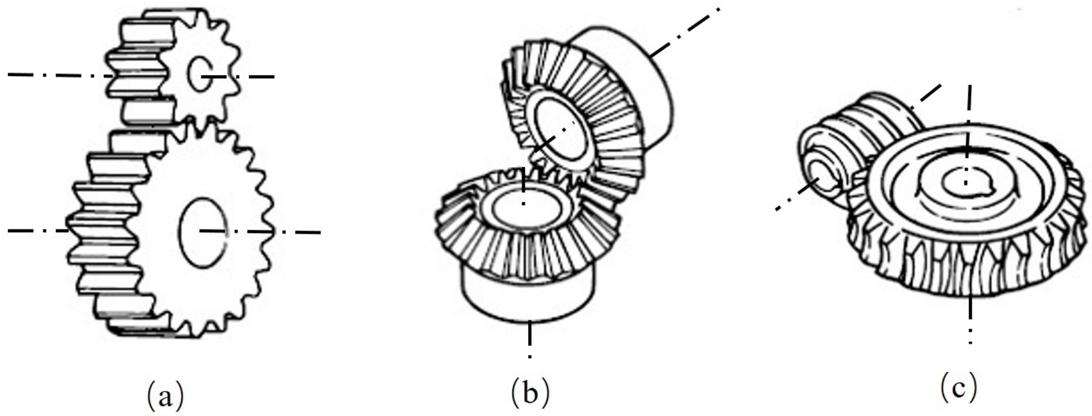

Fig. 1.2: Three types of gear systems: (a) parallel, (b) intersecting, (c) non-intersecting

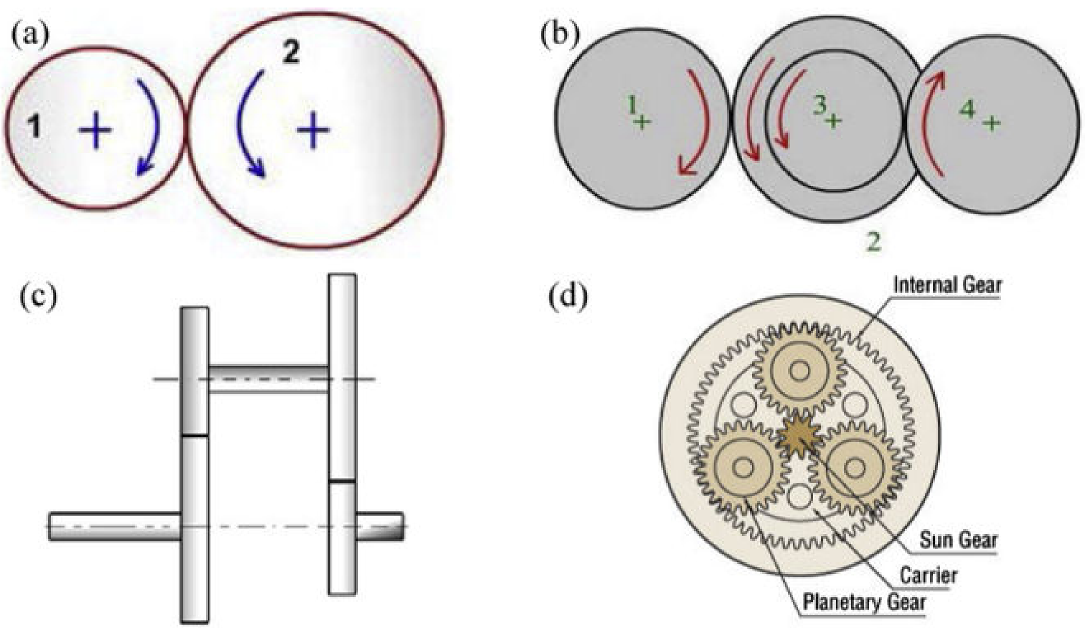

Fig. 1.3: Four types of gear systems: (a) simple gear systems, (b) compound gear systems, (c) reverted gear systems, and (d) planetary gear systems [3]

Parallel shaft gear systems are most commonly used and can be classified into four categories based on the transmission train: simple gear systems, compound gear systems, reverted gear systems, and planetary gear systems [3]. Fig. 1.3 gives examples for each type of parallel shaft gear systems. This classification method focuses on the relationship between gears and shafts, and the number of shafts is not restrained. For example, a simple gear system has only one gear mounted on each shaft while the number of shafts in the system can be more than two. For a compound gear system, there is more than one gear mounted on a shaft. For a reverted gear system, the axis of the driving gear shaft and the driven gear shaft are coaxial. If one gear rotates on its own axis and also revolves around the axis of another gear, this gear system is termed as a planetary gear system. A basic planetary gear system contains one sun gear, one internal gear (ring gear), one carrier, and several planet gears that mesh with the sun gear and the ring gear simultaneously.

The first three categories shown in Fig. 1.3 are collectively called fixed-axis gear systems since all gears only rotate on their own axis and all their axis are fixed. This thesis focuses on the fixed-axis gear system because it still has room to improve the understanding in the dynamics of the fixed-axis gear system. The development of fixed-axis gear dynamics will also give us a better understanding of planetary gear systems in the future.

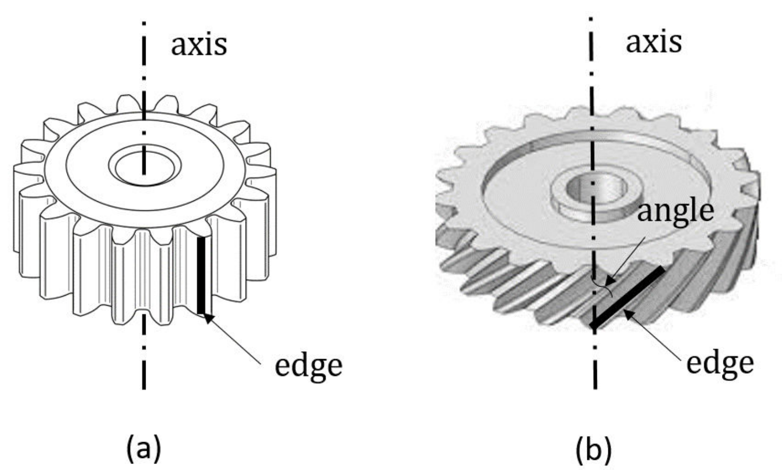

Fig. 1.4: Gear tooth comparison a) spur gear b) helical gear

According to the tooth type, there are mainly spur gears and helical gears. Fig. 1.4 shows the difference between the spur gear and the helical gear. Spur gears consist of a cylinder or disk with teeth projecting radially. The edges of each spur gear's tooth are straight and aligned parallel to the axis of rotation. The edges of helical gear's teeth are not parallel to the axis of rotation, but are set at an angle. Spur gears are used in low-speed applications while helical gears are used in high-speed applications or large power transmission systems [9].

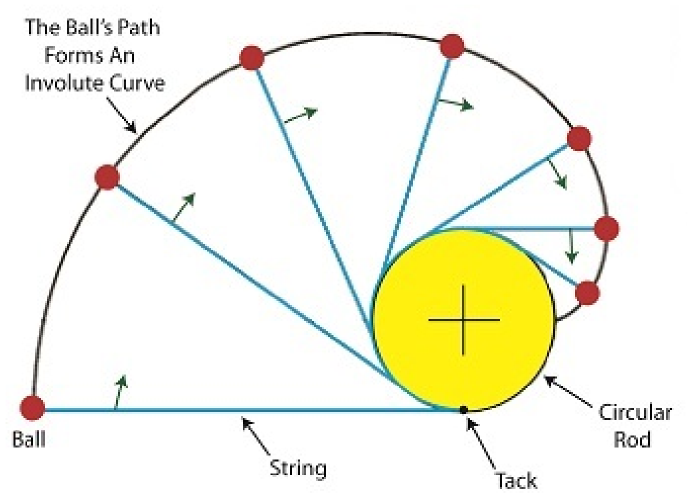

Fig. 1.5: An involute curve

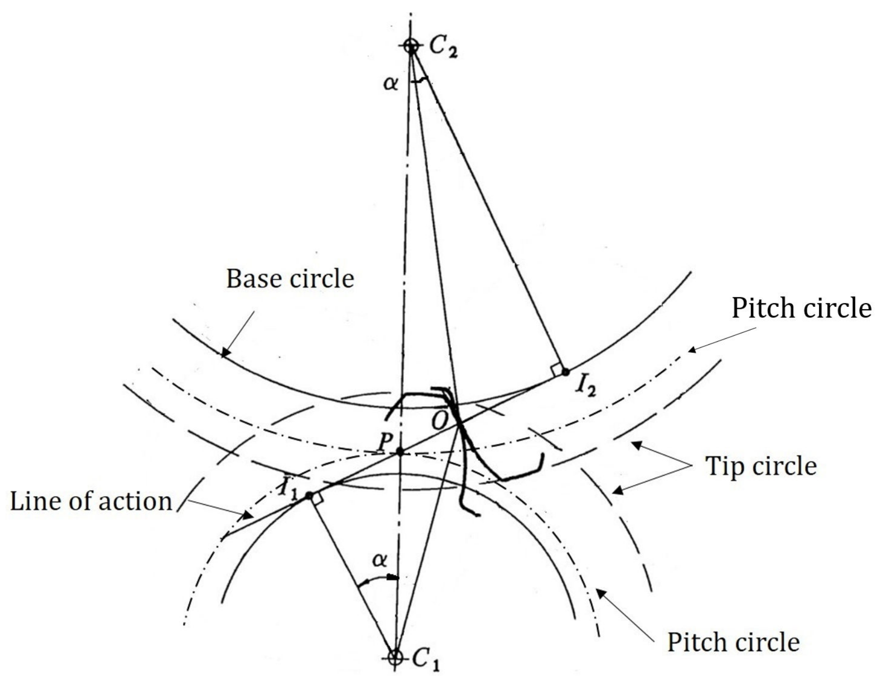

Fig. 1.6: An involute gear pair meshing

The involute gear profile is the most commonly used system for gearing today (e.g. spur involute gear and helical involute gear), such as clocks [10]. In an involute gear, the profiles of the teeth are involutes of a circle. Fig. 1.5 shows a string with one end fixed on a tack of a circular rod while the other end has a ball. The involute of a circle is the spiraling curve traced by the end of an imaginary taut string unwinding itself from that stationary circle (called the base circle). In a word, the path of the ball is called involute curve.

Spur gears and parallel-axis helical gears are involute gears. The contact point of the two involutes, as shown in Fig. 1.6, changes along the common tangent of the two base circles as rotation occurs. The common tangent is called the line of contact or the line of action. A pair of gears can only mesh correctly if the pressure angles are the same. Fig. 1.6 shows a pair of involute gear teeth meshing together. Base circles, tip circles, and pitch circles are shown in this figure. In addition, C_1 and C_2 are the center of two gears, I_1 and I_2 are tangent points on the line of action; α (pressure angle) is the complementary angle of $\overline{C_1C_2}$ and line of action, point O is the current pitch point (or contact point), and P is also a pitch point in the line of connecting centers.

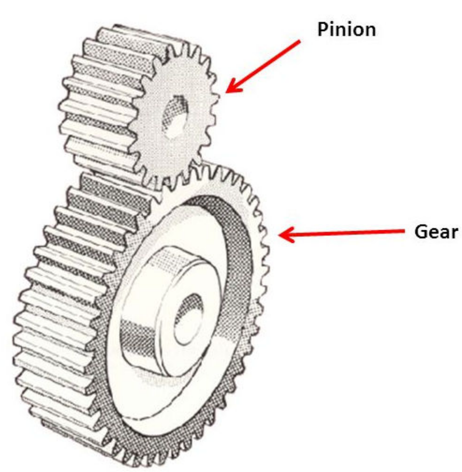

Fig. 1.7: An example of a spur gear pair

Fig. 1.7 gives an example of a spur gear pair which contains two spur gears marked as “pinion” and “gear”. “Pinion” (also called driving gear) usually means the smaller gear in a gear system while “gear” (also called driven gear) is the bigger one (see Fig. 1.7). Please note that the word “gear” has the specific meaning when it is mentioned with “pinion”. In other cases (e.g. “gear system”), the word “gear” holds a broader meaning.

1.1.2 Gear response generation

This section focuses on the basics of gear dynamics. The generation of gear responses will be introduced.

Spur gears are the most widely used type of gears in engineering applications. The dynamics of a spur gear pair has been explored. The gear dynamic modelling includes six aspects [11]:

1. Study the real motion of the gear system under given external forces.
2. Analyze the interaction forces between the gears.
3. Study the energy balance and load sharing during the operation of the gear system.
4. Investigate mechanical vibration.
5. Study the theory and mechanisms of motion.
6. Other comprehensive analysis.

Gear dynamic modelling provides several benefits in engineering corresponding to the above listed six aspects [11]:

1. Predict and analyze the behaviour of the gear system.
2. Find out the weakness of the gear system.
3. Reasonably arrange the load in the gear system.
4. Obtain the influences of different factors that cause vibration, noise and failure.
5. Help improve the control system.
6. A better design of gear systems which helps extend its life.

Thus, it is necessary to study the dynamics of a gear system. This thesis is limited to the dynamic model of a pair of fixed-axis spur gears as shown in Fig. 1.7. Many studies have been conducted on dynamic modelling of spur gear transmission systems. Dynamic modelling utilizes physical laws to simulate gear system responses, e.g. equilibrium, Conservation of Energy, and Newton's laws

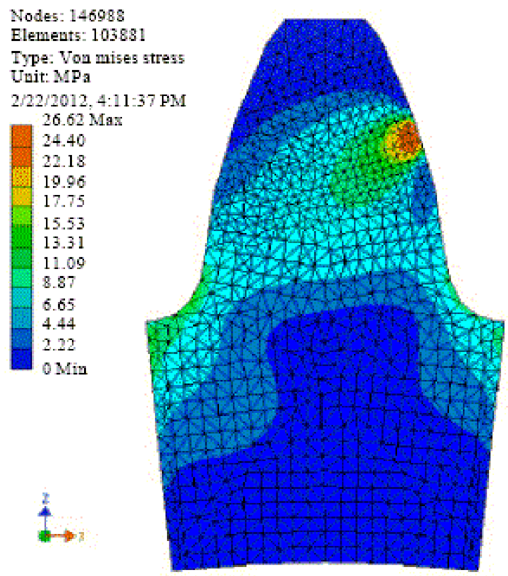

Fig. 1.8: An example of gear systems by FEM [4]

of motion [12]. Equilibrium refers to the net force on each component of a gear system being zero. The law of Conservation of Energy states that the total energy of an isolated gear system remains constant, it is said to be conserved over time. Newton's laws of motion describe the relationship between a gear, the forces acting upon it, and its motion in response to those forces. Dynamic response or response refers to the motion (including displacement, velocity, and acceleration) of a gear excited by forces or torques.

Lumped parameter modelling (LPM) and finite element modelling (FEM) are two commonly used techniques to model gear systems [13]. FEM discretizes a physical model into disjoint components of simple geometry (called finite elements). It obtains its system response by the summation of the responses of all elements [14]. Fig. 1.8 gives an example of gear systems' dynamic analysis using FEM. The gears in this figure are divided into a large number of disjoint simple geometries which are called finite elements. This figure utilizes colours to represent the amplitude level of the element stress simulated by FEM. Red element means the greatest stress while blue refers to the smallest stress. It is noted that the contact region elements have the greatest stress. There are a number of commercial FEM softwares, including ABAQUS [15], ANSYS [16], and so on.

A classic dynamic model of a gear pair is shown in Fig. 1.9. In this figure,

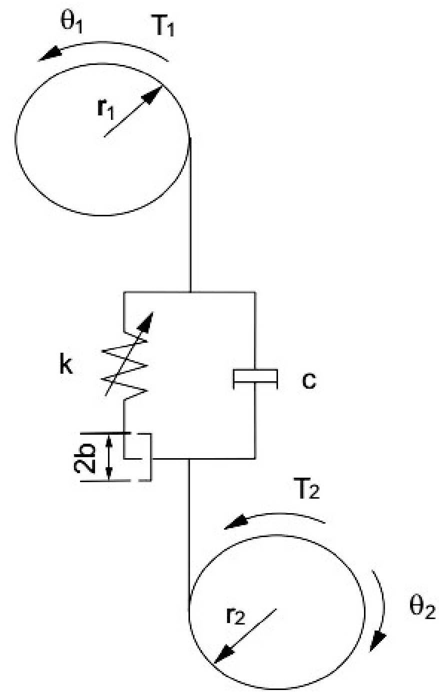

Fig. 1.9: Model of a gear system [5]

$T_i\ (Nm)$, $\theta_i\ (rad)$, and $r_i\ (m)$ are the torque applied to gear i, rotation angle of gear i, and base radius of gear i, where subscript $i\ (i = 1, 2)$ refers to the driving and driven gears. In involute gears, the tooth profile is generated by the involute of the base circle. Note that $k\ (N/m)$, $c\ (Nm/s)$, and $b\ (m)$ are time-varying mesh stiffness (TVMS), damping coefficient, and backlash, to be defined next.

TVMS is the rigidity of the mesh between two gears, which resists deformation in response to an applied force [17]. TVMS is usually time varying according to the status of meshing. Fig. 1.10 shows that TVMS is time-variant with two mesh statuses: single tooth contact and double tooth contact. Please note that the mesh stiffness is different from the concept of material stiffness. Material stiffness means inherent material property to resist deformation, which is usually a constant for a given material. Damping refers to the gradually decreasing vibration amplitude characteristics of a gear system, due to external effects (such as fluid resistance, friction, etc.) and the inherent nature of the system [18]. When two elastic bodies interact, most of the elastic strain energy is restored. However, a portion of it will be dissipated in heat due to random molecular vibration. The phenomenon can be considered as an internal damping effect during the impact. Fig. 1.11 gives an

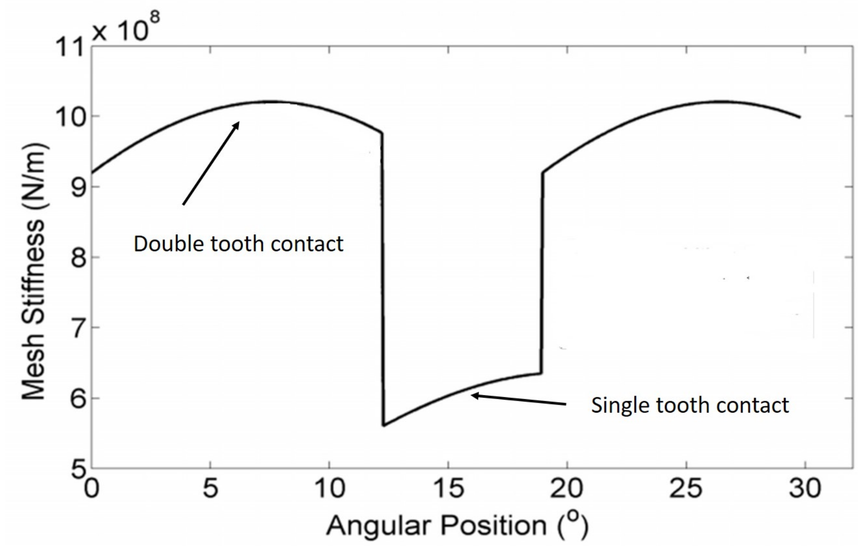

Fig. 1.10: An example of time-varying mesh stiffness (TVMS)

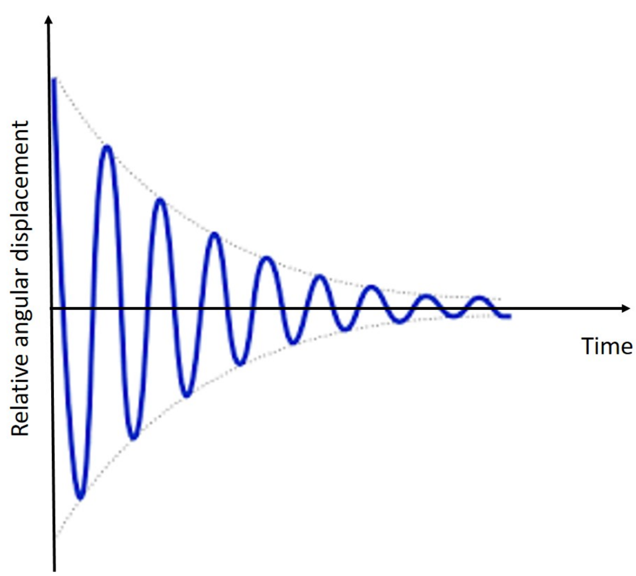

Fig. 1.11: An example of damping effects

example of damping effect on the value of relative angular displacement which is to be defined in Section 1.2. Backlash (see Fig. 1.12) is the amount of clearance between mated gear teeth. It can be seen when the direction of movement is reversed and the slack or lost motion is taken up before the reversal of motion is completed.

Lumped parameter modelling (LPM) considers the components to be solid with the masses concentrated at a set of points [19]. Ignoring the shape of gears,

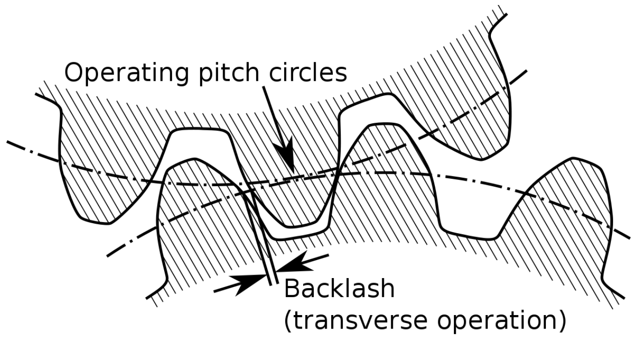

Fig. 1.12: Backlash [6]

LPM focuses on the dynamics of mesh point (see point O in Fig. 1.6) only. All the parameters (e.g. mass and damping) of all gears are treated equivalent to the mesh point, which is actually a mesh line considering the thickness of gear teeth. Taking rotation into account only, this is torque balance for the mesh point according to Newton's second law. Namely, a gear system in rotational equilibrium has no net external torque. Just as force makes object accelerate linearly, torque makes gears accelerate rotationally. The basic law is: torque = (moment of inertia) $\times$ (angular acceleration). Ordinary differential equation (ODE) is used to represent the dynamics of a gear system. We next illustrate a gear dynamic model described by LPM.

The corresponding mathematical model by LPM (considering rotation only) in Fig. 1.9 is shown as Eq. (1.1) [5]. Relative angular displacement is defined in Eq. (1.2).

$$\begin{aligned} J_1\ddot{\theta}_1 &= T_1 - \Big(k \cdot g(X) + c(r_1\dot{\theta}_1 - r_2\dot{\theta}_2)\Big)\, r_1 \\ J_2\ddot{\theta}_2 &= -T_2 + \Big(k \cdot g(X) + c(r_1\dot{\theta}_1 - r_2\dot{\theta}_2)\Big)\, r_2 \end{aligned} \tag{1.1}$$

$$\dot{X} = r_1\dot{\theta}_1 - r_2\dot{\theta}_2 \tag{1.2}$$

where J_i, T_i, $\ddot{\theta}_i$, and r_i are the moment of inertia, external torque, angular acceleration, and base circle radius of gear i ($i = 1, 2$), respectively, k is time varying mesh stiffness, and $g(X)$ is a function of backlash b, which is defined as following:

$$g(X) = \begin{cases} X - b, & X > b \\ 0, & -b \le X \le b \\ X + b, & X < -b \end{cases} \tag{1.3}$$

According to Eq. (1.1) and Eq. (1.2), we can obtain:

$$\ddot{X} + \bar{c}\dot{X} + \bar{k} \cdot g(X) = T \tag{1.4}$$

where

$$\bar{c} = c\left(\frac{r_1^2}{J_1} + \frac{r_2^2}{J_2}\right) \tag{1.5}$$

$$\bar{k} = k\left(\frac{r_1^2}{J_1} + \frac{r_2^2}{J_2}\right) \tag{1.6}$$

$$T = \frac{T_1 r_1}{J_1} + \frac{T_2 r_2}{J_2} \tag{1.7}$$

where X, $\dot{X}$, and $\ddot{X}$ are relative angular displacement, relative angular velocity, and relative angular acceleration, respectively, $\bar{c}$, $\bar{k}$, and T are equivalent damping coefficient, equivalent TVMS, and equivalent torque. In solving process, TVMS is treated as a series of time-varying certain values. In the rest of thesis, "gear dynamic model" usually refers to a second order ODE, such as Eq. (1.4).

After solving the dynamic model, we can obtain dynamic responses. "Dynamic responses" or "responses" refer to X, $\dot{X}$, and $\ddot{X}$ in Eq. (1.4). In other words, we can obtain the solution to the dynamic equation. Here, "model" and "response" are a pair while "equation" and "solution" are a pair.

Both LPM and FEM can deal with the dynamics of gear systems. Usually, FEM has an equal or higher accuracy than LPM. However, LPM is faster in simulation than FEM. LPM has some advantages when dealing with randomness in the model. In next section, we will explain that it is difficult for us to solve a dynamic model considering stochastic parameters. Thus, this study focuses on the dynamic modelling using LPM. Compared with existing studies, more aspects of nonlinearity of gear parameters will be considered in our study to explore gear dynamics. Later in our thesis, we will present more advanced studies to improve gear dynamic model.

1.1.3 Characterization of dynamic response

This section focuses on the dynamic characteristics of gear systems. "Dynamic characteristics" refer to the properties of system responses when a time-varying input is applied. It is different from "static characteristics" which refer to the results when a constant input is applied.

In the study of dynamic modelling, the dynamic characteristics of gear system are quite complex and directly affect its performance. The performance usually means the health condition of a gear system. The evaluation of dynamic characteristics is an important part of gear dynamic analysis. They reflect the gear system's performance and indicate gear faults and failure. A better understanding of the dynamic characteristics will be a perspective to implement appropriate models for reliability design. Reliability design is a process that encompasses tools and procedures to ensure that a gear system meets its reliability requirements within its lifetime. Reliability design is implemented in the design stage of a product to proactively improve gear system reliability. An example of gear system reliability design can be referred to [20]. Obtaining dynamic characteristics of gear systems is the precondition of conducting a reliability design. Thus, it is necessary to analyze dynamic characteristics of gear systems.

Dynamic characteristics are analyzed by obtaining dynamic responses first. The dynamic characteristics discussed in this thesis are mainly statistical properties, duration, periodicity, chaos, and stability of the responses. Duration refers to the time system spent in transient state. As an important aspect of this thesis, the dynamic characteristics studied in this thesis are listed as following:

1. **Statistical properties**
   Due to errors of manufacturing and assembling, gear systems contain inherent randomness. Meanwhile, environment factors (e.g. temperature) include randomness. Since the responses of the gear pair under stochastic load are random variables, it is necessary to give statistical information of responses. In dealing with random variables, the probabilistic method is a classical approach for uncertainty representation based on the well-developed probability theory [21].

   In statistics, dispersion (also called variability, scatter, or spread) is the extent to which a distribution is stretched or squeezed [22]. Common examples of measures of statistical dispersion are the variance, standard deviation, and interquartile range. Dispersion is contrasted with location or central tendency, and together they are the most common used statistical characteristics of distributions [21]. The descriptions of responses in the gear system under stochastic load are analyzed with probability density function (PDF) [23]. Let $f(X)$ denote the PDF of random variable X. Then, $f(X)$ is defined in Eq. (1.8) and (1.9), which could be clearly seen from Fig. 1.13. In the applications such as fatigue prediction and reliability, an actual PDF is needed.

$$\Pr[a \leq X \leq b] = \int_a^b f(X)\,dx. \tag{1.8}$$

$$\int_{-\infty}^{+\infty} f(X)dX = 1 \tag{1.9}$$

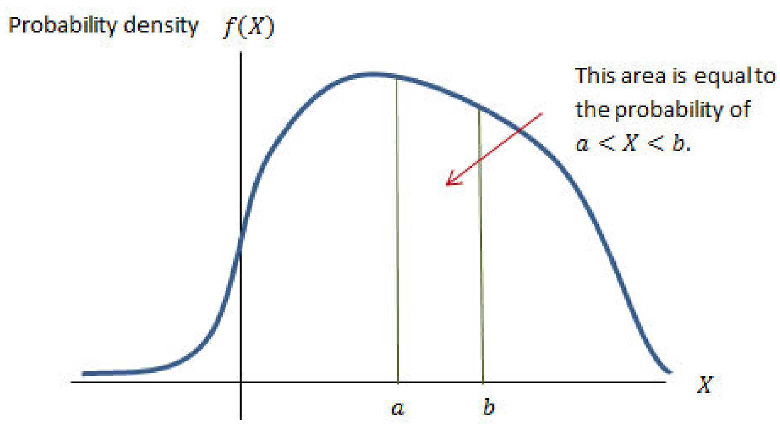

Fig. 1.13: Definition of PDF

2. **Duration** [24]
   Duration refers to the time a system spends in the transient state. If the responses vary beyond a given range (e.g., less than 5% variation), it is called the transient response and the state of the gear system is named as the transient state. In contrast, stationary responses mean the responses vary in a very small range or remain constant. The corresponding state of the gear system is called the steady state.

3. **Periodicity**
   Periodic behavior is defined as recurring at regular intervals, such as "every 24 hours". Quasi-periodicity is the property of a system that displays irregular periodicity. Quasi-periodic behavior is a pattern of recurrence with a component of unpredictability that does not lead itself to precise measurement.

4. **Chaos** [25]

   A dynamic system with chaotic behaviour must have three properties: 1) it must be sensitive to initial conditions; 2) it must be topologically mixing; 3) it must have dense periodic orbits. Fig. 1.14 shows the chaotic behaviour of three samples of responses.

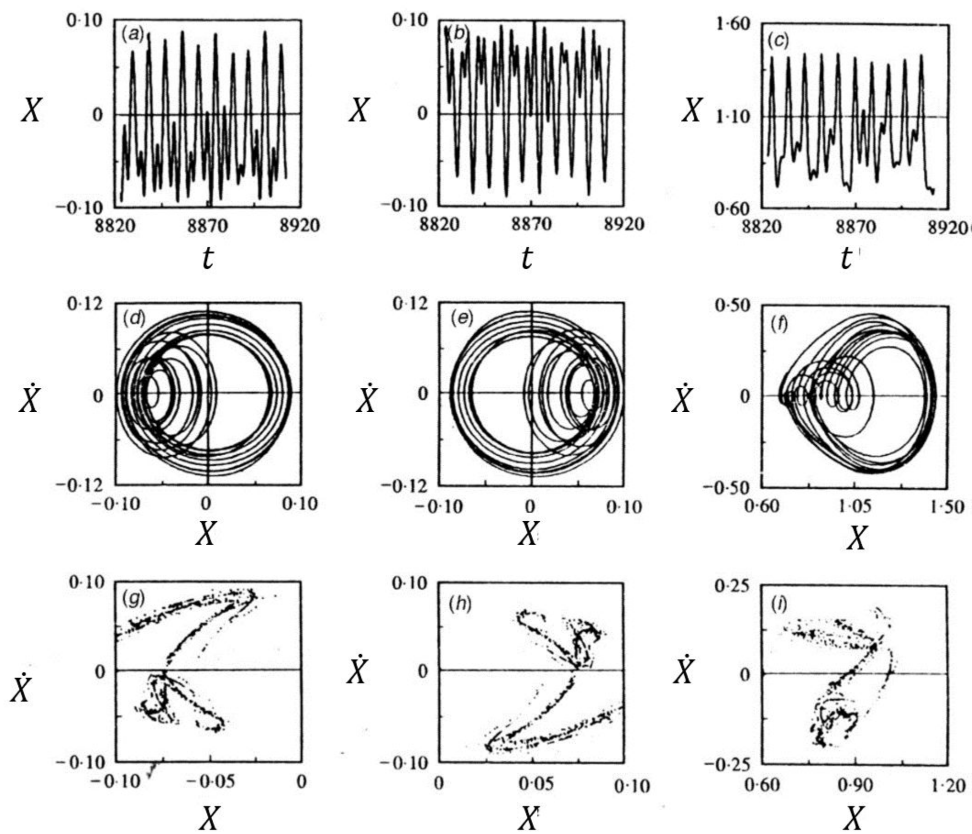

Fig. 1.14: Example of chaotic behaviour: (a-c) Time history of X; (d-f) phase plane; (g-i) Poincare' map [7]

Phase diagram and Poincare map are useful tools showing the periodicity and chaos of gear systems' dynamic responses. Here, Fig. 1.14 (d-f) depict three examples of phase diagram according to the responses in Fig. 1.14 (a-c). The overlapped loops in phase diagram indicating the responses are periodic. Fig. 1.14 (g-i) describe three examples of Poincare map according to responses in Fig. 1.14 (a-c). According to the graphical features of the visible points in Poincare maps, the periodic, quasi-periodic, and chaotic oscillations can be learned.

5. **Solution stability** [26]
   Solution stability addresses the stability of solutions of differential equations (and of trajectories of dynamic systems) under small perturbations of initial conditions. "Trajectories" refer to the time-history of X from $X_{t=0}$ to $X_{t=\tau}$. Stability has many different definitions. Lyapunov stability and asymptotically stability are adopted in this thesis. Their definitions are given in the next paragraph.

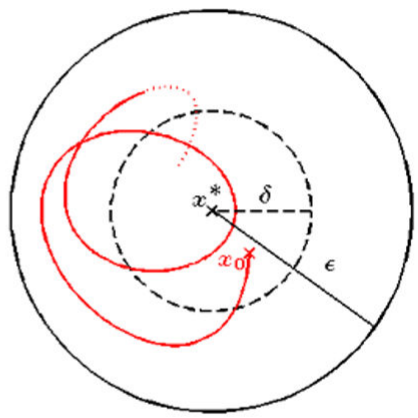

Fig. 1.15: Solution trajectory

Use an orbit diagram as an example (see Fig. 1.15). The response of the dynamic model starting from x_o converges to a certain orbit x^*. We can say that $X_{t=0} = x_0$ and $X_{t\to\infty} = x^*$. This equilibrium is said to be Lyapunov stable, if, for each $\epsilon > 0$, there exists a $\delta > 0$ such that, if $\|x_0 - x^*\| < \delta$, then for each $t \geq 0$ we have $\|x_t - x^*\| < \epsilon$. The equilibrium of the above system is said to be asymptotically stable if it is Lyapunov stable and there exists $\delta > 0$ such that if $\|x_0 - x_t\| < \delta$, then $\lim_{t\to\infty} \|x_t - x^*\| = 0$.

1.1.4 Factors affecting dynamic response

It is well-known that the characteristics of a gear system are affected by internal and external excitations [27]. Internal excitations include backlash, TVMS, transmission error, friction, and so on. Definitions of damping, backlash, and TVMS are introduced in Section 1.1.2. Transmission error is caused by assembling or manufacturing and it is the difference between the theoretical and practical rotation angle of the driven gear. Friction is induced by the teeth sliding at the mesh point of two gears. It is along the tangent direction of the contact force. External excitations contain external load, driving speed, and so on. External load here is limited to torque applied on gears in this study. Driving speed in this thesis refers to the rotational driving speed of the pinion.

We first look into a general ODE defined in Eq. (1.10). An ODE is defined to be unique and specific according to the initial condition and parameters of the equation. The parameters which affect the solution of an ODE are the internal and external excitations. Note that these excitations affect the dynamic responses. Internal excitations reflect in $q_1(X, \dot{X})$, $q_2(X, \dot{X})$, and $q_3(X, \dot{X})$ while external load is T. Researchers have been working on a better expressions of each parameter for decades. This work will continue to search for an improved model to approach the real systems.

$$\ddot{X} + q_1(X, \dot{X})\dot{X} + q_2(X, \dot{X})X + q_3(X, \dot{X}) = T \tag{1.10}$$

Many reported studies have dealt with gear systems under deterministic internal or external excitations [7] [24]. Deterministic excitation means, at an arbitrary time point, the value of the excitation is known and unique though they may be different at different time points. By contrast, stochastic excitation has an unknown value at each time point. These existing models reveal the mechanism of gear systems in these aspects and contribute to the understanding of gear dynamics. The restriction of the gear dynamics problems within the deterministic domain reduces the difficulties in obtaining dynamic responses of a gear system.

Due to errors of manufacturing, processing, assembling, wear, lubrication, operating environment, and other factors, the internal and external excitations may not be deterministic [2]. For example, considering the operating environment, wind force applied to each wind turbine in a wind farm at a certain time point is stochastic. Individual modelling of each gear system is not realistic. Thus, stochastic internal and external excitations have been considered and the gear models with stochastic internal and external excitations have been investigated.

Let's establish a dynamic model considering stochastic excitations to describe the general dynamic characteristics of a spur gear pair. There are three aspects in dealing with stochastic excitations [2]:

1. Modelling of the internal and external stochastic excitations.

2. Solutions to dynamic equations with stochastic excitations involved.

3. Analysis of the internal and external stochastic excitations' effects on dynamic characteristics.

1.1.5 Modelling deterministic and stochastic excitations

To model deterministic excitations, a certain deterministic expression is required for each factor. For example, damping coefficient can be considered as a constant. TVMS can be defined as a square wave function with certain period and amplitude [5]. More generally, deterministic load T_d can be given as Eq. (1.11), where T_0 is a constant (T_0 can be zero), $T_n(t)$ is a function of time, and n is a positive integer. In addition, $T_n(t)$ has a certain value for each time point t. Modelling deterministic excitations depends on a simplified physical model which can present majority properties of a gear system. Many researchers have worked on deterministic excitations and a detailed review can be referred to [7].

$$T_d = T_0 + T_1(t) + ... + T_n(t) \tag{1.11}$$

On the other hand, stochastic excitation has another form. Taking stochastic load T_s as an example, a general expression of T_s can be shown as:

$$T_s = T_d + rnd(t) \tag{1.12}$$

where $rnd(t)$ is the random part in the load.

To describe the randomness in gear systems, statistic model, interval model, and fuzzy model have been used [2]. If internal or external excitations contain randomness and its probability distribution can be estimated using data, a statistic model can be applied. For example, Fig. 1.16 shows the seasonal wind speed distribution in region La Ventosa in Mexico. Alonzo et al. [8] used the statistical model to study the entire seasonal distribution of the wind speed. If only the ranges of internal or external excitations are available, interval model can be utilized. For example, Ref. [28] studied a wind turbine gear system where the stiffness and damping are all uncertain but bounded. In addition, fuzzy model can describe the randomness in internal or external excitations when limited information is available [29].

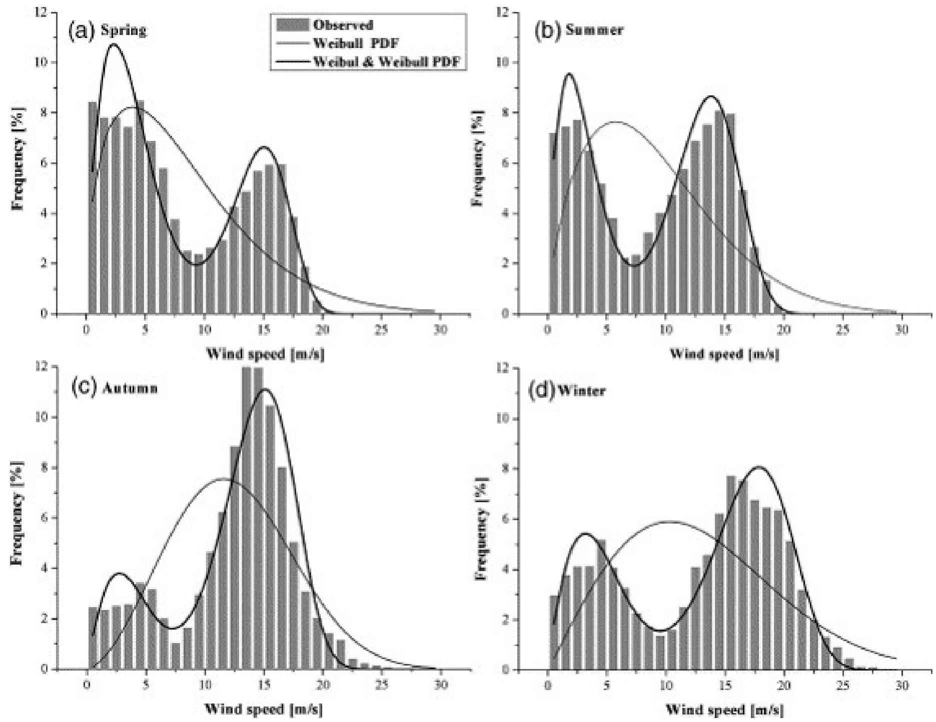

Fig. 1.16: Seasonal wind speed distribution [8]

Based on the amount and the type of available information, we can choose a proper model and the corresponding analysis method. Among these models, the statistical model is the most commonly used method and it has advantages in simulation and mathematical description than the other two methods. Our work focuses on using statistic models to describe the randomness in both internal and external excitations. In next paragraphs, we introduce some fundamentals to the statistical approach.

Among the studies investigating randomness of external load in gear systems' analysis model [30] [31], Gaussian white noise was widely accepted in describing randomness in external load [32]. The other model, Gaussian diffusion process, will be applied to model the external load in this study. We will define it next. Gaussian white noise is suitable for modeling the randomness in lab experiment condition (with small fluctuations in operating environment). Gaussian diffusion process is applicable in the occasion considering natural forces (with larger fluctuating than lab experiment condition), e.g., wind power.

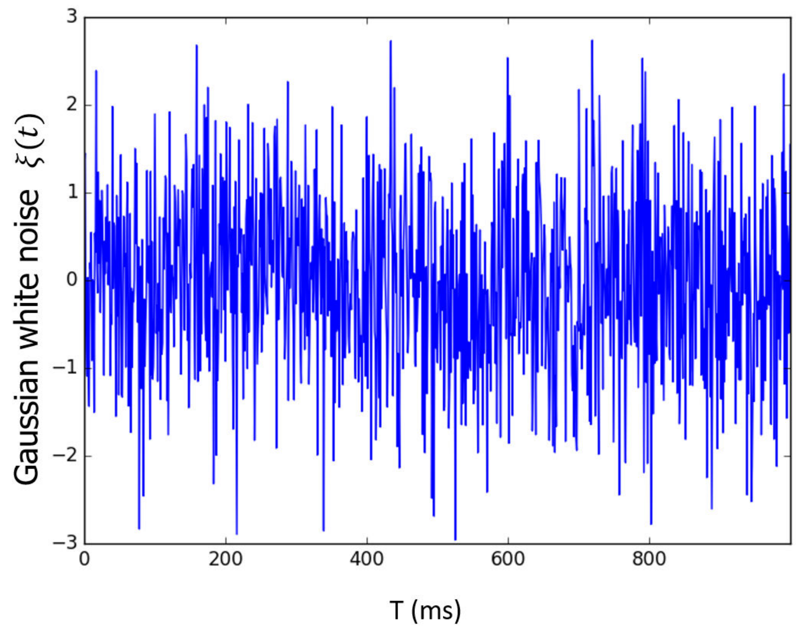

Fig. 1.17: A plot of Gaussian white noise signal

A sample of Gaussian white noise is depicted in Fig. 1.17. Gaussian white noise $\xi(t)$ is defined as:

$$E(\xi(t)) = 0 \tag{1.13}$$

$$E[\xi(t)\xi(t+\tau)] = \sigma^2\Theta(\tau) \tag{1.14}$$

where t is time, ξ is a Gaussian white noise with variance σ^2, and Θ is the Dirac Delta function (see Fig. 1.18) which is also known as unit impulse symbol.

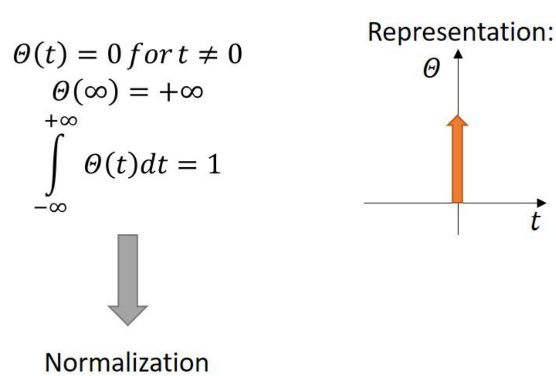

Fig. 1.18: Dirac Delta function

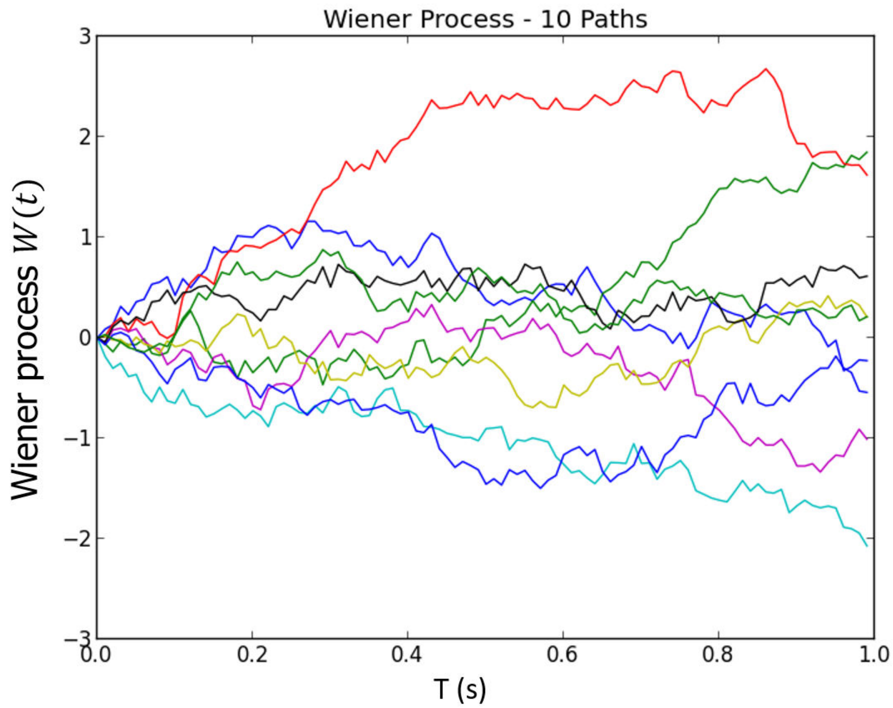

Fig. 1.19: An example Wiener process

A Gaussian diffusion process is used to simulate the equivalent external excitation Φ. It is the integration of Gaussian white noise. It is assumed that Φ can be approximated in the following form [33]:

$$d\Phi(t) = \lambda dt + \sigma dW(t) \tag{1.15}$$

where λ is the drift scalar, σ is the diffusion scalar, and $W(t)$ is a standard Wiener process. Wiener process is a continuous-time stochastic process and it is often called Brownian motion. An example of Wiener process is shown in Fig. 1.19, which contains 10 different paths. The standard Wiener process $W(t)$ is characterised by the following properties:

1. $W(t)$ has independent increments: for each $t > 0$, the future increments $W(t+\tau) - W(t),\ \tau \geq 0$, are independent of the past values $W(s),\ s < t$.

2. $W(t)$ has Gaussian increments: $W(0) = 0,\ W(t) - W(0)$ is normally distributed with mean 0 and variance $t,\ W(t) \sim \mathcal{N}(0,t)$.

3. $W(t)$ has continuous paths: $W(t)$ is continuous in t with probability 1.

Comparing Fig. 1.17 and Fig.1.19, the properties of the two types of stochastic model can be obtained. The main differences between the two types of stochastic model are shown as: 1) the mean of $\xi(t)$ equals to zero while the mean of $W(t)$ does not; 2) the variance of Gaussian white noise $\xi(t)$ is σ^2 while the variance of Gaussian diffusion process $\Phi(t)$ is $\sigma^2 t$.

1.1.6 Runge-Kutta and Monte Carlo (MC) approach

Current methods can solve a gear model's differential equations under stochastic load and with other deterministic factors that may include TVMS, backlash, damping ratio, and so on. Solving a gear model's differential equations under stochastic load and with at least one of the internal factors being stochastic is more difficult than when all factors are deterministic.

Runge-Kutta method is a family of iterative methods to obtain approximate solutions of an ODE [34]. Accordingly, an initial value problem is specified as follows,

$$\dot{y} = f(t, y) \tag{1.16}$$

$$y(t_0) = y_0 \tag{1.17}$$

where y is an unknown function of time t which needs to be approximated. By Runge-Kutta method, we can approximate the value of $y(t_n)$ at any time point t_n. The fourth-order Runge-Kutta method, also namely RK4, is the most widely used member of the Runge-Kutta family. The procedure of RK4 can be summarized as follows [35].

$$y_{n+1} = y_n + \frac{1}{6}\left(k_1 + 2k_2 + 2k_3 + k_4\right) \tag{1.18}$$

$$t_{n+1} = t_n + h \tag{1.19}$$

where $h > 0$ is the step-size, $n = 0, 1, 2, \cdots$, $k_1 = hf(t_n, y_n)$, $k_2 = hf(t_n + \frac{h}{2}, y_n + \frac{k_1}{2})$, $k_3 = hf(t_n + \frac{h}{2}, y_n + \frac{k_2}{2})$, and $k_4 = hf(t_n + h, y_n + k_3)$. Accordingly, y_{n+1} is the RK4 approximation of $y(t_{n+1})$. Note that the total accumulated error of RK4 is on the order of $O(h^4)$. Similarly, the accumulated error of the mth-order Runge-Kutta method is on the order of $O(h^m)$ [35].

Applying MC method combined with Runge-Kutta method [34] can also obtain the numerical solution to such model but with high calculation cost. Runge-Kutta

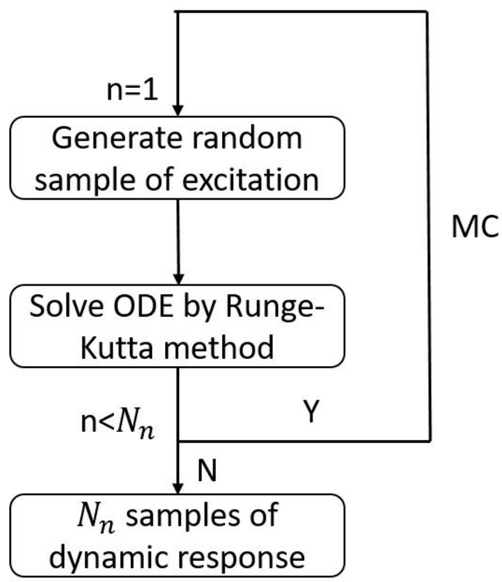

Fig. 1.20: Flowchart of the Runge-Kutta and MC approach

method is a numerical approximation approach for an ODE. Conducting Runge-Kutta method can obtain one sample of results for each time. The flowchart of Runge-Kutta and MC approach is given in Fig. 1.20. A large number of samples are needed for MC to obtain reasonable statistical properties of gear system responses at each time point. The corresponding study on numerical solution will be shown in Chapter 2 and Chapter 3.

1.1.7 Path integration (PI) method

Analytical solution has advantages in calculation efficiency compared with numerical solution. Analytical solution or closed form expression is a mathematical expression that can be evaluated in a finite number of mathematical operations. It may contain constants, variables, certain well-known operations (e.g., $+$, $-$), and functions (e.g., nth root, exponent, logarithm), but usually not the limit operator. Some researchers have explored the analytical solution to a gear dynamic model under stochastic load with all internal excitations being deterministic. However, there is no reported work giving analytical solution to a gear model under stochastic load and with at least one of the internal factors being stochastic. A general analytical solution is needed for such model to be solved fast.

PI method is a method providing analytical solution to an ODE with the zero-order term being stochastic and the first and the second order terms being deterministic. PI method's key idea is assuming that the transition process follows the Gaussian distribution. Then, the PDF of the response can be calculated by doing integration in a finite phase plane space [36]. The corresponding study on PI method will be shown in Chapter 4.

In summary, we have given the background information of the thesis in this section. We first introduced the basic concepts of gear systems, gear dynamics, and generation of dynamic responses. Then, the effects of different kinds of dynamic characteristics and the modelling of deterministic and stochastic excitations were explained. The basic ideas of numerical and analytical approaches were given at the end of this section. In Section 1.2, the related literature is surveyed.

1.2 Literature review

In this thesis, we focus on a single degree of freedom (SDOF) gear model shown in Eq. (1.10) considering different internal and external excitations. There is no doubt that the dynamic model is closer to reality by considering more stochastic internal and external excitations. However, it was pointed out that gear transmissions are complicated and it is hard to model all details of a transmission [12]. Our work is to explore those internal and external excitations which have not been considered in the gear dynamic modelling and their effects on gear dynamic characteristics. Meanwhile, considering more excitations in a gear dynamic model increases the complexity (or nonlinearity) in solving the dynamic equation in Eq. (1.10). Providing a better strategy of solving gear dynamic equations is another important aspect in this thesis.

This section reviews existing works on modelling stochastic internal and external excitations in a gear pair, analyzing each internal or external excitation's effects on gear dynamic characteristics, and obtaining analytical solution to a gear dynamic model. Section 1.2.1 recalls the reported gear model under stochastic load and Section 1.2.2 reviews internal excitations in a gear pair. The studies related to another external excitation, driving speed, are reviewed in Section 1.2.3. Section 1.2.4 reviews the developments of solving techniques for gear models under stochastic load.

1.2.1 Deterministic and stochastic load considered in a gear pair

Dynamic modelling is the foundation of studying the gear dynamics. Recalling Eq. (1.10), T is considered as load in a gear dynamic model. A general expression of deterministic load is shown in Eq. (1.11). For a stochastic load, it is considered as a summation of deterministic load and a random part (see Eq. (1.12)). This section reviews existing works on deterministic and stochastic load considered in a gear pair.

Gear dynamics under deterministic load has been explored for decades. Wang et al. [7] reviewed the reported models and approaches used in gear dynamics. Khabou et al. [24] investigated the dynamic behavior of a spur gear system under deterministic load and concluded that adequate external load should be chosen to reduce vibration.

However, the assumption of deterministic external load faces its shortcomings in many practical occasions, e.g., uneven road, ocean flows, and wind power. For example, the wind power is unpredictable and its effects on the wind turbine gear system are unknown. The assumption of deterministic load in wind turbine gear system is not suitable for the case with fluctuating wind.

A few studies investigated randomness of external load in gear system analysis. Utagawa and Harada [30] investigated the influence of randomness of dynamic loads for high speed gears. Tobe et al. [31] investigated stochastic load, which was treated as Gaussian white noise. Their results were validated by comparing with the experimental results reported in [37]. Ref. [37] reported studies in gear stochastic dynamics and examined the randomness of external load via lab experiments. Wang et al. [38] studied a wind turbine generator working in stochastic wind with varying directions and loads.

Gaussian white noise (refer to Eq. (1.13) and Eq. (1.14)) is suitable for the circumstances with small environment influence. However, the suitable application environment of Gaussian white noise is limited. Considering the complexity of working condition, other stochastic load models are required for different environments. Compared with Gaussian white noise, Gaussian diffusion process (refer to Eq. (1.15)) has fluctuating mean values, which is more appropriate in large varying noise of load situations to study the transient characteristics caused by the randomness of load.

Existing works modelled Gaussian white noise as the random part in external load. Nevertheless, they did not utilize Gaussian diffusion process to model the randomness in load. The assumption of Gaussian diffusion process may be better on the occasions, for example, wind turbines suffering from time varying load and frequent start-up [21]. It is necessary to point out that we are not saying Gaussian diffusion process is suitable for all circumstances. For instance, Gaussian white noise may be a realistic representation of real gear systems with small varying noise of load. It is still worth to consider stochastic load as Gaussian diffusion process in gear modeling for some cases (i.e., a large varying noise of load).

Both Gaussian white noise and Gaussian diffusion process will be utilized in this thesis to model the stochastic excitations including external load and driving speed. Gaussian white noise is adopted to model external load and driving speed in Section 2.4 and Section 3.2.2, respectively. In Section 2.5, Eq. (1.15) is adopted to model external load. For stochastic external excitation, it is the first time to model external load using Gaussian diffusion process and model driving speed using Gaussian white noise. Corresponding work can be referred to Chapter 2 and Chapter 3.

1.2.2 Internal excitations considered in a gear pair

Researchers have considered that many internal excitations affect gear dynamics. Theodossiades and Natsiavas [39] introduced the gear systems with periodic stiffness and backlash under the action of external excitation, caused by torsional moments and gear transmission errors. They considered the transmission errors as static errors, which means that the error is time invariant. The meshing stiffness was expressed in a Fourier series form and backlash was adopted as Eq. (1.3). Wang et al. [7] reviewed internal excitations, including backlash, tooth mesh stiffness, transmission error, friction, etc., used in gear dynamics under deterministic load. Many different types of mathematical models for internal excitations have been proposed. Generally, the models of internal excitations can be classified into four main groups. The following paragraph gives an introduction to the category of internal excitations.

The first group consists of linear time-invariant (LTI) models, and an extensive review was given by Ozguven and Houser [13]. In the second group, linear time-varying (LTV) mesh stiffness is included [40] [41]. Accordingly, a geared system is excited parametrically by static transmission induced by kinematical errors and tooth deflections. The third group takes nonlinear gear backlash and time-invariant average mesh stiffness (NTI) [42] [43] into account. It should be noted that backlash is bounded due to design or manufacturing error. In the last group, both gear backlash and mesh stiffness variation are considered simultaneously as nonlinear time-varying (NTV). This group of models is mainly used in the study of multi-parameters nonlinear vibration.

Compared to the many studies on the gear deterministic internal excitations under deterministic load, the investigations on the gear deterministic internal excitations under stochastic load are limited. Yang [44] investigated a gear dynamic model under Gaussian white noise and assumed constant mesh stiffness and constant damping coefficient. Recently, Wen and Yang [5] developed a gear pair's dynamic model considering constant damping coefficient, time-varying mesh stiffness, and backlash. They considered time-varying mesh stiffness as a square wave function and backlash as in Eq. (1.3).

Many internal factors for a gear system have random variations and greatly affect the system's dynamic characteristics. Lu et al. [45] studied the influence of stochastic perturbations of damping ratio and backlash on dynamic behavior of gear systems. Stochastic perturbations in [45] referred to a combination of a constant and a Gaussian white noise. Handschuh [46] and Inalpolat et at. [47] investigated the impact of random spacing errors on transmission error and root stresses of a spur gear pair. This transmission error function assumes an infinite number of harmonics with normally distributed indexing errors. However, some internal factors (e.g., friction), which affects gear systems significantly under stochastic load, have not been studied.

Friction has been identified as a cause of vibration, noise, and failure of a gear system under deterministic load [48]. Many researchers have reported the effects of friction on gear dynamics under deterministic excitation. A detailed review of friction prediction in gear teeth was conducted by Martin [49], which stated that the values of coefficients of friction could be predicted reasonably according to various lubrication theories. Yang et al. [50] proposed a model of a spur gear pair considering friction, Hertzian damping, and bending under deterministic load. Iida et al. [51] investigated vibrational characteristics of a gear system affected by friction under deterministic load. Krupka et al. [52] studied the effects of surface lubrication film on vibrational characteristics of a gear system. He et al. [53] reported several sliding friction models in spur gear dynamics to analyze friction forces. Guilbault et al. [54] studied the effects of nonlinear damping in cylindrical gear dynamic modeling, which integrated the friction contribution. Ericson [55] applied FEM to study the stiffness of a gear pair under various deterministic loads.

However, friction has not been considered in a gear pair's dynamic model under stochastic load. Friction's effects on gear dynamic model under stochastic load have not been investigated. Though the coupling of friction and stochastic load adds difficulty to the solving process, the dynamic characteristics (such as periodicity, stability, and dispersion) are useful indicators in analyzing gear systems' health condition. For two factors which have independent effects labeled as 1, their effects on the system satisfy $1 + 1 = 2$. In classical mechanics, coupling is a connection between two nonlinear factors which leads to a result as $1 + 1 \neq 2$.

Friction is considered in Chapter 2 to study its effects on gear dynamic characteristics with stochastic load. The stochastic load is assumed to be Gaussian white noise or Gaussian diffusion process. The two kinds of load profiles have their own applicable situations. Two load profiles together with the consideration of friction will be studied and compared in Chapter 2.

1.2.3 Stochastic driving speed in gear model

Except load, the fluctuation of driving speed is another external excitation. The causes of the fluctuation of driving speed could be engine [56] or natural force (e.g., wind [57]) as shown in Fig. 1.21. Driving speed fluctuation is found as a common source of noises in some engines, such as, four stroke four cylinder inline diesel engine [24]. For a combustion engine, many forces arise due to gas pressure, bore, stroke of engine, and inertia of moving parts during the power stroke. The engine does generate driving speed fluctuations and torque fluctuation.

A few studies investigated the influence of driving speed caused by engine in gear systems. Qiu et al. [58] considered the influence of input velocity on

Fig. 1.21: Drivers of a gear system (a) engine (b) wind

the time-varying mesh stiffness and introduced a velocity modulated stiffness model. Liu et al. [26] investigated the driving speed in a spur gear system under deterministic load. They concluded that the driving speed was a non-negligible source of instability in gear systems.

Most previous work usually modelled the driving speed to be deterministic. However, deterministic assumption of driving speed may not be proper at some conditions. Some researchers modelled the randomness of the driving speed. Tutak and Jamrozik [59] studied the flow field turbulence in the combustion chamber and modelled the crankshaft velocity (performed a conversion between reciprocating motion and rotational motion) randomness of internal combustion engine. Pruvost et al. [60] proposed an improved filter to separate the noise (e.g., random part of rotation speed signal) and validated their designed filter in the diesel combustion engine experiment. Randall [61] summarized kinds of methods to deal with the random speed fluctuation in combustion engine. Except the deterministic fluctuation in the driving speed, the randomness raises our attention and the coupled effects of stochastic driving speed and stochastic load are worth to be investigated.

However, the gear model under stochastic load considering both friction and driving speed has not been evaluated. The effects of driving speed, friction, and load on the dynamic characteristics have not been studied. Neither deterministic nor stochastic driving speed has been considered for modeling a gear system with stochastic load. In Chapter 3, the driving speed is taken into consideration for a pair of spur gears under stochastic load. Two cases of driving speed (deterministic and stochastic) are studied and their effects on the dynamic characteristics are compared. The influences of driving speed on dynamic characteristics of gear systems are investigated, which can be referred to Chapter 3.

1.2.4 Approaches for solving gear dynamic model

Given a gear pair model, how to solve the model is another significant research topic. For an ODE like Eq. (1.1), it is usually solved by analytical or numerical methods. Runge-Kutta method [5] [44] [62] is a numerical method and is commonly used for solving ODEs without stochastic terms. The toolbox in Matlab for this approach is known as "ode".

Solving a gear dynamic model with stochastic excitations (internal or external or both of them) is more complicated than that under deterministic excitations. The gear model becomes a stochastic differential equation (SDE). There are different approaches to solve gear dynamic models with stochastic excitations involved. Computation efficiency and accuracy are two major reasons for choosing a proper approach. Taking the results by MC method as a standard, computation efficiency refers to the time saved compared to MC method and the accuracy refers to the relative errors compared to MC method.

As introduced in Section 1.1.5, statistic model, interval model, and fuzzy model have been used to describe the randomness in gear systems [2]. Based on available data, the internal or external excitations' probability distribution can be estimated and a statistic model can be applied. Thanks to the well developed probabilistic theory, statistical method is the most commonly used method and it has advantages in simulation and mathematical description than interval method and fuzzy method. Our work focuses on using statistic method to model the randomness in both internal and external excitations.

In Section 1.2.4.1, statistical methods related to solving an SDE will be reviewed. The solution types of an SDE can be divided into analytical solution and numerical solution. Since the analytical solution has computation advantage, we will focus on analytical solution of gear dynamic models. Analytical solution for a gear model with one additional stochastic internal excitation will be introduced in Section 1.2.4.2.

1.2.4.1 Summary of solving approaches

Statistical methods are usually used to obtain the responses of a gear system under stochastic load. Statistical methods include statistical linearization method [63], stochastic averaging approach [64], MC method [65], Path integration method (or cell mapping) [66] [67], statistical Newmark method [68], and so on. In order to get the responses of a gear model by statistical methods, researchers usually focus on getting the statistical characteristics of the responses, such as, mean, variance, and PDF [69]. PI method and stochastic averaging method give analytical solutions while statistical linearization method, MC method, statistical Newmark method are numerical methods. Wei et al. [2] reviewed the main ideas and statistical characteristics of each statistical method as shown in Table 1.1. In the table, number "1" means the worst performance while number "5" refers to the best performance in accuracy and efficiency.

Table 1.1: Typical statistical methods and their performance [2]

Name	Accuracy	Efficiency
Statistical linearization method	1	4
Stochastic averaging method	3	2
Statistical Newmark method	2	3
Runge-Kutta & MC	5	1
Path integration method	4	5

Statistical linearization method [63] approximates the original nonlinear system to a similar linear system with the minimum error, which provides the variance of responses. It has the lowest accuracy and second fastest calculation speed among the mentioned five methods.

Stochastic averaging method [64] transforms the time varying parameters to time invariant parameters with averaging method and derives an approximate analytical solution, which gives PDF to a small damping nonlinear system.

Statistical Newmark method [68] utilizes the recursive equation of each discrete time point to derive mean and variance of responses. Both of the stochastic averaging method and statistical Newmark method have the medium performance in both accuracy and efficiency.

Runge-Kutta method obtains single numerical solution of a gear dynamic model for each time. Then, MC method uses numerical simulation to generate a number of response samples and then provides a high accuracy PDF. Let MC method denote the Runge-Kutta and MC method. MC method has the highest accuracy and slowest calculation speed.

PI method assumes transition PDF within a short time interval as Gaussian distribution and gives the analytical expression of the response PDF. PI method [66] [67] has the fastest calculation speed and its accuracy is relatively high if the load follows Gaussian distribution. If the time step length or the space discretion does not satisfy some relationship determined by drift factor and diffusion factor, PI method has a low accuracy.

It is known that analytical solutions have advantages in calculation efficiency compared with numerical solutions. In the following section, we will focus on how to obtain the analytical solution of a gear system considering stochastic internal and external excitations as reported by other researchers. In addition, the problems that have not been addressed or solved will be illustrated briefly.

1.2.4.2 Analytical approach for single stochastic internal factors

Researchers have explored the analytical solution to a gear dynamic model under stochastic load. Sato [70] studied the analytical solution of a gear system under random load with consideration of transmission error and TVMS. Naess et al. [67] derived the analytical solution to a gear system considering constant stiffness, constant damping coefficient, and backlash under the excitation of Gaussian white noise. Wen et al. [5] obtained the analytical solution of the gear system considering constant damping coefficient, TVMS, and backlash under the combination of deterministic load and stochastic load including Gaussian white noise.

Current methods have provided analytical solutions to a gear model under stochastic load and with other factors being deterministic that may include TVMS, backlash, damping ratio, and so on. However, they have not given analytical solutions to a gear model under stochastic load and with at least one of the internal factors being stochastic [71]. Thus, it is necessary to develop a method to derive the analytical solution to such a model.

Among the approaches reviewed in Section 1.2.4.1, PI method gives an analytical solution to the gear dynamic model. The analytical solution is in the analytical form of PDF. In the applications such as fatigue prediction and reliability analysis, and accurate PDF is needed [36]. PI method is a practical approach for capturing the PDF evolution in time. PI method is accurate when Gaussian white noise or Poisson white noise is used as noise terms [72].

Sun and Hsu [73] proposed PI method by assuming that the transition PDF within a short time was a Gaussian diffusion process. Köylüolu et al. [72] applied PI method to study a single degree of freedom oscillators subject to Gaussian and Poisson random excitations. By assuming that the conditional PDF is Gaussian, the PDF of the response can be obtained by integration in a finite phase plane space [36].

When at least one of the internal factors is stochastic, PI method cannot deal with the dynamic model under stochastic load directly [74]. On the other hand, modifying PI method to solve such a model will lose some accuracy. A method based on PI method and supervised learning will be proposed. Thus, obtaining such analytical solution with consideration of both accuracy and efficiency is to be addressed in Chapter 4. The results can be used to provide approximate analytical solution of the model in topic 1 (Chapter 2) with one of the internal excitations, friction, to be stochastic. Note that the proposed method in topic 3 (Chapter 4) is not limited to the model in topic 1 (Chapter 2). It can be used to solve the gear model with any one stochastic internal excitation under stochastic load. However, the proposed method in topic 3 (Chapter 4) cannot solve the model in topic 2 (Chapter 3) with two external stochastic excitations. Future research is needed to develop efficient approaches to solve multiple external stochastic excitations involved problem.

1.3 Objective and outline

Based on the reviews summarized in Section 1.2, three main issues have been identified that will be addressed in this thesis. The overall objectives are to investigate the dynamics of a spur gear pair considering different stochastic internal and external excitations via LPM and provide corresponding solutions either numerically or analytically. Fig. 1.22 summarizes the internal and external excitations with the challenges when considering them.

Our basic assumptions in this thesis are listed as follows:

- Both of the gears are involute spur gears.
- The transmission error, influence from the shaft, and bearing effects are not considered or they are assumed perfect or constant.
- The whole system is simplified as a single degree of freedom (SDOF) lumped mass model.
- The gear tooth is treated as a cantilever beam.
- The gear mesh interface is modeled as a spring-damper system.

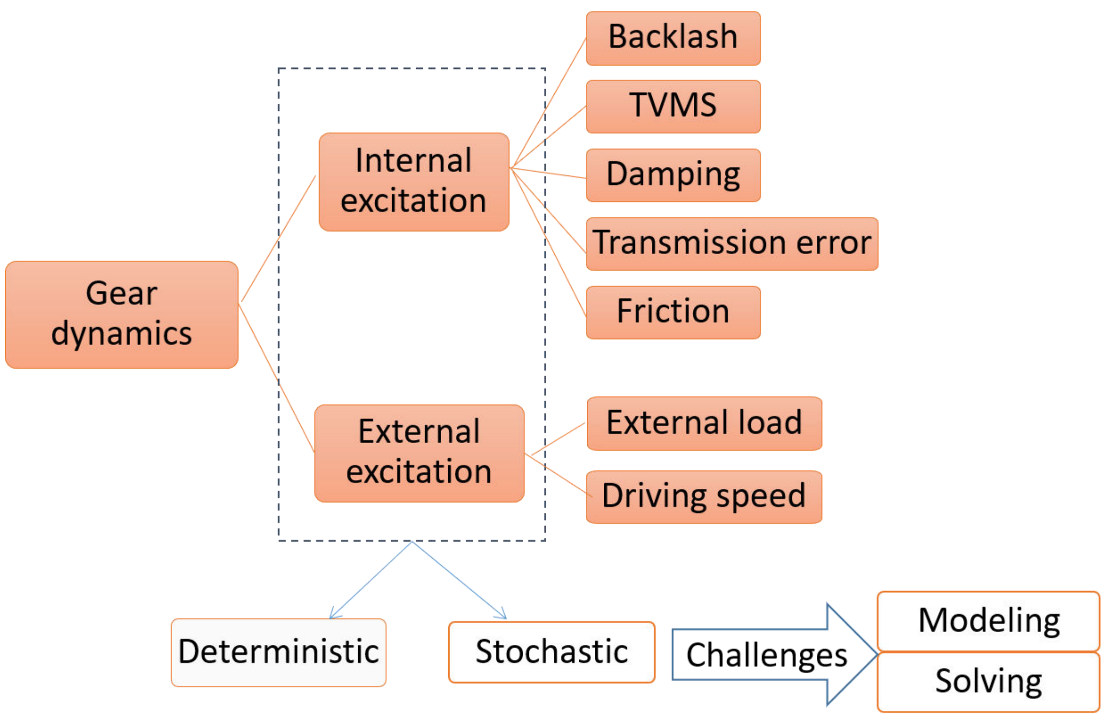

Fig. 1.22: Excitations and the challenges involved

According to the state of the art in dealing with gear systems' stochastic excitations, the three proposed research topics are:

- Build an improved dynamic model considering both friction and stochastic load
- Develop an improved dynamic model considering driving speed and s-tochastic load
- Provide a method for solving the gear model with one stochastic internal excitation and stochastic load

The structure of the thesis and the relationship among the three topics are given in Fig. 1.23. Topic 1 proposes an improved gear model under stochastic load and takes one more internal excitation, friction, into consideration. Then, developing from topic 1, one more external excitation (driving speed) has been considered in topic 2. There are three stochastic excitation (friction, load, and driving speed) in topic 2 while other excitations are deterministic. Topic 3 provides an approximate analytical solution to the model with one of the internal factors treated to be stochastic under stochastic load, e.g., the model in topic 1. This stochastic internal factor could be TVMS, backlash, damping ratio, or friction, etc. But only one of them can be stochastic.

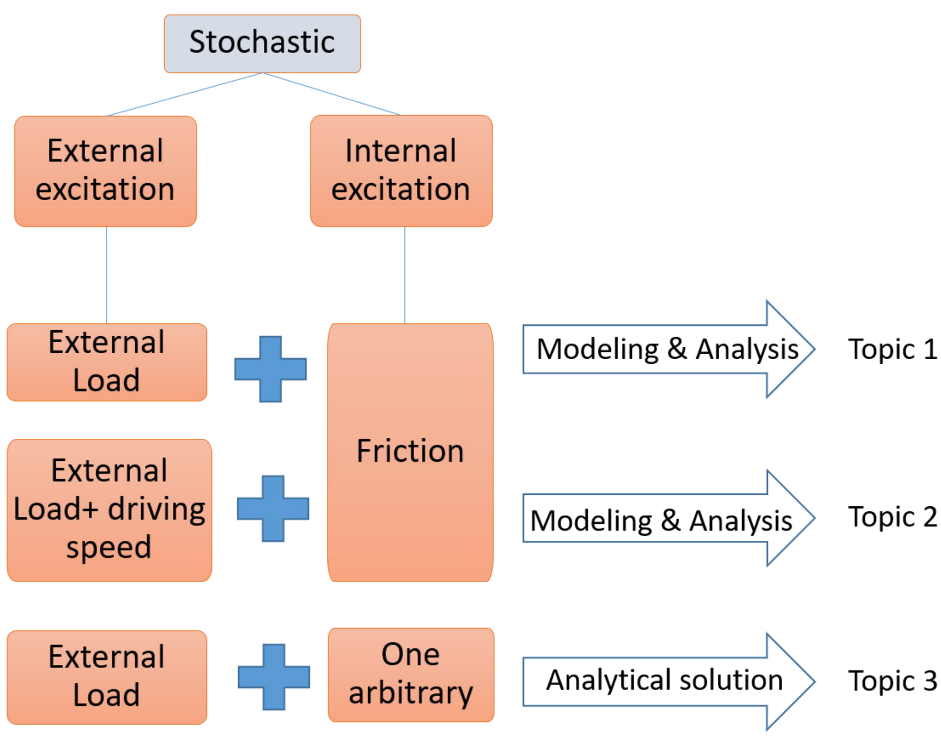

Fig. 1.23: Structure of the thesis

In topic 1, a gear stochastic dynamic model for a spur gear pair considering TVMS, gear mesh damping, backlash, friction, and stochastic load is established. The dynamic responses of this model are investigated using numerical simulation and compared with previous work. Two cases with different load profiles are studied and compared. For case 1, load is modeled as Gaussian white noise with a certain friction coefficient ($\mu = 0.04$). For case 2, load is modeled as Gaussian diffusion process with five friction coefficient values ($\mu = \{0.01,\ 0.02,\ 0.03, 0.04, 0.05\}$).

In topic 2, a gear stochastic dynamic model for a spur gear pair considering TVMS, gear mesh damping, backlash, friction, stochastic driving speed, and stochastic load is established. Driving speed is the first time to be taken into consideration under stochastic external excitations. Two profiles of driving speed (deterministic and stochastic) are studied and compared. The dynamic responses of this model are investigated using numerical simulation and compared with previous works.

Topic 3 proposes an approximate analytical solution to a spur gear dynamic model with stochastic load and one stochastic internal factor. The analytical solution is derived using PI method and then updated using a supervised learning algorithm. A case study taking friction as an example of the single stochastic internal element is used to validate our proposed method. The dynamic responses of this model are investigated using our proposed method and then compared with MC results.

The remaining parts of this thesis are structured as follows. Chapter 2, Chapter 3, and Chapter 4 give details of the three research topics, respectively. The summary and future work are presented in Chapter 5.

This thesis is written using the paper based template which meets the formatting requirements of University of Alberta.

2

Effects of Friction and Stochastic Load on Transient Characteristics

The dynamic modeling of gear systems under deterministic excitations has been widely investigated in existing studies. However, the existence of randomness in external load of geared systems is widely known. Stochastic load induces more vibration and noise than deterministic load. To better demonstrate gear systems, a nonlinear dynamic model is developed considering time-varying mesh stiffness (TVMS), backlash, sliding friction, and stochastic external load in this chapter[1]. Friction is the first time introduced in a spur gear pair nonlinear dynamic model under stochastic load. Monte Carlo (MC) simulation is applied to analyze the transient characteristics focusing on the effects caused by stochastic load and friction. The results show that stochastic load makes the system have a longer duration in the transient state and lower transient stability compared with the results under deterministic load. Friction causes higher dispersion of the gear pair's relative angular displacement in the transient state while lower dispersion in the steady state compared with the case without considering friction. In addition, the system's transient stability and the response's dispersion vary with the increase

[1]The following two papers based on the work of this chapter have been published.
Y. Fang, X. Liang, and M. J. Zuo, "Effect of sliding friction on transient characteristics of a gear transmission under random loading," in *Proceedings of 2017 IEEE International Conference on Systems, Man, and Cybernetics (SMC)*. IEEE, Banff, Canada, Oct. 5-8, 2017, pp. 2551–2555.
Y. Fang, X. Liang, and M. J. Zuo, "Effects of friction and stochastic load on transient characteristics of a spur gear pair," *Nonlinear Dynamics*, vol. 93, no. 2, pp. 599–609, Jul. 2018.

of friction coefficient. The friction coefficients that cause the lowest transient stability and highest dispersion of relative angular displacement are identified.

2.1 Introduction

Gear systems are widely used in modern power transmission systems. Many studies have been performed on dynamic modelling of spur gear transmission systems [12]. The dynamic characteristics of a gear system are affected by internal and external excitations [27]. Internal excitations include backlash [75], TVMS [76], transmission error [77] [78], and so on. Many studies focused on the investigation of internal excitations while only a few did investigation on external excitations (e.g., varying load [79]).

Gear dynamics under deterministic load has been explored for decades. The models and approaches used in gear dynamics are reviewed by Wang et al. [7]. Khabou et al. [24] investigated the dynamic behavior of a single stage spur gear system under deterministic load and concluded that adequate external load should be chosen to reduce vibration. Shao and Chen [27] proposed an analytical model of a spur gear pair with tooth root crack under deterministic load. These existing models reveal the mechanism of gear systems and contribute to the understanding of gear dynamics. However, they restricted the gear dynamics problems in the deterministic domain, and thus, it reduces the difficulties in obtaining dynamic responses of a gear system.

A few studies investigated randomness of external load in gear system analysis. Utagawa and Harada [30] investigated the influence of randomness on dynamic loads for high speed gears. Tobe et al. [31] investigated stochastic load, which was treated as Gaussian white noise. Their results were validated by comparing with the experiment results reported in [37]. Ref. [37] was one of the earliest reported studies in gear stochastic dynamics and the randomness of external load was examined via lab experiments. Wang et al. [38] studied a wind turbine generator suffering from stochastic wind with varying directions and loads. The extensions of the models from deterministic domain to stochastic domain lead to more realistic representation of real gear systems.

Patil et al. [21] analyzed the effects of wind stochastic energy variation on gear system's steady and transient states. Drago [22] studied the influence of stochastic start-up load to the potential failure of gears. Gear vibrations and noises are mainly induced by load variation at gear transient state [24]. It is necessary to consider the stochastic external load in gear system modelling especially at transient state.

Researchers have made some improvements in modelling gear dynamics under stochastic load. Wang and Zhang [32] considered the speed-dependent stochastic errors in the modelled one-dimensional spur gear pair. Theodossiades and Natsiavas [39] introduced the gear systems with periodic stiffness and backlash and they considered the transmission errors as static errors. Yang [44] investigated a gear multi-mesh dynamic model under Gaussian white noise while with constant mesh stiffness and damping coefficient. Recently, Wen and Yang [5] developed a gear pair's dynamic model considering constant damping coefficient, backlash and TVMS. It was solved by numerical and analytical methods.

Friction has been identified as a cause of vibration, noise and failure of gear systems [48]. Many researchers have reported the effects of friction on gear dynamics under deterministic excitation. Martin [49] conducted a detailed review of friction prediction in gear teeth and concluded that the values of coefficients of friction could be predicted reasonably according to various lubrication theories. Yang et al. [50] proposed a model of a spur gear pair considering friction, Hertzian damping and bending under deterministic load. He et al. [80] investigated vibrational characteristics of a gear system affected by friction under deterministic load. Krupka et al. [52] studied the effects of surface lubrication film on vibrational characteristics under transient conditions. He et al. [53] reported several sliding friction models in spur gear dynamics to analyze friction forces. Guilbault et al. [81] studied the modeling and monitoring of tooth fillet crack growth under a spur gear set, which integrated the friction contribution.

Friction has not been considered for modelling a gear system with stochastic load. In this chapter, friction is taken into consideration for a pair of spur gears under stochastic load. Transient characteristics of this gear system are studied. The influences of stochastic load and surface sliding friction on gear system stability are investigated.

The remaining parts of this chapter are organized as follows. In Section 2.2, the proposed stochastic dynamic model for a spur gear pair is described. Section 2.3 validates the proposed model by comparing it to reported work. Section 2.4 illustrates the effects of friction coefficient and stochastic load (modelled as Gaussian white noise) on gear transient characteristics. Section 2.5 investigates the effects on gear transient characteristics by friction and stochastic load (modelled as Gaussian diffusion process). Section 2.6 draws the conclusion.

2.2 Nonlinear stochastic gear dynamic model considering friction

In this section, a single degree of freedom (SDOF) nonlinear dynamic model of a spur gear pair is developed based on the model reported in [50]. TVMS, backlash, sliding friction and stochastic load are considered in our model. The model of the geared system is shown in Fig. 1.9. Only rotation of the gear is considered in this model. Fig. 2.1 gives the TVMS used in this study, which is simpler comparing to the TVMS model shown in Fig. 1.10. In order to investigate the influence of friction in this chapter, we keep everything else the same as [5]. Thus, we adopt the same TVMS profile with that of [5]. The whole derivation process for Eq. (2.1) and Eq. (2.2) is based on [50] and no new contributions are claimed in this part.

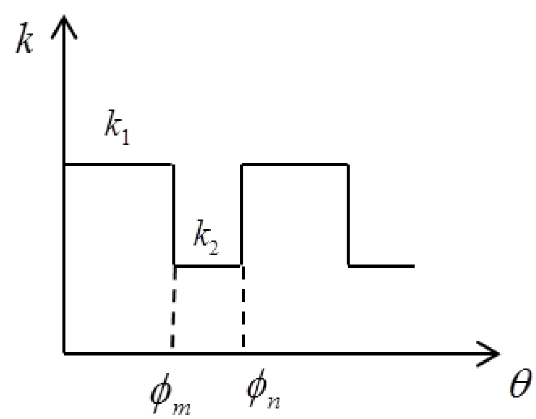

Fig. 2.1: Time varying mesh stiffness [5]

The equations of the motion for the system given in Fig. 1.9 can be expressed as

$$\mathrm{J}_1\ddot{\theta}_1 = \mathrm{T}_1 - (F+G)R_{b1} - F_f X_1 \tag{2.1}$$

$$\mathrm{J}_2\ddot{\theta}_2 = \mathrm{T}_2 + (F+G)R_{b2} + F_f(l_p - X_1) \tag{2.2}$$

where J_i, T_i, $\ddot{\theta}_i$, and R_{bi} are the moment of inertia, external torque, angular acceleration, and the radius of the base circle of gear i $(i = 1, 2)$, respectively, F is the total elastic force between the contact teeth shown in Fig. 2.2, G is the damping force, F_f is the sliding friction, X_1 denotes the distance between the tangent point C_1 on the action line and the force contact point B_1, and l_p is the length of the action line from point of C_1 for gear 1 to the corresponsing point C_2 for gear 2. Since the contact point and the direction of the normal force would change, the direction of the friction force also changes. Note that the direction of the friction force is perpendicular to the normal force and opposite to the tooth sliding direction. For more details, please refer to [50].

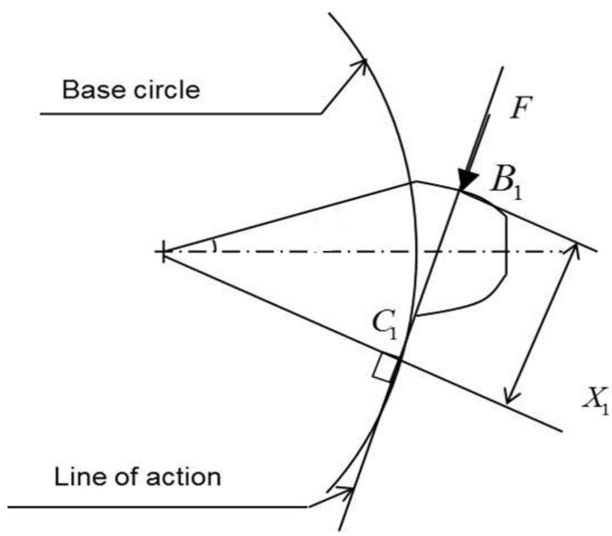

Fig. 2.2: Elastic force on the tooth of gear 1

Multiply Eq. (2.1) by R_{b1}/J_1 and Eq. (2.2) by R_{b2}/J_2, and then subtract the second from the first one. We can get the expression shown in Eq. (2.3).

$$R_{b1}\ddot{\theta}_1 - R_{b2}\ddot{\theta}_2 = \left(\frac{T_1 R_{b1}}{J_1} - \frac{T_2 R_{b2}}{J_2}\right) - (F+G)\left(\frac{R_{b1}^2}{J_1} + \frac{R_{b2}^2}{J_2}\right) - F_f\left[\frac{X_1 R_{b1}}{J_1} + \frac{(l_p - X_1)R_{b2}}{J_2}\right] \tag{2.3}$$

Let $\delta = R_{b1}\theta_1 - R_{b2}\theta_2$. The gear pair's equation is reduced to an SDOF nonlinear system with TVMS (i.e., Eq. (2.18)), backlash (i.e., Eq. (2.17)), and friction (i.e., Eq. (2.5)). Thus, we have

$$\ddot{\delta} = \Phi - \left(K\delta + \alpha\delta\dot{\delta}\right) q_3 - \mu\left(K\delta + \alpha\delta\dot{\delta}\right)(q_1 + \theta_1 q_2) \tag{2.4}$$

where

$$F_f = \mu(F+G) \tag{2.5}$$

$$l_p = (R_{b1} + R_{b2}) \sin \alpha_0 \tag{2.6}$$

$$X_1 = (a_0 + \theta_1 + \theta_{b1}) R_{b1} \tag{2.7}$$

$$\theta_{b1} = \frac{\pi}{2Z_1} + \tan \alpha - \alpha \tag{2.8}$$

$$F = Kg(\delta) \tag{2.9}$$

$$G = \alpha \delta \dot{\delta} \tag{2.10}$$

$$\Phi = \frac{T_1 R_{b1}}{J_1} - \frac{T_2 R_{b2}}{J_2} \tag{2.11}$$

$$q_1 = \alpha_0 \left(\frac{R_{b1}^2}{J_1} + \frac{R_{b2}^2}{J_2} \right) + \theta_{b1} \left(\frac{R_{b1}^2}{J_1} - \frac{R_{b1} R_{b2}}{J_2} \right) \tag{2.12}$$

$$q_2 = \frac{R_{b1}^2}{J_1} - \frac{R_{b1} R_{b2}}{J_2} \tag{2.13}$$

$$q_3 = \frac{R_{b1}^2}{J_1} + \frac{R_{b2}^2}{J_2} \tag{2.14}$$

In Eqs. 2.5–2.14, θ_{b1} is half of the tooth angle (see Fig. 2.2), α_0 denotes the pressure angle, K is the effective mesh stiffness, δ gives the relative angular displacement of the gear pair, α is the damping coefficient, Φ represents the equivalent external excitation, μ is the friction coefficient, and q_1, q_2, and q_3 denote polynomials as shown in Eqs. 2.12–2.14, respectively.

Rewriting Eq. (2.4), a second order ordinary differential equation (ODE) is obtained as

$$\ddot{\delta} + Q(\theta_1) g(\delta) \alpha \dot{\delta} + Q(\theta_1) K(\theta_1) g(\delta) = \Phi \tag{2.15}$$

The expressions of $Q(\theta_1)$, $g(\delta)$, and $K(\theta)$ are given as following.

$$Q(\theta_1) = q_3 + \mu(q_1 + \theta_1 q_2) \tag{2.16}$$

$$g(\delta) = \begin{cases} \delta - b, & \delta > b \\ 0, & -b \le \delta \le b \\ \delta + b, & \delta < -b \end{cases} \tag{2.17}$$

$$K(\theta) = \begin{cases} k_1 & \multirow{2}{*}{for} \quad (n-1)\phi_n \le \theta < (n-1)\phi_n + \phi_m \\ k_2 & \quad (n-1)\phi_n + \phi_m \le \theta < n\phi_n \end{cases} \tag{2.18}$$

where $Q(\theta_1)$ is a function of θ_1, $g(\delta)$ denotes the function of backlash (shown in Fig. 2.3), ϕ_n and ϕ_m represent gear rotation angles during a mesh circle and the single tooth pair mesh duration in a mesh circle, respectively. We assume that the gear system is in a closed box with adequate lubrication oil. Also, the lubrication condition affects the friction coefficient μ. Though there is this influencing effect, in this thesis, it has been actually assumed that the lubrication condition is perfect and no lubrication effects on μ are considered in this thesis.

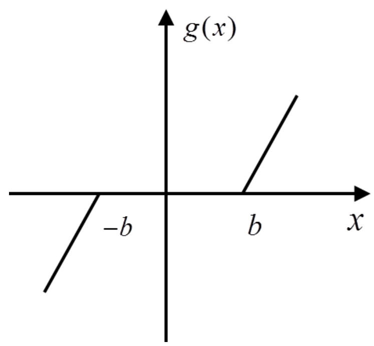

Fig. 2.3: Function of backlash [5]

The classic way to model the external load is using Gaussian white noise. In Section 2.3, the excitation Φ is modeled as a combination of a constant deterministic part Φ_0 , a deterministic periodical part Φ_1, and a random part $\xi(t)$.

$$\Phi(t) = \Phi_0 + \Phi_1 \cos(\omega t) + \xi(t) \tag{2.19}$$

A Gaussian diffusion process is used to simulate the equivalent external excitation Φ. It is the integration of Gaussian white noise. It is assumed that Φ can be approximated by an Itô stochastic differential equation (SDE) [82], which is given as the following form [33]:

$$d\Phi(t) = \lambda dt + \sigma dW(t) \tag{2.20}$$

where λ is the drift scalar, σ is the diffusion scalar, and $W(t)$ is a standard Wiener process. In Section 2.5, Eq. (2.20) is adopted to model external load.

Recently, a stochastic dynamic model was investigated in [5]. They considered the excitation as a combination of constant deterministic part f_0, a deterministic periodically changing part $f_1 \cos(\Omega_m t)$, and Gaussian white noise $\xi(t)$. Their nonlinear system equation is given as follows:

$$\ddot{\delta} + \alpha\dot{\delta} + K(\theta_1)g(\delta)=f_0 + f_1 \cos(\Omega_m t) + \xi(t) \tag{2.21}$$

In the above equation, f_0, f_1, and Ω_m are constant. Comparing Eq. (2.15) with Eq. (2.21), the damping coefficient in [44] is a constant α, while the $Q(\theta_1)g(\delta)\alpha$ in our model is dependent on δ. Expand $Q(\theta_1)g(\delta)\alpha$ and all relevant parameters are shown:

$$Q(\theta_1)g(\delta)\alpha = [q_3 + \mu(q_1 + \theta_1 q_2)]\, g(\delta)\alpha \tag{2.22}$$

where q_1, q_2, q_3, $g(\delta)$ and α are deterministic. Due to stochastic external load, θ_1 is a stochastic variable. Since $g(\delta)$ is nonlinear and $Q(\theta_1)$ is stochastic, there is no doubt that our proposed model in Eq. (2.4) reflects more nonlinearity than the existing model and is more difficult to solve.

2.3 Validation of the proposed model

The validation is done by comparing with the result reported in [75], which proposed a model of a spur gear pair under deterministic load considering TVMS and backlash. TVMS was modeled the same way as shown in Fig. 2.1.

The gear pair parameters used in [75] will be also used in our proposed model (see Table 2.1).

Table 2.1: Gear pair parameters

Density	$\rho = 7.8 \times 10^{-6} Kg/mm^3$
Young's modulus	$E_1 = E_2 = 2.068 \times 10^5 N/mm^2$
Poisson ratio	$\nu_1 = \nu_2 = 0.03$
Radius of gears	$r_1 = 20mm, r_2 = 80mm$
Pressure angle	$\alpha_0 = 20°$
Number of teeth	$Z_1 = 20, Z_2 = 80$
Thickness of gear	$L = 10mm$
Backlash	$b = 0.05mm$

If we assume that the friction coefficient equals to 0.04, Eq. (2.15) is the same as the model in [50]. Angular displacements of the two gears during free vibration

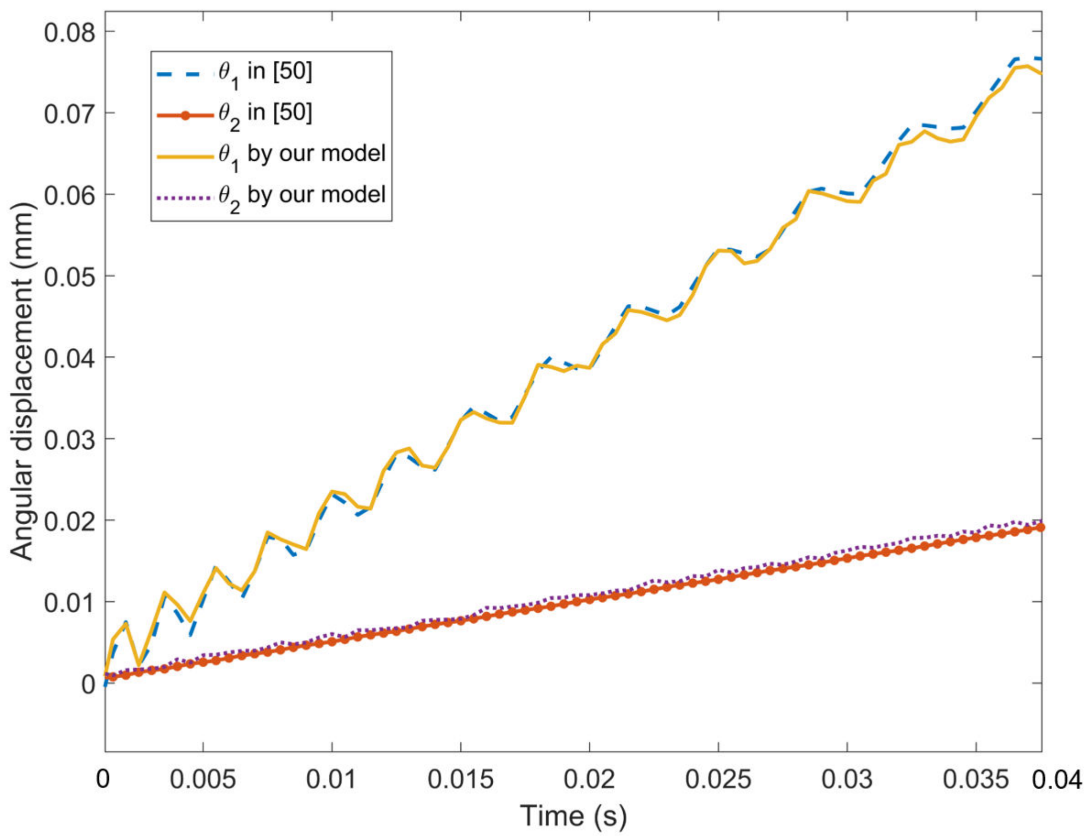

Fig. 2.4: Angular displacement comparison

are solved here. Ref. [50]'s results and our results are given in Fig. 2.4. Compared to [50], our results (angular displacements) are almost the same in both magnitude and tendency.

Although this validation is conducted under deterministic load, it still supports the correctness of our model to some degree. And the model can be extended to stochastic external excitation to explore the characteristics in stochastic gear dynamics.

2.4 Dynamic characteristics analysis while load is modelled as Gaussian white noise

To analyze the dynamic characteristics of the proposed model while load is modeled as Gaussian white noise, this section gives the numerical simulation results. The main objective of this section is to investigate the friction and stochastic load effects on system's transient characteristics.

Numerical solutions to the equations of the motion are obtained with Matlab using "ode15s". All the stochastic load in this section are using a certain Gaussian white noise model as given in Table 2.2. The stochastic load is modeled in Eq. (2.19) and a sample of the load is shown in Fig. 2.5.

Table 2.2: The scenario of the load in Eq. (2.19)

Φ_0	2×10^4
Φ_1	5×10^3
Type of $\xi(t = t_1)$	Normal distribution
Mean of $\xi(t = t_1)$	0
Standard deviation of $\xi(t = t_1)$	5×10^3

Section 2.4.1 will study the stochastic load effects on transient characteristics, such as vibration. Section 2.4.2 will study the friction coefficient effects on transient characteristic, namely, dispersion.

2.4.1 Load effects on dynamic characteristics

This section shows the effects of stochastic and deterministic load on a gear system's dynamic characteristics, respectively. According to [49], the friction coefficient in a gear system varies from 0.02 to 0.08. In this section, we fix the friction coefficient at 0.04 to illustrate the load effects on gear dynamic characteristics.

Fig. 2.6 and Fig. 2.7 present the relative angular displacement δ and the contact

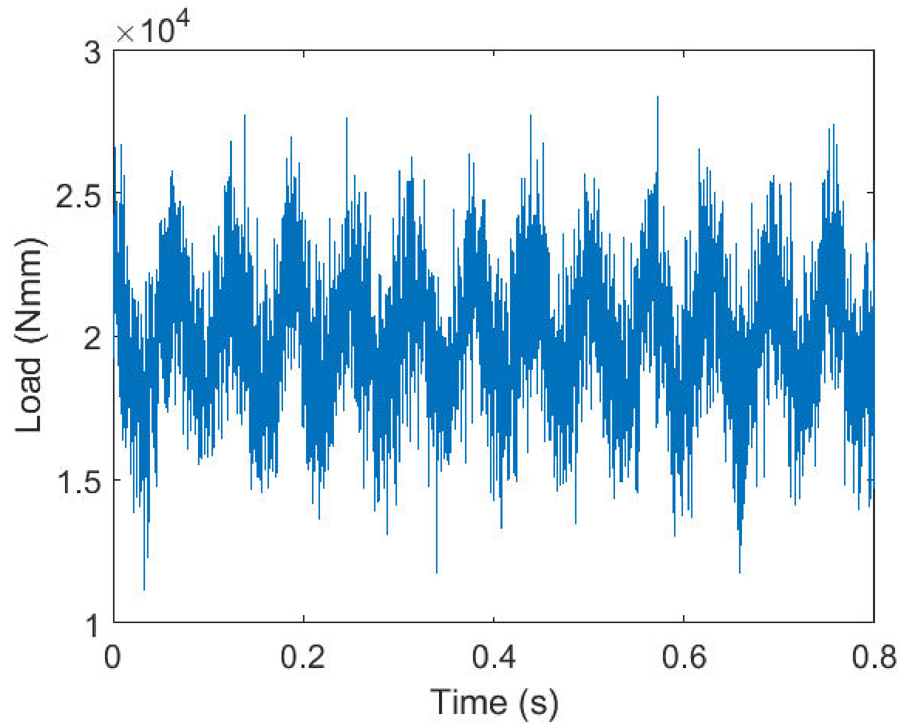

Fig. 2.5: A sample of the load

force of the gear pair under stochastic and deterministic load.

As time goes, when the relative angular displacement becomes stable, the system is considered to be in the steady state. Fig. 2.6 shows that the system used about 0.6 seconds (s) to reach the steady state under the stochastic load. Under the deterministic load, the system only costed 0.3 s to reach the steady state. Therefore, the system with stochastic load uses much longer time to reach steady state than that with deterministic load.

Fig. 2.7 shows the contact force fluctuation under deterministic and stochastic load. In the transient state ($t < 0.3\ s$), the contact force has similar fluctuation level under the two load conditions. However, in the steady state ($t > 0.6\ s$), the fluctuation level under stochastic load is higher than that under deterministic load.

In the steady state, system's vibration under stochastic load is higher than that under deterministic load. The possible reason for this phenomenon is that the higher variation of magnitude in load (caused by the stochastic term in the external load) leads to a longer adjustment time for a gear system to approach to the steady

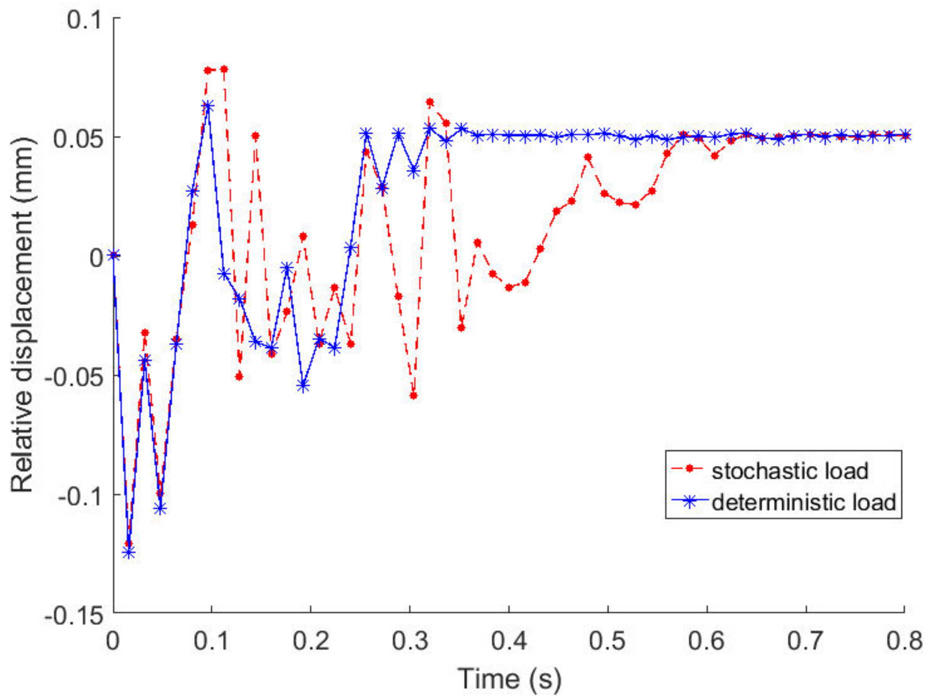

Fig. 2.6: Relative angular displacement under two types of load

state. Hence, we should pay more attention to the health monitoring of gearboxes when the external load is stochastic.

2.4.2 Friction effects on dynamic characteristics

This section evaluates the influence of friction on the dynamic characteristics of the gear system under stochastic load. Two cases ($\mu = 0$ and $\mu = 0.04$) are illustrated and compared, where μ is friction coefficient.

From Fig. 2.8, we can see that the system without friction took about 0.2 s to reach the steady state while the system with friction used about 0.6 s to reach the steady state. Therefore, the transient state will be longer if the system has friction. In addition, the system with friction has a larger fluctuation of relative angular displacement in the transient state ($t < 0.2s$). The friction affects the time duration of the transient state and also the strength of the vibration in transient state.

Probabilistic distributions have been used to characterize stochastic responses [83] [84]. We adopt the MC method to obtain a number of responses. In the following part of this chapter, the PDFs of the relative angular displacement of

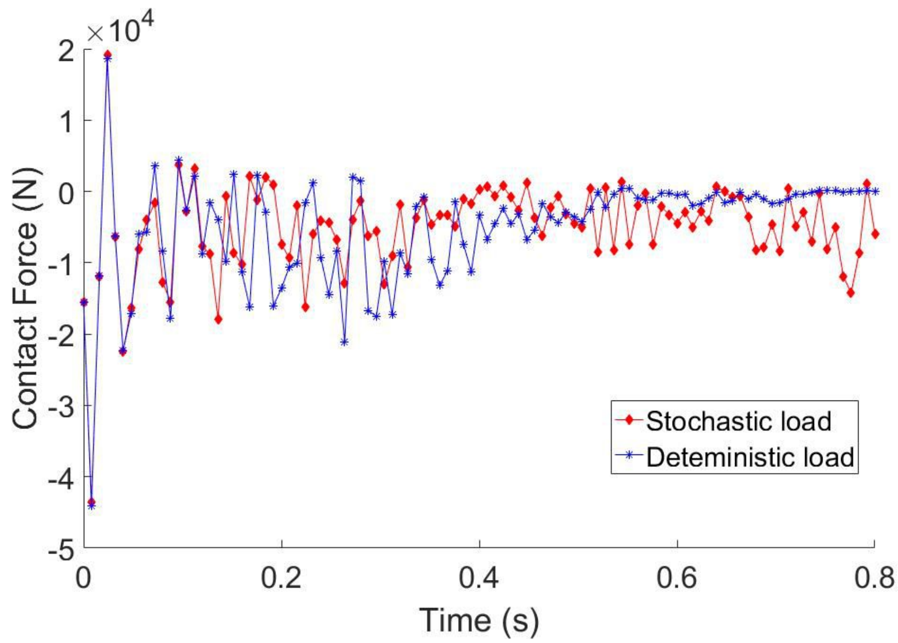

Fig. 2.7: The contact force under two types of load

the system are given in Fig. 2.9 and Fig. 2.10. The PDFs of the relative angular velocity of the system are given in Fig. 2.11 and Fig. 2.12.

Fig. 2.9 depicts the PDF of the relative angular displacement at $0.1s$ (transient state). The values of system response here mean the magnitude of the relative displacement between two meshing gear tooth surfaces. Due to the randomness in load, the relative displacement obtained under generated stochastic load profiles is also stochastic. The average value of the response is equal to -0.0296 with $\mu = 0$ while it is -0.0293 with $\mu = 0.04$. The average values are very close to each other under these two friction conditions. The standard deviation of the response is 0.0322 with $\mu = 0$ while it is 0.0414 with $\mu = 0.04$. The standard deviation for the case with friction is much higher than that for the case without friction.

Fig. 2.10 describes the PDF of the relative angular displacement at $0.7s$ (steady state). The average value of the relative angular displacement is 0.0450 with $\mu = 0$ while it is 0.0412 with $\mu = 0.04$. These two average values are quite close to each other, indicating that the influence of friction is not that big in this case. The standard deviation of the response is 0.0265 with $\mu = 0$ while it is 0.0194 with $\mu = 0.04$. The standard derivation of the responses without friction in the steady state is higher than the case with friction. The dispersion of the response is higher

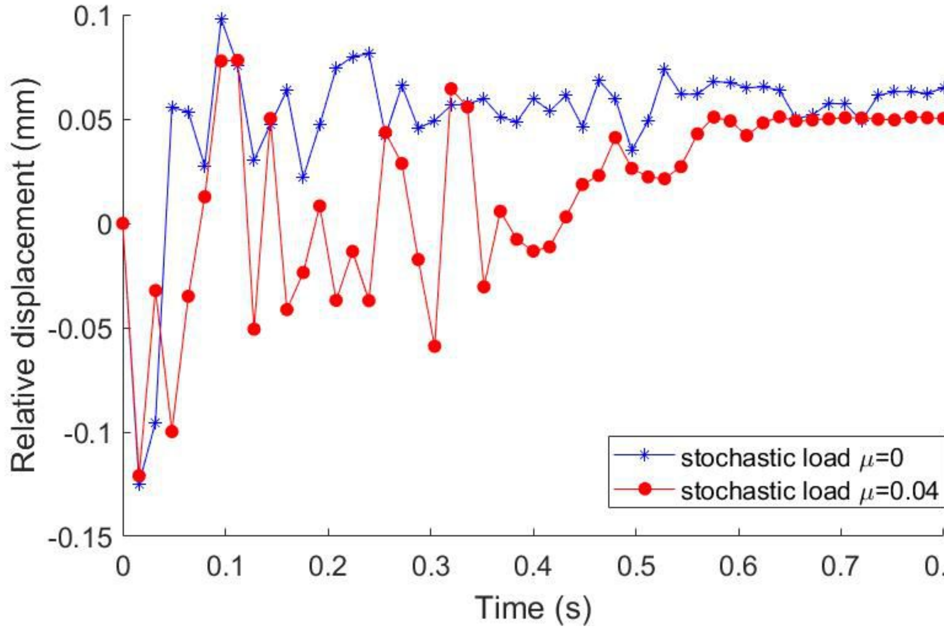

Fig. 2.8: Relative angular displacement under stochastic load with or without friction

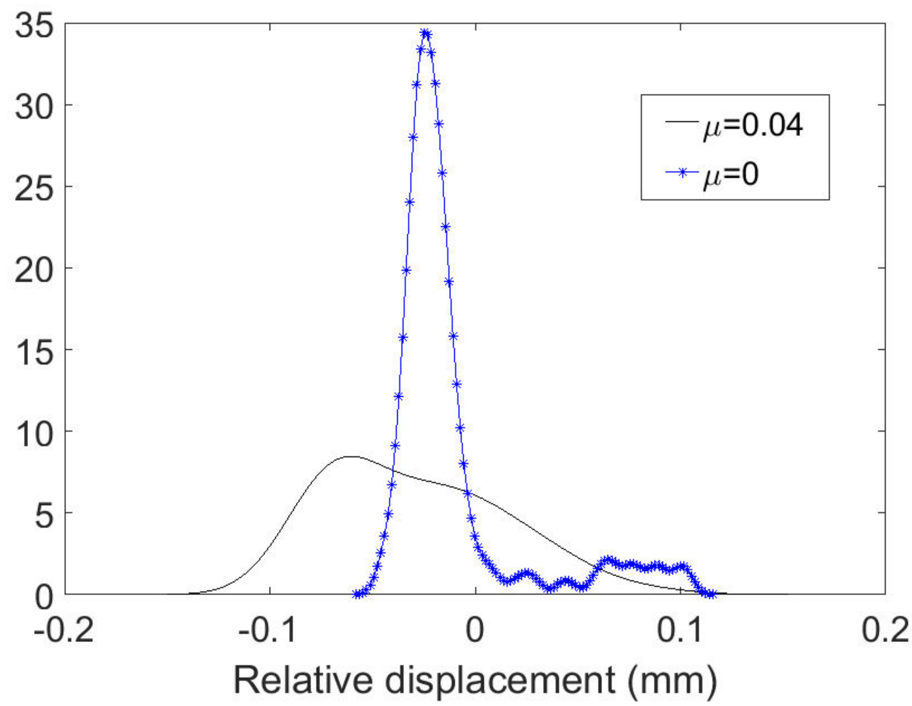

Fig. 2.9: PDF of the relative angular displacement at t=0.1s

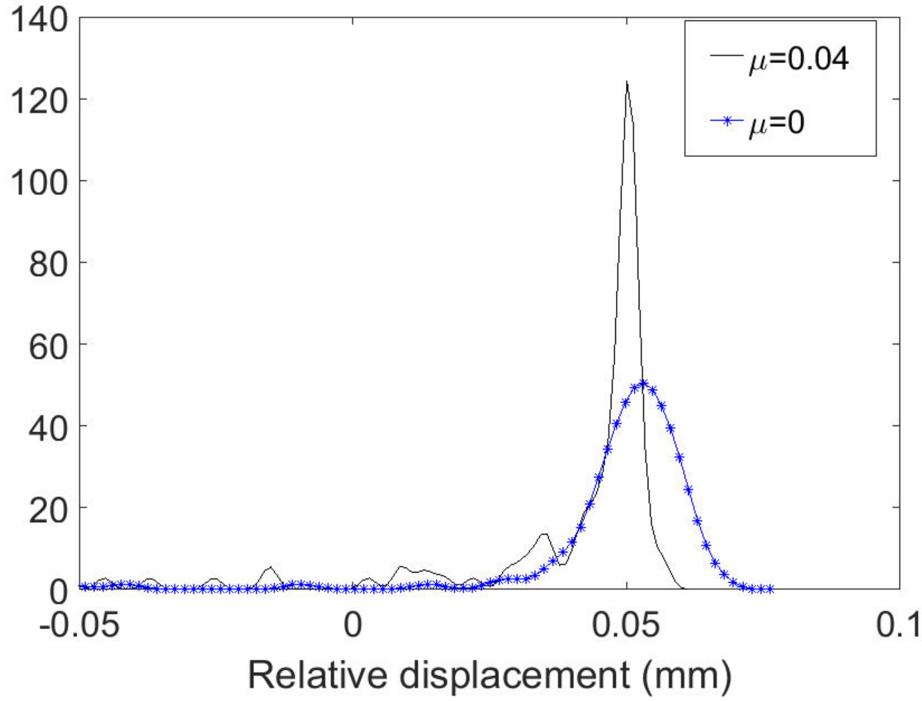

Fig. 2.10: PDF of the relative angular displacement at t=0.7s

in the system without friction. This phenomenon may be caused by the coupling of load randomness.

When we examine the difference in the average values of relative angular displacement at $0.7s$ (a steady state case in Fig. 2.10) and at $0.1s$ (a transient state case in Fig. 2.9), the difference of the average values between the friction case and the friction-less case becomes a little bigger at $0.7s$ than that at $0.1s$.

Similarly, Fig. 2.11 depicts the PDF of the relative angular velocity at $0.1s$ (transient state). The values of system responses here mean the magnitude of the relative velocity between two meshing gear tooth surfaces. There is no doubt that the relative velocity obtained under generated stochastic load profiles is also stochastic. The average value of the response is equal to -0.196 with $\mu = 0$ while it is -0.283 with $\mu = 0.04$. The average values are very close to each other under these two friction conditions. The standard deviation of the response is 0.322 with $\mu = 0$ while it is 0.814 with $\mu = 0.04$. The standard deviation for the case with friction is much higher than that for the case without friction.

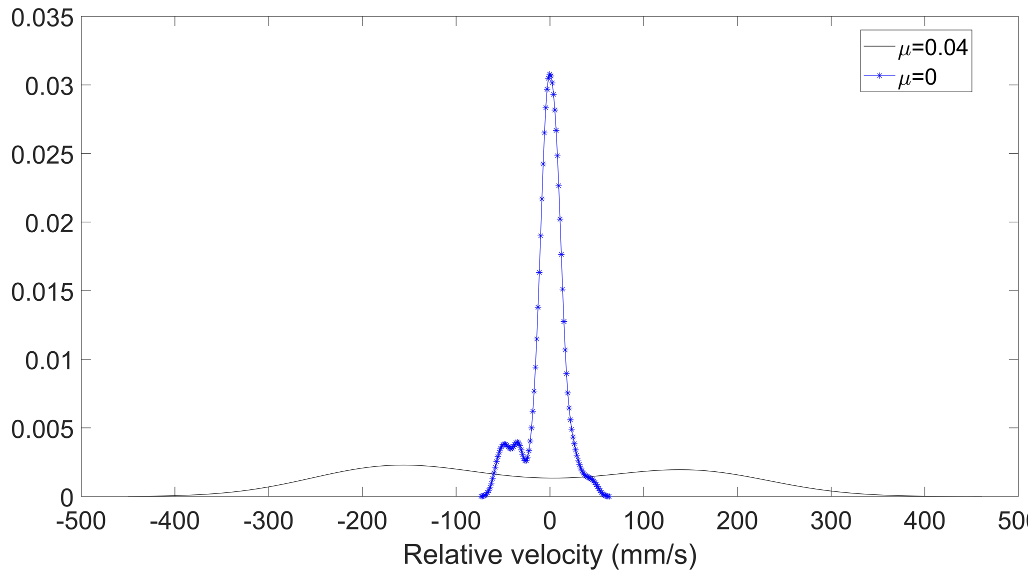

Fig. 2.11: PDF of the relative angular velocity at t=0.1s

Fig. 2.12 describes the PDF of the relative angular displacement at 0.7 s (steady state). The average value of the relative angular displacement is 0.231 with $\mu = 0$ while it is 0.376 with $\mu = 0.04$. These two average values are quite close to each other, indicating that the influence of friction is not that big in this case. The standard deviation of the response is 0.185 with $\mu = 0$ while it is 0.294 with $\mu = 0.04$. The standard derivation of the responses without friction in the steady state is higher than the case with friction. The dispersion of the response is higher in the system without friction. This phenomenon may be caused by the coupling of load randomness.

When we examine the difference in the average values of responses at $0.7s$ (a steady state case in Fig. 2.12) and at $0.1s$ (a transient state case in Fig. 2.11), the difference of the average values between the friction case and the friction-less case becomes a little bigger at $0.7s$ than that at $0.1s$. From Fig. 2.11, the standard deviation of the relative velocity becomes closer for the two cases than that of the relative displacement at $0.7s$.

In a conclusion, friction causes more dispersion to the transient state than that to the steady state. The friction effects on dispersion reflected in relative displacement is bigger than that in relative velocity.

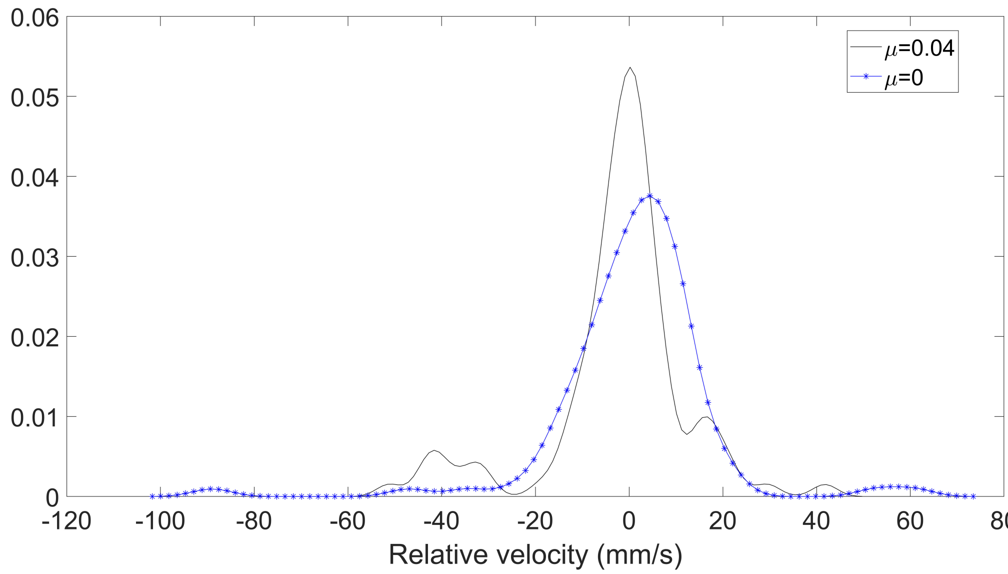

Fig. 2.12: PDF of the relative angular velocity at t=0.7s

2.5 Dynamic characteristics analysis while load is modelled as Gaussian diffusion process

To analyze the dynamic characteristics of the proposed model while load is modeled as Gaussian diffusion process, this section gives the numerical simulation results. The main objective of this section is to investigate the friction and stochastic load effects on system's transient characteristics.

Numerical solutions to the equations of the motion are also obtained by Matlab. All the simulations in this section are under a constant load or a certain Gaussian diffusion process modeled as given in Eq. (2.20). This load scenario is shown as Table 2.3, which is used for all stochastic loads simulated in this section. The gear pair's parameters are given in Table 2.1.

Recall [49], the friction coefficient in a gear system may vary from 0.01 to 0.08. In this section, we fix the friction coefficient at 0.04 to illustrate the load effects on gear dynamic characteristics.

Section 2.5.1 will study the stochastic load effects on transient characteristics, such as periodicity, chaos and stability. Section 2.5.2 will study the friction coefficient effects on transient characteristics, namely, stability and dispersion.

Table 2.3: The scenario of Gaussian diffusion process

λ	0
σ	5×10^3
Type of $\Phi(t = 0)$	Normal distribution
Mean of $\Phi(t = 0)$	2×10^4
Standard deviation of $\Phi(t = 0)$	5×10^3

2.5.1 Load effects on dynamic characteristics

This section shows the effects of stochastic and deterministic loads on a gear system's dynamic characteristics. In this section, we fix the friction coefficient at 0.04 to illustrate the load effects on gear dynamic characteristics.

Fig. 2.13 shows three loading processes: S_1 is a constant loading process. S_2 and S_3 are two realizations of the Gaussian diffusion process.

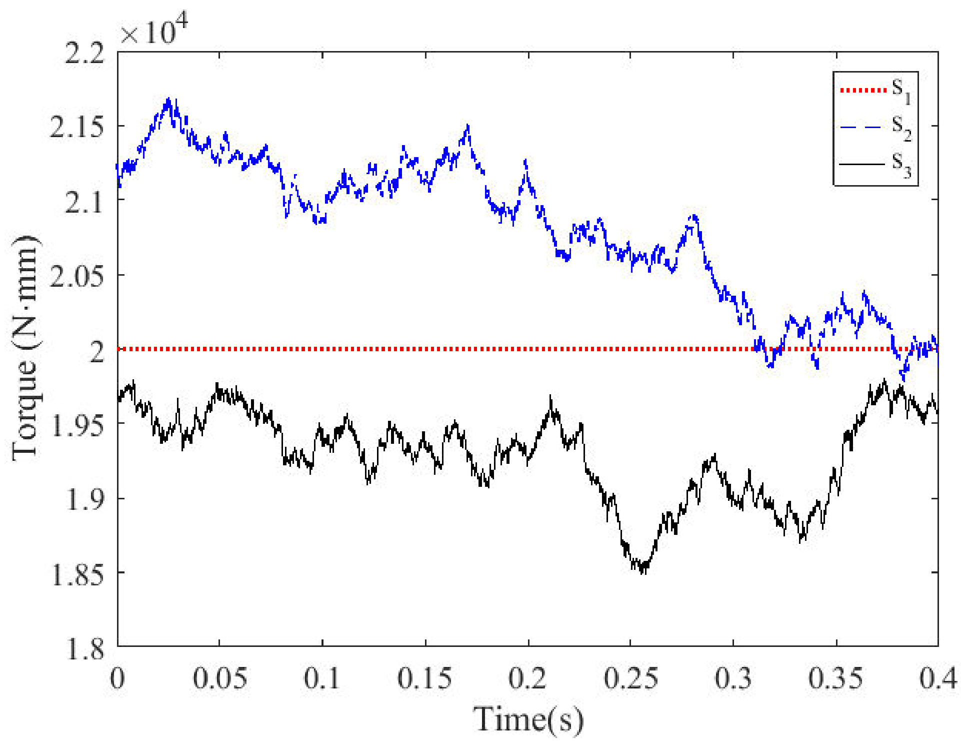

Fig. 2.13: External load processes

The external load is assumed to be a summation of a deterministic load component and Gaussian white noise [31], [37], [5]. Compared with Gaussian white noise, Gaussian diffusion process has fluctuating mean values, which may be appropriate in some cases to study the transient characteristics caused by the randomness of load. The assumption of Gaussian diffusion process may be suitable on some occasions, for example, wind turbine suffering from time varying load [22].

The friction coefficient usually varies with load and speed in real applications. Under stochastic load, it is not easy to precisely analyze the friction mechanism as many factors are involved (e.g., lubrication, surface roughness, load, sliding velocity, and temperature) [80], [85]. According to the research results from [80] [85], the friction coefficient has a small variation when the load and relative velocity vary in a small range.

Ref. [53] compared the influence of five different friction coefficient models on gear dynamic responses under constant load. One model used constant friction coefficient while others adopted time varying friction coefficients. According to their results, gearbox systems behave similarly in many aspects even though the friction models are different. They concluded that the simplified assumption of constant friction coefficient is still adoptable to some extent compared to those time-varying friction coefficient models.

The purpose of this chapter is not to analyze the friction mechanism but to investigate the transient characteristics affected by friction under stochastic load. Even though a constant friction model is used in this study, the proposed model can still generate reasonable results especially when the variation of load and relative velocity is small. If the variations of load and velocity are large, further research is needed.

2.5.1.1 Duration in transient states

Numerical solutions to the equations of the motion are obtained by Matlab. Fig. 2.14 presents the relative angular displacement δ of the gear pair under stochastic and deterministic loads.

As time goes, when the relative angular displacement keeps stable, the system

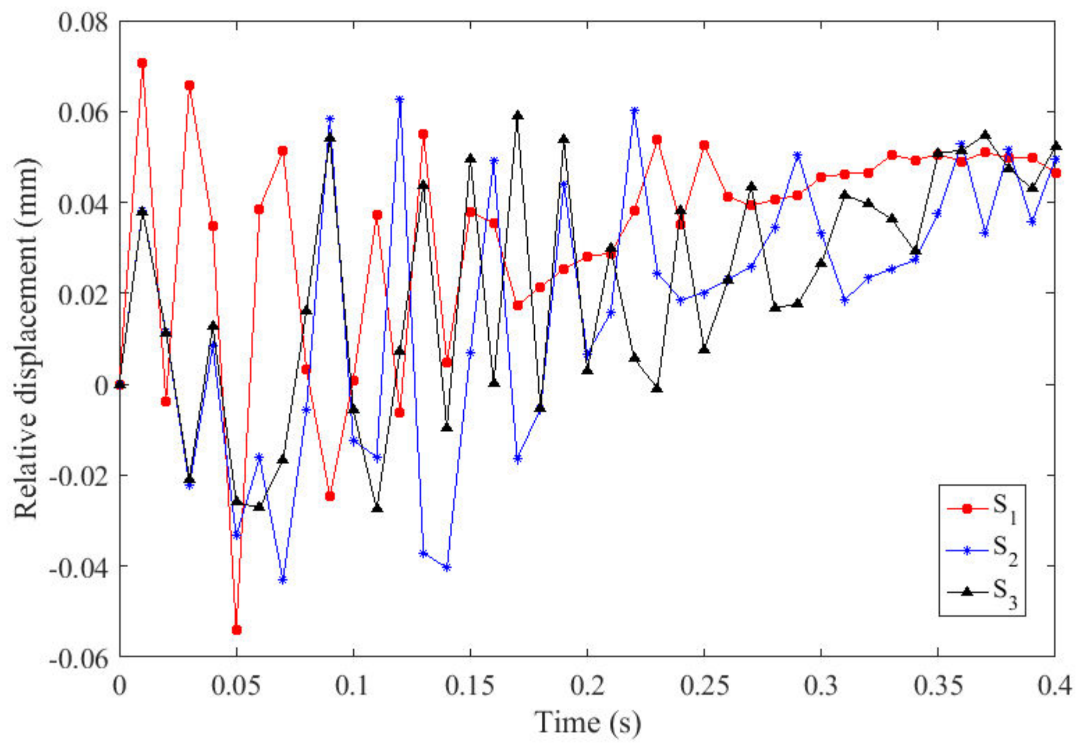

Fig. 2.14: Relative angular displacement under three load processes

is considered to be in the steady state. Fig. 2.14 shows that the system used about 0.35 s to reach the steady state under the deterministic load (S_1). Under the stochastic load (S_2 and S_3), the system has not reached the steady state before 0.4 s.

Therefore, the system with stochastic load uses much longer time to reach steady state than that with deterministic load.

2.5.1.2 Periodicity and chaos

In this section, the dynamic characteristics including periodicity and chaos are studied.

The chaotic oscillation cannot be intuitively observed in S_2 or S_3 compared to that in S_1. There are two possible reasons:

(a) The chaos of responses under this scenario of Gaussian diffusion process is not strong enough to appear in this scale.

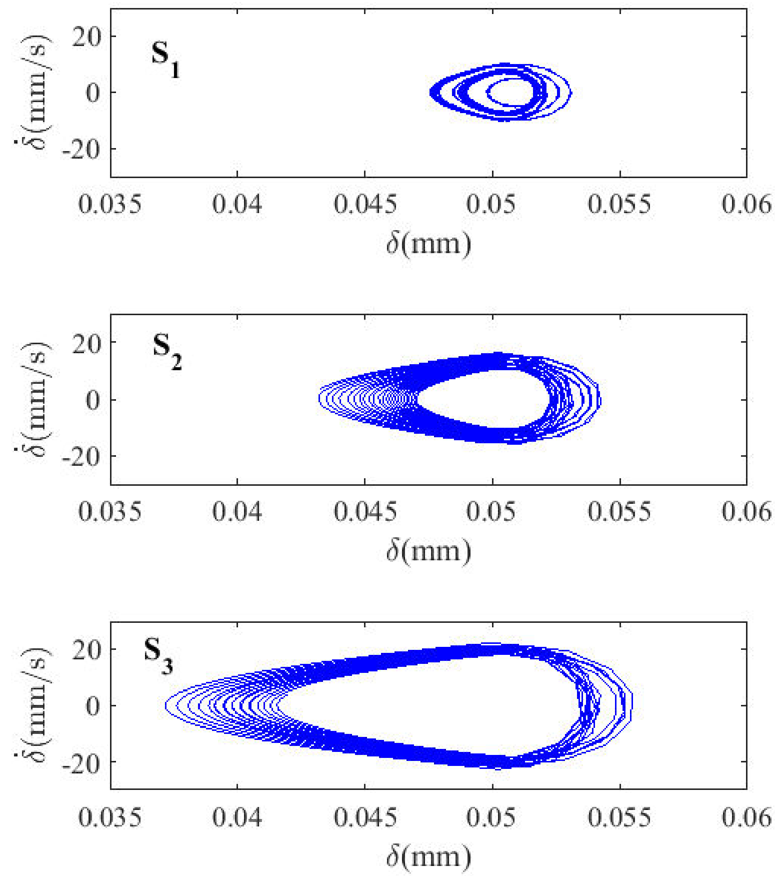

Fig. 2.15: Phase diagrams of relative angular displacement and relative angular velocity in the time interval [0.35, 0.4]s under three loading scenarios, S_1, S_2, and S_3

(b) The coupling of the friction and the randomness weakens the chaotic oscillation.

The chaotic oscillation of the system could be addressed using the secondary Poincaré map [86] in future work beyond this PhD thesis. The periodic and quasiperiodic dynamical oscillations can exist simultaneously [86], [87]. Most periodic behaviors are not perfect periodic and neither quasiperiodic nor chaotic as well [86]. From Fig. 2.15, the phase diagram of S_1 shows overlapped loops while the phase diagrams of S_2 and S_3 give independent loops.

Thus, the gear system under deterministic load holds the properties of periodic and quasiperiodic oscillations simultaneously. Under stochastic load, gear system shows quasiperiodic oscillation. This phenomenon needs further investigation with more samples and varying conditions.

2.5.1.3 Transient asymptotic stability

To investigate the performance of a gear system in the transient state, one of the most important aspects is the transient stability [21]. According to [21], the responses of a gear system will converge to a certain orbit. In our case, the convergency of responses under stochastic load can be visualized in Fig. 2.14 while the convergence orbit is not clear to identify.

However, we can utilize the convergence orbit obtained under deterministic load in [50] for reference, which δ has a small perturbation near 0.05 (value of backlash) and $\dot{\delta}$ has a small perturbation near zero. The gear system is approaching to a stable state with the relative motion decreasing and transmission ratio approaching to a constant. This phenomenon is asymptotically stable [88].

We apply an indicator to quantify such transient asymptotic stability. Choose a certain time interval and define center distance as Eq. (2.23). The center distance indicates the range of vibration response in a certain time interval. The transient state is more stable with a lower center distance.

$$\begin{aligned} d &= \sqrt{\{[\max(\delta) - 0.05] - [\min(\delta) - 0.05]\} \cdot \left\{\left[\max(\dot{\delta}) - 0\right] - \left[\min(\dot{\delta}) - 0\right]\right\}} \\ &= \sqrt{[\max(\delta) - \min(\delta)] \cdot \left[\max(\dot{\delta}) - \min(\dot{\delta})\right]} \end{aligned} \tag{2.23}$$

When $t \in [0.35, 0.4]$ and $\mu = 0.04$, we found $d = 0.34\,mm/s^{\frac{1}{2}}$ for S_1, $d = 0.44\,mm/s^{\frac{1}{2}}$ for S_2, and $d = 0.59\,mm/s^{\frac{1}{2}}$ for S_3. Even if S_2 and S_3 follow the same scenario, they show quite some differences in center distance from each other.

Since the responses (δ and $\dot{\delta}$) of the gear pair under Gaussian diffusion process are random variables, it is necessary to give statistical information of transient stability under stochastic load. In dealing with random variables, the probabilistic method is a classical approach for uncertainty modelling based on the well-developed probability theory [83] [89].

To obtain statistical results, we adopt direct MC method instead of path integration method [66], [67], [73], [74] or the stochastic perturbation method [90], [91]. Although MC method takes more calculation time, we can achieve the desired accuracy by increasing simulation time. In this simulation, each realization follows the same scenario in Table 2.3.

When $t \in [0.35, 0.4]$ and $\mu = 0.04$, we simulated 100 realizations and obtained corresponding center distances. There are 93 center distances greater than that obtained under deterministic load. We conclude that the center distance under stochastic load had 93% possibility greater than that under deterministic load. Therefore, it can be concluded that there is lower transient stability under the stochastic load.

2.5.2 Friction effects on dynamic characteristics

This section evaluates the effects of different friction coefficient values on the dynamic characteristics of the gear system under a certain stochastic load with the same scenario in Table 2.3. Six cases of the friction coefficient values ($\mu = \{0,\ 0.01,\ 0.02,\ 0.03, 0.04, 0.05\}$) are used and responses are compared with one another. The effects of friction coefficient on the transient stability will be studied in Section 2.5.2.1. Section 2.5.2.2 will investigate the friction coefficients' influence on the dispersion of responses.

2.5.2.1 Transient asymptotic stability

This section shows the effects of different friction coefficient values on the transient stability. Firstly, the center distances under three loadings (S_1, S_2, S_3) are shown in Fig. 2.16. Then, the statistical analysis of the center distance under stochastic load is shown in Fig. 2.17.

Fig. 2.16 shows the comparison of center distances as a function of friction coefficient for the three loading scenarios. From Fig. 2.16, the trend of the center distance of S_2 shares similarity with that of S_1. However, the trend of S_3 is different from S_1 and S_2. Even S_2 and S_3 follow the same scenario, they show great differences from each other in amplitude. It should be noticed that the change of center distance with the increasing of friction coefficient is not monotonous. A small friction coefficient does not guarantee a better transient stability from the observation in Fig. 2.16.

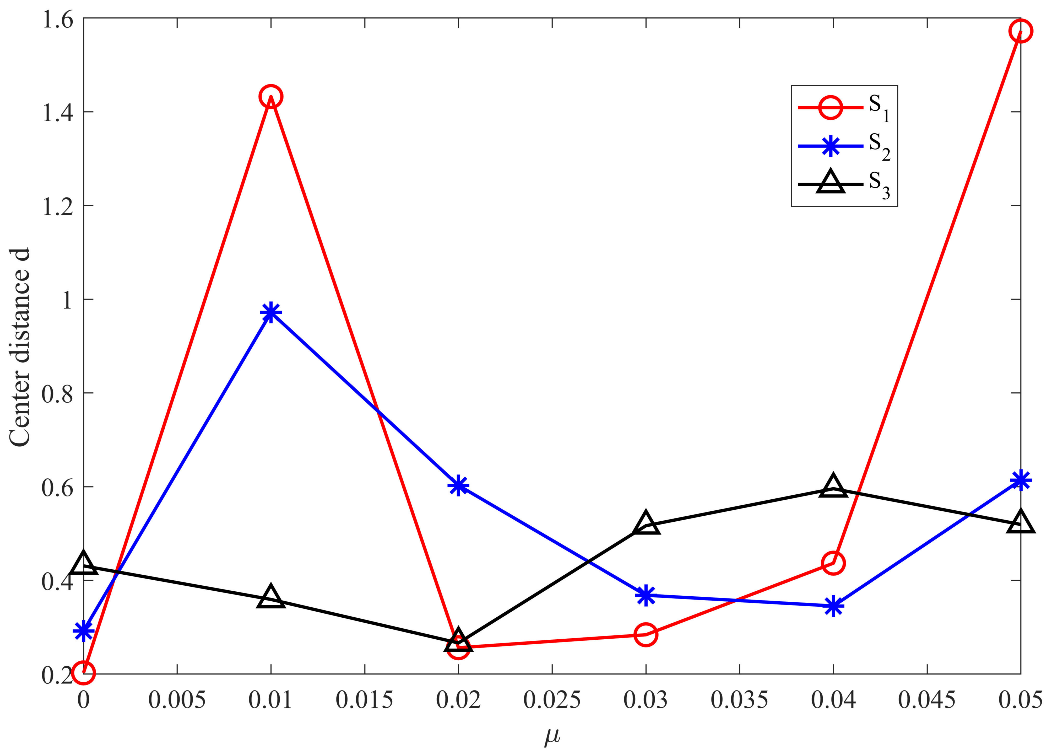

Fig. 2.16: Comparison of center distances as a function of friction coefficient for the three loading scenarios

Fig. 2.17 is a boxplot that denotes the statistical properties of center distances under each friction coefficient value. The dot in a circle is the median, the block with solid line is the interquartile range, and the dash line is the range of the minimum and maximum. From Fig. 2.17, the range of center distance with the friction coefficient being 0 is smaller than most of the cases with positive friction coefficient.

Thus, friction causes more instability in transient state. But there is no obvious trend between the center distance and friction coefficients. In those cases with positive friction coefficient values, the minimum range of center distance is found at $\mu = 0.02$, and the maximum range of center distance is found at $\mu = 0.01$ or $\mu = 0.03$.

In a word, gear system has worst transient stability with $\mu = \{0.01, 0.03\}$ and best transient stability with $\mu = \{0, 0.02\}$. According to this result, we should find

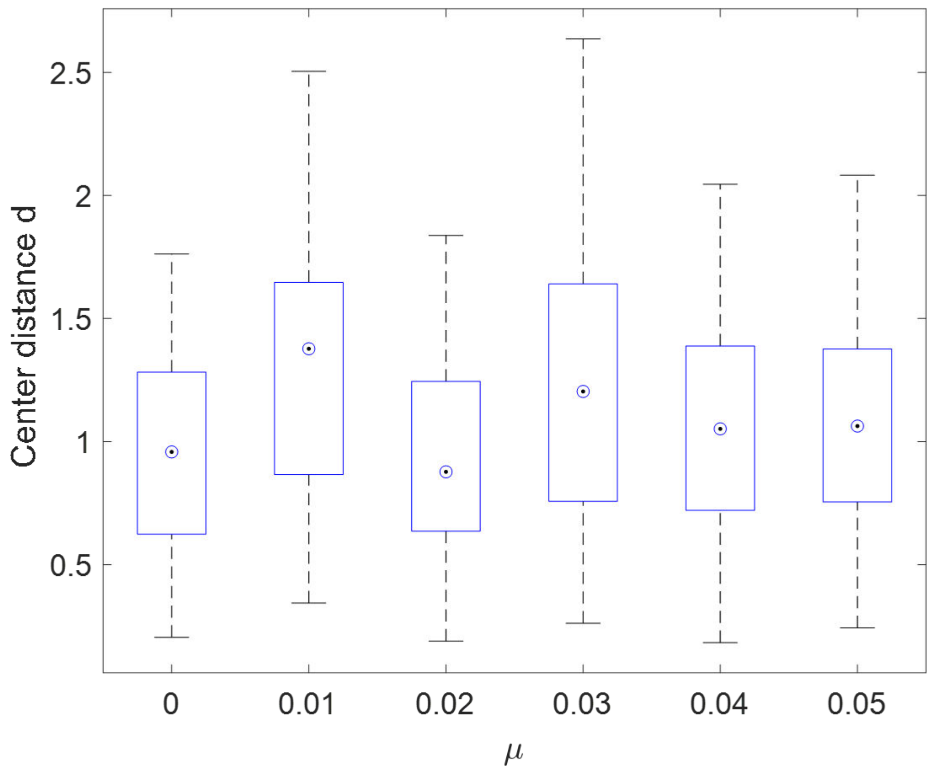

Fig. 2.17: Boxplot of the center distance as a function of friction coefficient for loading scenario S_2

out and avoid the friction coefficient which will worsen transient stability in the gear design phase. At the same time, the friction coefficient should be adjusted to a suitable value in gear system to increase transient stability.

2.5.2.2 Dispersion of responses

The descriptions of responses in the gear system under stochastic load are analyzed with PDFs [84]. Fig. 2.18 describes the PDF evolution during the time range [0.3, 0.4]s with $\mu = 0.04$. With increase of time, the joint PDFs between the relative angular displacement and the relative angular velocity become more concentrated. It indicates that the system approaches a stable state. Hence, in this simulation, $t = 0.4s$ is the most stable state for a gear system under stochastic load. If a rule of this evolution can be found, the PDF prediction can be done with an initial PDF.

Since $t = 0.4s$ is considered as the most stable state, the following discussion is limited to that time point. Fig. 2.19 and Fig. 2.20 show the instantaneous

Table 2.4: Responses under deterministic load

μ	0	0.01	0.02	0.03	0.04	0.05
δ	0.0515	0.0431	0.0511	0.0515	0.0508	0.0453
$\dot{\delta}$	-2.167	-10.59	7.079	6.854	-9.459	-28.38

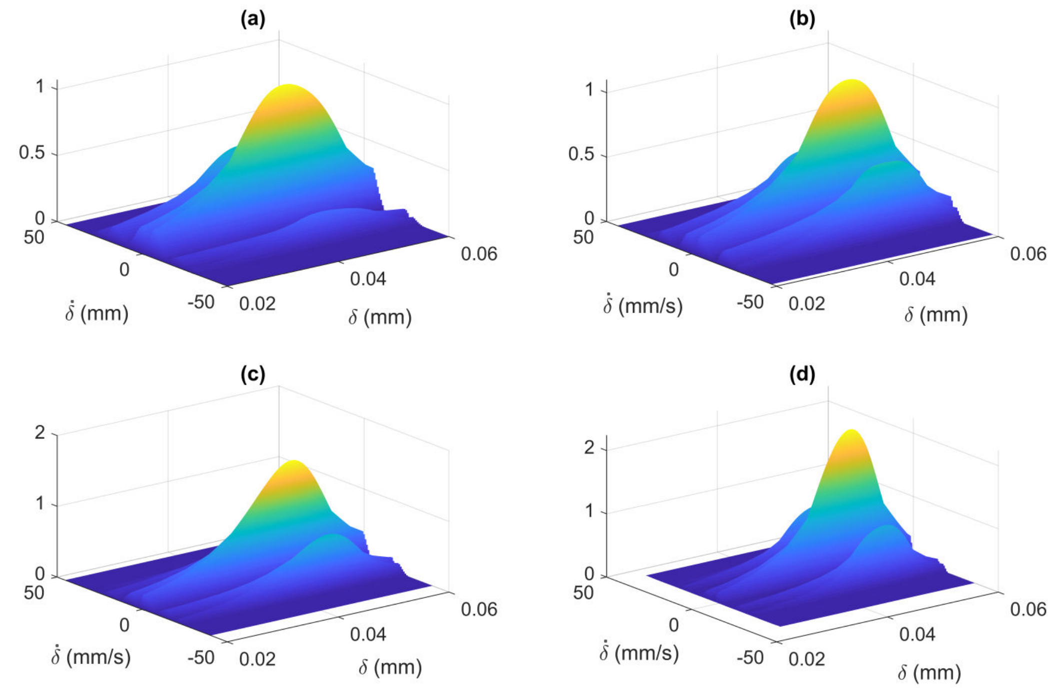

Fig. 2.18: PDF evolution plot depicting its changing within 0.1s at different time points: (a) at 0.3s, (b) at 0.33s, (c) at 0.36s, and (d) at 0.4s

PDFs of relative displacement and relative velocity respectively at $t = 0.4s$. The corresponding solutions of the deterministic case at the same time point are shown in Table 2.4. Due to the calculation difficulty, deterministic responses are easier to obtain than stochastic responses. If the responses under stochastic load fall in the center region of the responses under deterministic load, we can predict the stochastic responses corresponding to the deterministic responses. Compare Fig. 2.19-2.20 and Table 2.4, the results of relative angular displacement in Fig. 2.19 falls in the center regions around the results of deterministic load. But the mean of relative angular velocity did not fall in the center regions around the result of deterministic load.

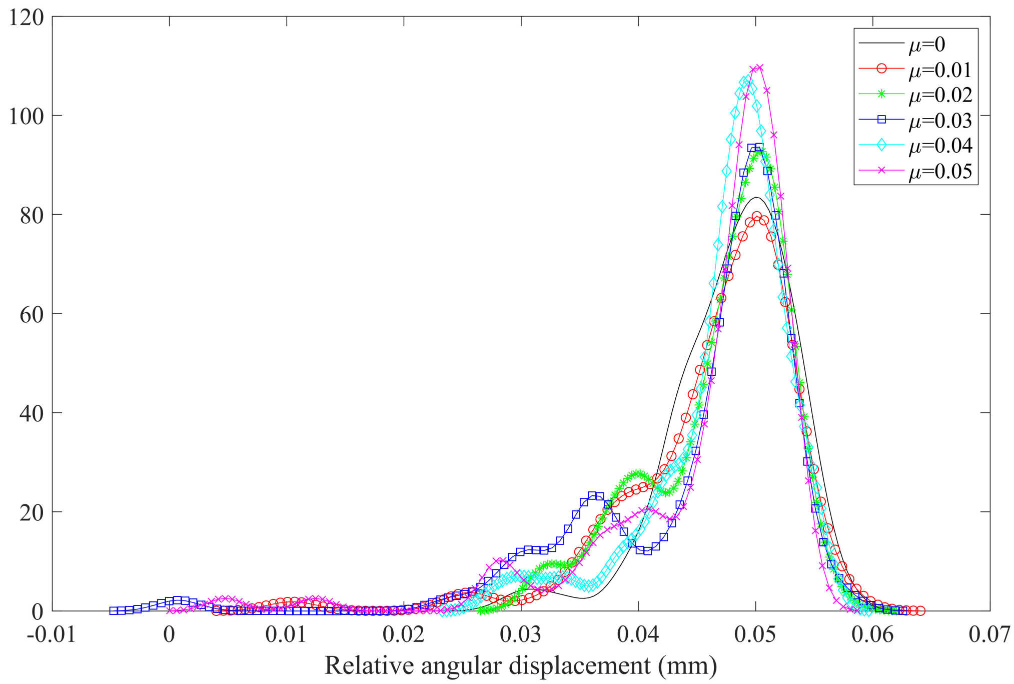

Fig. 2.19: PDFs of the relative angular displacement with different friction coefficient values at t=0.4s

For a practical gear pair, the PDFs of relative displacement and relative velocity are definitely different from the perfect gear case (without fault). According to the dispersion property investigated in the previous paragraph, the relative displacement is more appropriate to be an indicator of fault diagnoses for further study. Thus, these PDFs of relative angular displacement obtained by our study for perfect gear system may be used as references in gear health monitoring.

On the other hand, according to Fig. 2.19 and Fig. 2.20, the differences in the PDFs of different coefficients are obvious. It also proves that the friction cannot be ignored in dealing with gear stochastic dynamics. However, the relationship between friction, stochastic load, and time is not given. This will be further explored in our future work.

The probabilities of gear system responses (relative angular displacement and relative angular velocity) in a safety interval are given in Table 2.5. Safety interval means the gear system responses have a high possibility occur in a chosen interval. If the responses exceed the safety interval, there is a higher possibility that the gear

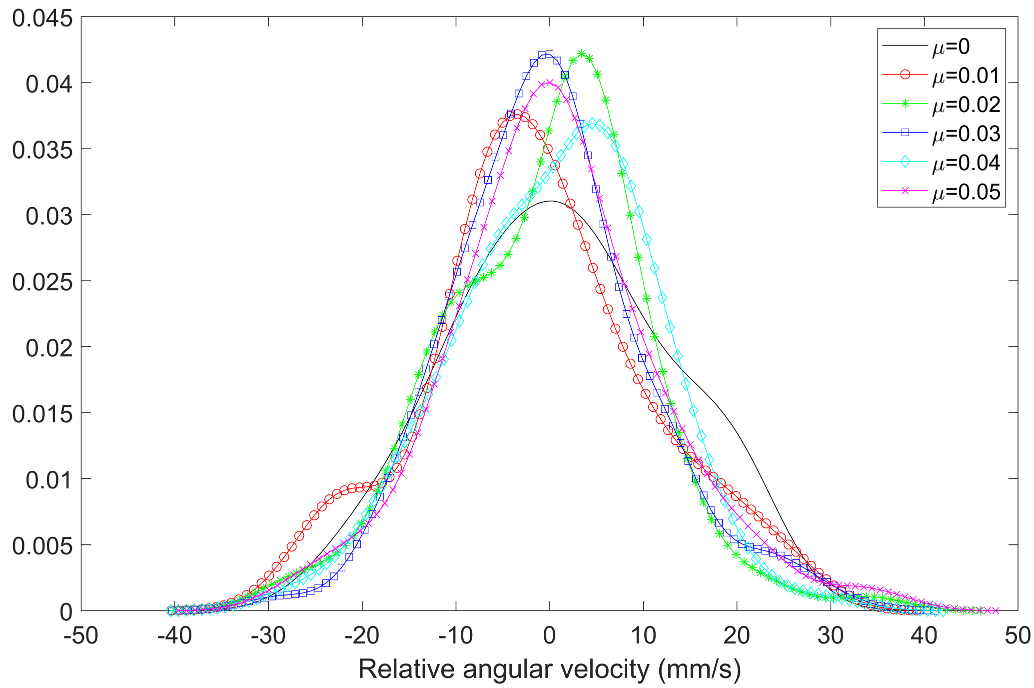

Fig. 2.20: PDFs of the relative angular velocity with different friction coefficient values at t=0.4s

Table 2.5: The probabilities of a safety interval under each friction coefficient value (%)

μ	0	0.01	0.02	0.03	0.04	0.05
$\delta \in [0.04, 0.055]$	91	89	85	**76**	87	85
$\dot{\delta} \in [-16, 16]$	80	**79**	90	90	89	87

system has failure [92]. We can select a proper safety interval based on accuracy demand. In Table 2.5, the safety intervals are chosen based on the rule that there are at least 75% data fall in the safety intervals. According to our model, we choose $\delta \in [0.04, 0.055]$ and $\dot{\delta} \in [-16, 16]$ for analysis. When $\delta \in [0.04, 0.055]$, it is noticed that the probability of δ is the lowest under the friction coefficient $\mu = 0.03$. When $\dot{\delta} \in [-16, 16]$, the probability of $\dot{\delta}$ is the lowest with $\mu = 0.01$. The lower interval probability indicates higher data dispersion. The higher dispersion of the values always reflects higher uncertainty in the data [84]. It is concluded that gear responses have a higher proportion exceeding a certain safety interval and have a higher potential failure probability with $\mu = 0.01$ or 0.03.

2.6 Conclusion

In this study, a gear stochastic dynamic model for a spur gear pair considering TVMS, gear mesh damping, backlash, friction, and stochastic load is established. The dynamic responses of this model are investigated using numerical simulation and compared with previous work. Two cases with different load profiles are studied and compared. For case 1, the random part of load is modeled as Gaussian white noise with a certain friction coefficient ($\mu = 0.04$). For case 2, the random part of load is modeled as Gaussian diffusion process with five friction coefficient values ($\mu = \{0.01,\ 0.02,\ 0.03, 0.04, 0.05\}$).

- Case 1: The random part of load is modeled as Gaussian white noise:

The analysis results demonstrate that (a) under the same friction coefficient ($\mu = 0.04$), stochastic load generates longer duration in the transient state and higher fluctuation in the steady state compared with those under deterministic load; (b) under stochastic load, the case with friction produces larger difference in the average value of the system's relative angular displacement at the steady state compared with that of the case without friction; (c) the case with friction generates higher dispersion of relative angular displacement in the transient state and lower dispersion in the steady state compared with those of the case without friction.

- Case 2: The random part of load is modeled as Gaussian diffusion process:

The analysis results demonstrate that (a) the established SDOF gear dynamic model is more realistic than reported models which did not consider friction, (b) under the same friction coefficient value ($\mu = 0.04$), the stochastic load generates longer duration and more quasi-periodicity in the transient state than those of the deterministic load. Stochastic load causes lower transient stability than deterministic load, (c) under stochastic load, the gear system has the worst transient stability with $\mu = 0.01$ or 0.03 and best transient stability with $\mu = 0$ or 0.02. Friction generates high dispersion of the relative angular displacement with $\mu = 0.01$ or 0.03 in the transient state.

Overall, this analysis gives us better understanding on the effects of stochastic load and friction on the gear dynamic characteristics. The proposed gear dynamic model and numerical results can be used as a reliable tool to investigate the gear random dynamics. Future work will design corresponding experiments to validate our numerical findings. Moreover, our gear model can be further extended by incorporating varying friction coefficients and analyzing the effects of different friction models on gearbox dynamics under stochastic load in our future work.

In summary, this chapter addressed the problem of investigating a more realistic gear dynamic model, and thus, a model considering one more internal factor (i.e., friction) was proposed. The effects of the stochastic load and friction on the gear dynamic characteristics were studied. This model will be used later in Chapter 3 and Chapter 4. In Section 3.2, one more external factor is considered based on this model. In addition, Section 4.4 takes this model to validate the proposed approximate analytical method.

3

Effects of Driving Speed Variation on Gear Dynamic Characteristics under Stochastic Load

Although a more practical gear model with consideration of a stochastic internal factor is proposed and analyzed in Chapter 2, only a kind of external excitation (i.e., stochastic load) is considered in that model. In reality, there are some other stochastic external excitations remaining to be explored. In this chapter, one more external excitation (i.e., driving speed) is considered based on the model in Chapter 2. As we known, engine drive gear systems are widely used in vehicles, coal mining machines, and other mechanical equipment. Engine is known as a source of external excitations to a gear system. Due to the manufacturing error, energy loss, possible change of the engine status, and variation of operating environment, the driving speed and external load are not deterministic in the future. Thus, this chapter[1] aims to investigate the effects of the driving speed variation (including deterministic or stochastic driving speed) on

[1]The work of this chapter has been accepted or submitted for peer review as follows:
Y. Fang, M. J. Zuo, and Y. Li, "Investigation of gear dynamic characteristics under stochastic external excitations," in *Proceeding of 2019 International Conference on Advances in Materials, Mechanical and Manufacturing (AMMM)*, Beijing, China, Mar. 22-24, 2019. Accepted on Jan. 3, 2019.
Y. Fang, X. Liang, and M. J. Zuo, "Effects of driving speed variation on gear dynamic characteristics under stochastic loading," *Mechanism and Machine Theory*. Submitted on Oct. 8, 2018.

gear dynamic characteristics under stochastic load for the first time. Monte Carlo (MC) simulation is applied to analyze the characteristics. The results show that the random element in the driving speed affects the gear response a lot which should not be ignored. Under the stochastic load, a small ratio of randomness in driving speed greatly increases the dispersion in responses. In addition, the dispersion in responses is more sensitive to the uncertainty of the driving speed than that of the load.

3.1 Introduction

Gear systems play an important role in modern power transmission systems [12]. Many researchers have studied the dynamic modelling of spur gear transmission systems. Excitations are widely discussed in gear dynamic modelling and they affect the dynamics of gear systems. There are two categories of excitations, internal excitations and external excitations. Internal excitations include time-varying mesh stiffness (TVMS) [17] [93], backlash [94], transmission error [77], and so on. Many studies have studied the effects of internal excitations on gear dynamics while less attention has been paid to the effects of external excitations on gear dynamics.

In reality, the gear system can be driven by engine [56] or nature force (e.g., wind [57]). In this work, we restrict to the engine drive gear systems. Accordingly, the external excitations contain the external load [79] [95] and driving speed of the pinion [1]. Note that the driving speed is provided by the engine. Under deterministic domain, external excitations have been investigated in some existing works. Wang et al. [7] reviewed the mathematical models and the solving approaches for the nonlinear dynamics of gear systems under deterministic load. An analytical model of a spur gear pair with tooth root crack was proposed in [27] under deterministic load. Qiu et al. [58] considered the influence of deterministic input rotating speed on stiffness and introduced a velocity modulated stiffness model. Liu et al. [26] investigated the effects of speed on gear dynamics and concluded that the variation of the pinion's speed was a non-negligible source of instability in a gear system. The transient dynamic behavior of the gear system, which is affected by the variation of the external excitations, was investigated in [24]. Pruvost et al. [60] proposed an improved filter to separate the noise from engine signals and validated it using diesel combustion engine experiments. In addition, they investigated the variation of rotation speed and load, and their effects on engine transfer functions between the cylinder and the listening spot.

It is widely known that randomness of the external excitations exists in the gear systems driven by nature force (i.e., wind turbine) [96]. Similarly, due to manufacturing error, energy loss, possible change of the engine status, and variation of operating environmental, the external excitations in engine drive gear systems may also not be deterministic [2] [60]. Several works focused on the studies of randomness in the engine. Tutak and Jamrozik [59] studied the flow field turbulence in the combustion chamber and modelled the crankshaft velocity (the crankshaft performs a conversion between reciprocating motion and rotational motion) randomness of an internal combustion engine. Randall [61] summarized the methods to deal with random speed fluctuations in combustion engines. To obtain more realistic representation of gear systems, the stochastic properties should be considered in the anticipated load profile and anticipated speed profile.

In recent works about modeling gear systems, attention of researchers has transferred from the deterministic domain to the stochastic domain. In [30], the stochastic property of dynamic loads for high speed gears was observed. Tobe et al. [31] modeled the randomness in the load as Gaussian white noise and validated their model through experiment results reported in [37]. Chaari et al. [97] investigated the dynamic behavior of a spur gear system under cyclic and random load, respectively. Wen et al. [94] investigated the random dynamic response of a gear pair. The dynamic model in Ref. [94] considered constant mesh stiffness, constant damping coefficient, and stochastic external load by adding Gaussian white noise. Later, they developed a model considering backlash, TVMS, and constant damping coefficient [5]. Fang et al. [23] considered one more excitation, friction, than the model proposed in [5]. Ref. [23] investigated the effects of friction on the dynamic characteristics of a spur gear pair under stochastic load.

Although researchers have made some improvements in modelling gear dynamics under stochastic load, there are still short of investigations about the effects of driving speed on gear dynamics with stochastic load.

In this chapter, we modeled the driving speed (deterministic or stochastic) and investigated its effects on gear dynamics under stochastic load. The major contributions of this work are summarized as follows.

1. The existing works only considers the effects of the driving speed variation on gear dynamic characteristic under deterministic load. In reality, however, the stochastic load exists widely in gear systems [30]. The extension of the models from deterministic domain to stochastic domain leads to more realistic representation of real gear systems. In addition, investigating the effects of the driving speed variation on gear dynamic characteristics under stochastic load is a significant part of the gear random dynamics study.

2. The driving speed is generally modelled as deterministic in existing works. However, the randomness in the driving speed is found by many researches, e.g., [59] [61]. Therefore, the effects of stochastic driving speed variation on gear dynamic characteristics under stochastic load is investigated in this work. A mathematic model is developed.

3. By the Monto Carlo method, we analyzed the dynamic characteristics focusing on the effects caused by the driving speed (deterministic or stochastic) under stochastic load. Some insightful conclusions are summarized by the simulation results.

The remaining parts of this chapter is organized as follows. In Section 3.2 the proposed stochastic dynamic model for a spur gear pair is described. Section 3.3 illustrates the effects of the driving speed on gear dynamic characteristics. Section 3.4 draws the conclusion.

3.2 Nonlinear stochastic gear dynamic model

In this section, a single degree of freedom (SDOF) nonlinear dynamic model of a spur gear pair is developed based on the model reported in [23]. Backlash, TVMS, sliding friction, and stochastic load are considered in [23]. Keeping everything the same as in [23], a time-varying modulated driving speed is considered in our model and described in Section 3.2.1. The external load and driving speed of the pinion are modelled in Section 3.2.2.

3.2.1 Proposed model considering driving speed

In this section, the proposed model is based on Ref. [23] while considering a time-varying modulated driving speed. Note that only an initial speed is given in the model of Ref. [23]. The model reported in [23] is given in Eq. (3.1) and (3.2) while it transforms to Eq. (3.11) with the consideration of our modelled driving speed.

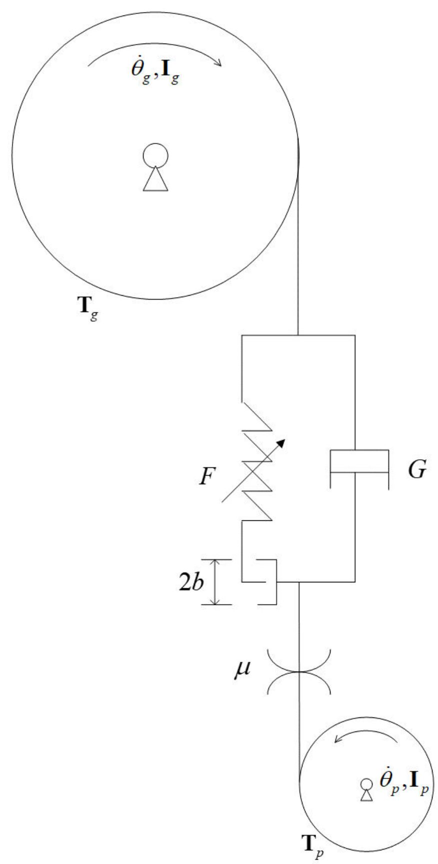

Fig. 3.1: Dynamic model of a gear pair

The equations of the motion for the system given in Fig. 3.1 can be expressed as [1]

$$\mathrm{I}_p\ddot{\theta}_p = \mathrm{T}_p - (F+G)R_p - \mu(F+G)X_1 \tag{3.1}$$

$$\mathrm{I}_g\ddot{\theta}_g = \mathrm{T}_g + (F+G)R_g + \mu(F+G)(l-X_1) \tag{3.2}$$

where $\mathrm{I_p}$, T_p, $\ddot{\theta}_p$, and R_p are the moment of inertia, external torque, angular acceleration, and base circle of pinion (similarly subscript g is used to denote the gear), respectively; F is the total elastic force between the contact teeth shown in Fig. 2.2, G is the damping force, μ is the friction coefficient, X_1 denotes the tangent distance in the action line, $l = (R_p + R_g)\sin\alpha_0$ means the length of the action line, and α_0 denotes the pressure angle. For more details, please refer to Ref. [23] and Ref. [50].

Subtract Eq. (3.2) from Eq. (3.1) and then divide both sides by I_g . The following expression can be obtained.

$$\ddot{\theta}_g = \left[\mathrm{I}_p\ddot{\theta}_p + \mathrm{T}_g - \mathrm{T}_p + (F+G)(R_g - R_p + \mu(R_g + R_p)\sin\alpha_0)\right]/\mathrm{I}_g \tag{3.3}$$

Let $\delta = R_p\theta_p - R_g\theta_g$, where δ gives the relative angular displacement of the gear pair. Then Eq. (3.3) transfers to Eq. (3.4).

$$\ddot{\theta}_g = \left[\mathrm{I}_p\ddot{\theta}_p + \mathrm{T} + (K\delta + \alpha\dot{\delta})L\right]/\mathrm{I}_g \tag{3.4}$$

where

$$F = Kg(\delta) \tag{3.5}$$

$$G = c\dot{\delta} \tag{3.6}$$

$$L = R_g - R_p + \mu(R_g + R_p)\sin\alpha_0 \tag{3.7}$$

$$\mathrm{T} = \mathrm{T}_g - \mathrm{T}_p \tag{3.8}$$

In Eqs. (3.5)–(3.8), K is the effective mesh stiffness, $g(\delta)$ denotes the function of backlash, L is the equivalent length of the force arm, and c is the damping coefficient, and T is the equivalent torque (i.e., the external load in this study) that reflects the combined fluctuation of T_g and T_p.

The expressions of $g(\delta)$, and $K(\theta)$ (see Fig. 2.1) are given below

$$g(\delta) = \begin{cases} \delta - b, & \delta > b \\ 0, & -b \le \delta \le b \\ \delta + b, & \delta < -b \end{cases} \tag{3.9}$$

$$K(\theta) = \begin{cases} k_1, & (n-1)\phi_n \le \theta < (n-1)\phi_n + \phi_m \\ k_2, & (n-1)\phi_n + \phi_m \le \theta < n\phi_n \end{cases} \tag{3.10}$$

where b denotes the backlash, ϕ_n and ϕ_m represent a mesh period of gear teeth and the double pairs of teeth mesh duration in a mesh period, respectively.

Rewriting Eq. (3.4), a second-order ODE is finally obtained as

$$\ddot{\theta}_g = \left\{\mathrm{I}_p\ddot{\theta}_p + \mathrm{T} + [Kg(\theta_pR_p - \theta_gR_g) + c(\dot{\theta}_pR_p - \dot{\theta}_gR_g)]L\right\}/\mathrm{I}_g. \tag{3.11}$$

Observe Eq. (3.11), the inputs (excitations) in this ODE are T, θ_p, $\dot{\theta}_p$, and $\ddot{\theta}_p$ while the outputs are θ_g, $\dot{\theta}_g$, and $\ddot{\theta}_g$ (or called the responses of gear dynamic model).

The comparison between the model in Ref. [23] and the proposed model is shown in Table 3.1. From Table 3.1, both models have the equivalent load $\mathrm{T}(t)$ and the initial condition of the gear $\theta_g(t=0),\ \dot{\theta}_g(t=0)$ as input. The main difference in inputs between the two models is the motion of pinion ($\theta_p(t),\ \dot{\theta}_p(t),\ \ddot{\theta}_p(t)$). In the proposed model, the motion of the pinion is fully specified while only the initial condition of the pinion motion is given in model of Ref. [23].

Correspondingly, the outputs (or solution) to the model (or equation) in Ref. [23] include the motions of both pinion and gear ($\theta_p,\ \dot{\theta}_p\ ,\theta_g,\ \dot{\theta}_g$). Only the motion of gear ($\theta_g,\ \dot{\theta}_g$) needs to be solved in the proposed model. The proposed model is a kind of velocity modulated model.

Table 3.1: The comparison between two models

	Model in Ref. [23]	The proposed model
Equation	Eq. (3.1) and Eq. (3.2)	Eq. (3.11)
Input	$\mathrm{T}(t), \theta_g(t=0),\ \dot{\theta}_g(t=0)$ $\theta_p(t=0),\ \dot{\theta}_p(t=0)$	$\mathrm{T}(t), \theta_g(t=0),\ \dot{\theta}_g(t=0)$ $\theta_p(t),\ \dot{\theta}_p(t),\ \ddot{\theta}_p(t)$
Output	$\theta_p,\ \dot{\theta}_p\ ,\theta_g,\ \dot{\theta}_g$	$\theta_g,\ \dot{\theta}_g$

In the next section, the modelling of excitations in Eq. (3.11) including $\mathrm{T}(t)$, $\theta_p(t)$, $\dot{\theta}_p(t)$, and $\ddot{\theta}_p(t)$, will be investigated. The models of $\theta_p(t)$, $\dot{\theta}_p(t)$, and $\ddot{\theta}_p(t)$ have not been studied in Ref. [23].

3.2.2 External load and driving speed formulation

In this section, the purpose is to make Eq. (3.11) solvable by numerical method, i.e., Runge-Kutta method.

To solve Eq. (3.11), the key point is to obtain $\theta_p(t)$ and $\ddot{\theta}_p(t)$ under any given $\dot{\theta}_p(t)$. Two cases of $\dot{\theta}_p(t)$, deterministic and stochastic models, will be studied in Section 3.2.2.1 and Section 3.2.2.2, respectively. The adopted deterministic model of $\dot{\theta}_p(t)$ is reported in Ref. [24]. The stochastic model of $\dot{\theta}_p(t)$ is based on the model in Ref. [1] with additional consideration of the randomness studied in Ref. [61].

It should be noted that the effects of both deterministic and stochastic driving speed on gear dynamics under stochastic load are still short of investigation. In addition, the derivation of $\theta_p(t)$ and $\ddot{\theta}_p(t)$ according to stochastic $\dot{\theta}_p(t)$ is considered in gear dynamic modelling for the first time.

3.2.2.1 Deterministic model of $\dot{\theta}_p,\ \theta_p,\ \ddot{\theta}_p$ as reported in Ref. [1]

For a combustion engine, due to many factors such as gas pressure, bore, stroke of engine, and inertia of moving parts during the power stroke, the engine generates stochastic velocity $\dot{\theta}_p(t)$ and torque T [1] [24]. In this study, the energy loss in the connection of engine and pinion is ignored. The excitation speed of pinion $\dot{\theta}_p(t)$ from an internal combustion engine, fluctuates significantly between low (around the compression stage) and high (around the ignition stage) values [26]. Therefore, the model of the total driving speed in pinion can be assumed to be a summation of a constant angular velocity term and a small variation [26].

Therefore, a general expression of $\dot{\theta}_p$ can be formulated as reported in Ref. [1]:

$$\dot{\theta}_p(t) = \chi_0 + \sum_n \chi_n \sin(\rho_n t + \psi_n) \tag{3.12}$$

where t is the time in second (s), χ_0 is a constant which represents the mean of the driving speed, n denotes the harmonic of the driving speed, and ρ_n, χ_n, and ψ_n are the corresponding angular frequency, amplitude and initial phase, respectively.

If the conditions of θ_p and $\ddot{\theta}_p$ at $t = t_0$ are known, the absolute angular displacement θ_p and acceleration $\ddot{\theta}_p$ can be analytically determined by integration and differentiation to velocity $\dot{\theta}_p$, respectively.

Assuming a time interval $\Delta t = t - t_0$, the angular displacement θ_p and the angular acceleration $\ddot{\theta}_p$ of the pinion at arbitrary time t can be expressed as follows

$$\theta_p(t) = \theta_p(t_0) + \chi_0 \Delta t + \sum_n \chi_n \frac{\sin(\rho_n t) - \sin(\rho_n t_0)}{\rho_n} \tag{3.13}$$

$$\ddot{\theta}_p(t) = -\sum_n \chi_n \rho_n \sin(\rho_n t) \tag{3.14}$$

3.2.2.2 Stochastic model of $\dot{\theta}_p,\ \theta_p,\ \ddot{\theta}_p$

The objective of this section is to derive the model of θ_p and $\ddot{\theta}_p$ based on stochastic $\dot{\theta}_p$. Considering randomness, Eqs. (3.17), (3.22), and (3.23) reveal reality on some occasions and make an improvement compare to the existing work.

The expression of the rotational motion in the pinion ($\dot{\theta}_p,\ \ \theta_p,\ \ \ddot{\theta}_p$) within deterministic domain are given in Eqs. (3.12)–(3.14). Due to errors of manufacturing, processing, assembling, wear, lubrication, operating environment, and other factors, the combustion engine's rotational speed and external load may not be deterministic [2]. Accordingly, the random part in the anticipated external load and anticipated driving speed needs to be considered. According to the studies in [61] and [5], it is assumed the randomness in the driving speed and load are Gaussian white noise $\xi_i(t)$, ($i = 1, 2$).

$$E(\xi_i(t)) = 0 \tag{3.15}$$

$$E[\xi_i(t)\xi_i(t+\tau)] = r_i\Theta(\tau) \tag{3.16}$$

where $\xi_i(t)$ is a Gaussian white noise with variance r_i, subscript $i = 1$ represents driving speed, $i = 2$ refers to the load, and Θ is the Dirac Delta function.

Thus, Eq. (3.12) can be rewritten as:

$$\dot{\theta}_p(t) = \chi_0 + \sum_n \chi_n \sin(\rho_n t + \psi_n) + \xi_1(t) \tag{3.17}$$

The physical meaning of this driving speed profile can be explained as [56]:

1. The pistons move up and down periodically in their cylinders,
2. The periodic behavior can be expressed as a combination of a series of sinusoidal functions (i.e., Fourier series),
3. Considering kinds of factors (e.g., manufactory errors), the randomness is expressed as Gaussian white noise [5] [61].

Similarly, the profile of the driving torque is also periodic. We consider the case that T_g is periodic or constant. For example, centrifugal pump or wheels is the load in output of a gear system. Accordingly, the external load T can also be expressed via Fourier series combined with Gaussian white noise as following:

$$\mathrm{T}(t) = f_0 + \sum_j f_j \cos(\nu_j t + \beta_j) + \xi_2(t) \tag{3.18}$$

where f_0 is a constant, j denotes the harmonic of the torque, ν_j, f_j, and β_j are the corresponding angular frequency, amplitude, and initial phase, respectively. Note that the adopted speed profile and load profile in this study are also widely adopted in lots of existing works. For example, the similar speed profile (i.e., Eq. (3.17)) is also adopted in [1], [2], and [24], and the similar load profile (i.e., Eq. (3.18)) is also adopted in [94], [60], and [96].

Recall Ref. [1], the external load T is modelled as:

$$\mathrm{T}(t) = f_0 + \sum_j f_j \cos(\nu_j t + \beta_j) \tag{3.19}$$

As we known, Gaussian diffusion process $\Phi(t)$ is the integration of Gaussian noise. $\Phi(t)$ can be approximated as follow by $\mathrm{It\hat{o}}$ [98] SDE [99].

$$d\Phi(t) = \lambda dt + \sigma dW(t) \tag{3.20}$$

where λ is the drift scalar, σ is the diffusion scalar, and $W(t)$ is a standard Wiener process. In addition, $dW(t)$ can be approximated as $dW(t) \sim \sqrt{\Delta t}$ [82] [100]. For a Gaussian white noise $\xi_1(t)$, $\lambda = 0$ and $\sigma = \sqrt{r_1}$. The approximate integration of Eq. (3.17) can be obtained as follows:

$$\theta_p(t) = \theta_p(t_0) + \chi_0 \Delta t + \sum_n \chi_n \frac{\sin(\rho_n t) - \sin(\rho_n t_0)}{\rho_n} + \sqrt{r_1 \Delta t} \tag{3.21}$$

On the other hand, $\ddot{\theta}_p$ can be defined in Eq. (3.22). Here, the slope of two points has been used to approximate the derivate. Although there is accuracy loss, this assumption has calculation benefit in numerical simulation.

$$\ddot{\theta}_p(t) = -\sum_n \chi_n \rho_n \sin(\rho_n t) + \frac{\xi_1(t) - \xi_1(t_0)}{\Delta t} \tag{3.22}$$

For dynamic modelling of the gear system under stochastic load, the proposed model (Eq. (3.11) combining with Eqs. (3.17), (3.21), and (3.22)) considers randomness in the pinion rotational motion for the first time.

To avoid confusing, Table 3.2 shows the comparison of the models between existing works and the proposed model. In these three models, TVMS, backlash, damping, and friction are all taken into account. Although both of Ref. [23] and Ref. [1] modelled the sliding friction, the friction model in Ref. [23] reflects reality more than that in Ref. [1]. Thus, the proposed model adopts the friction model in Ref. [23]. The existing works [1] [24] [26] only considered deterministic driving speed under deterministic load. However, the proposed model considers both deterministic and stochastic $\dot{\theta}_p$ under stochastic load.

Table 3.2: Comparison of the model between existing works and our work

	External load T	Driving speed $\dot{\theta}_p$
Ref. [23]	Stochastic Eq. (3.18) with $j = 1$	None (i.e., free vibration)
Ref. [1]	Deterministic Eq. (3.19)	Deterministic Eq. (3.12)
Proposed model	Stochastic Eq. (3.18)	Deterministic Eq. (3.12)
		Stochastic Eq. (3.17)

The challenge in this proposed model deals with one or two more stochastic factors in the gear dynamic modelling which adds complexity in solving the model and in the results analysis.

3.3 Results and discussion

To analyze the dynamic characteristics of the proposed model, this section gives the numerical simulation results. The main objective of this section is to investigate the driving speed effects on system's dynamic characteristics under stochastic load. The reported work is duplicated in Section 3.3.1 to validate the proposed model. The investigations of the proposed model are shown from Section 3.3.2 to Section 3.3.4.

In Section 3.3.1, the dynamic responses under deterministic driving speed and deterministic load are obtained. Section 3.3.2 gives the dynamic characteristics under deterministic driving speed and stochastic load. Section 3.3.3 studies the dynamic characteristics under stochastic driving speed and stochastic load. The results of Section 3.3.2 and Section 3.3.3 are compared with each other. Section 3.3.4 investigates the coupled effects and sensitivity.

3.3.1 Validation of the proposed model

The driving speed has been studied in Ref. [1], which studied a model of a spur gear pair under deterministic load considering TVMS, backlash, friction, and deterministic driving speed. This model has been validated with a finite element model. It was concluded that this model captured the salient behaviour of the actual system.

To conduct validation, it is necessary to keep parameters in the proposed model and the model in Ref. [1] the same. However, there are two differences in the two models:

1. the friction model in Ref. [1] is simplified as sign function;
2. external load in Ref. [1] is deterministic while it is stochastic in the proposed model. If Eq. (3.17) is replaced by Eq. (3.19), namely, removing the random term in load, the proposed model is reduced to the model in Ref. [1].

The gear pair parameters in Table 3.3 are adopted for validation and they will be used in the following sections' simulations. The friction coefficient usually varies with load [80] [53] but the variation in the friction coefficient can be ignored with small variations in load [85]. In this study, the friction coefficient is fixed at 0.04 to illustrate the driving speed effect on gear dynamic characteristics.

Table 3.3: Gear pair parameters

Inertia moment of pinion	$I_p = 2.6 \times 10^{-4}\ Kg \cdot m^2$
Inertia moment of gear	$I_g = 0.0045\ Kg \cdot m^2$
Base circle	$r_p = 0.034\ m,\ r_p = 0.052\ m$
Pressure angle	$\alpha_0 = 20^\circ$
Stiffness	$k_1 = 1.6 \times 10^8 N/m, k_2 = 0.9 \times 10^8 N/m$
Friction coefficient	$\mu = 0.04$
Backlash	$b = 0.05mm$

The relative displacements by the proposed model and Ref. [1] (see Fig. 3.2) are almost the same. It illustrates that the proposed model and the model in Ref. [1]

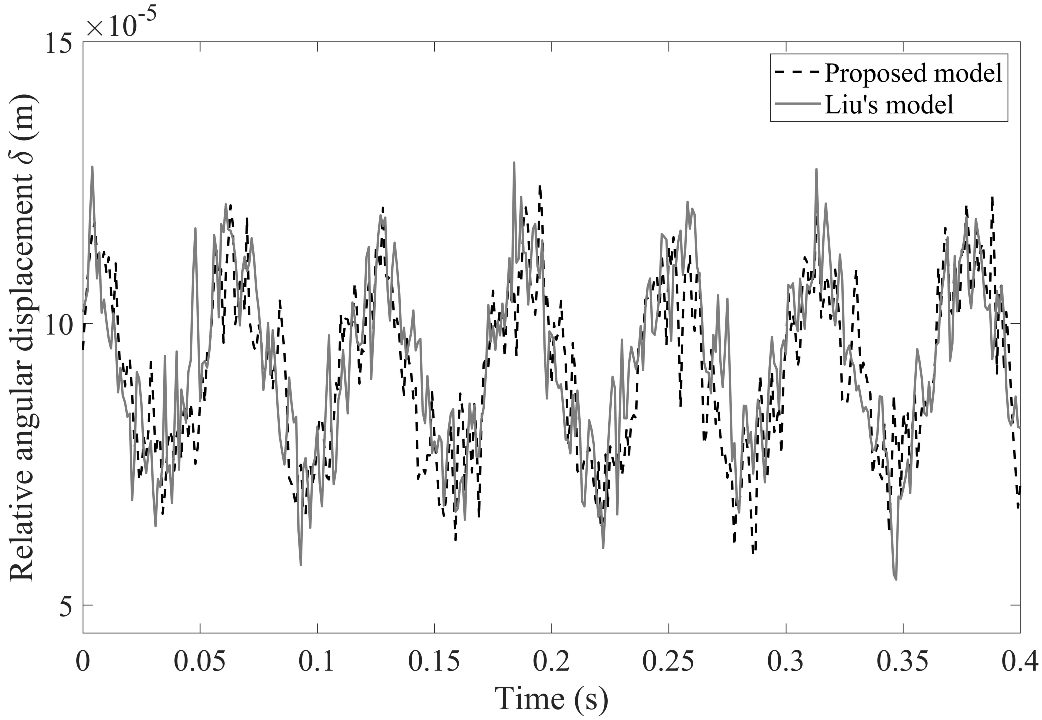

Fig. 3.2: Relative angular displacement comparison between two methods

can be considered as the same in dynamic performance with a small error range. Note that Liu's Model in Fig. 3.2 means the model in Ref. [1]. Although the friction models are slightly different, the validation still supports the correctness of our model to some degree.

3.3.2 Dynamic responses under deterministic driving speed and stochastic load

In this section, a numerical example is studied with two external excitations: deterministic driving speed and stochastic load. This assumption might be reasonable for certain occasions, e.g., the engine is in quite good condition and assembled advanced speed control equipment. Here, the randomness in $\dot{\theta}_p(t)$ is negligible. The dynamic responses are obtained by Matlab after solving single degree of freedom ODE using the Runge-Kutta method [101].

The stochastic load is set in Eq. (3.23) with $r_2 = 2500$:

$$\mathrm{T}(t) = 500 + 50\cos(100t) + \xi_2(t) \tag{3.23}$$

In order to study the effects of $\dot{\theta}_p(t)$ on dynamic characteristics, a coefficient λ_1

is introduced in the speed equation to adjust its amplitude.

Five cases with $\lambda_1 = \{0.5,\ 0.75,\ 1,\ 1.25,\ 1.5\}$ will be compared and other parameters will be the same. The driving speed is formulated as:

$$\dot{\theta}_p(t) = \lambda_1 \left[800 + 80\cos(100t + \pi/2) + 20\cos(80t + \pi/2)\right] \tag{3.24}$$

With initial condition $\theta_p(t = 0) = 0$, the examples of $\theta_p(t_i)$ and $\ddot{\theta}_p(t_i)$ can be obtained correspondingly.

$$\begin{aligned}\theta_p(t_i) = \lambda_1 [\theta_p(t_{i-1}) + 800\Delta t + 0.8\cos(100t) - 0.8\cos(100t_{i-1}) \\ +0.2\cos(80t) - 0.2\cos(80t_{i-1})]\end{aligned} \tag{3.25}$$

$$\ddot{\theta}_p(t_i) = \lambda_1 \left[-8000\sin(100t_i + \pi/2) - 1600\sin(80t_i + \pi/2)\right] \tag{3.26}$$

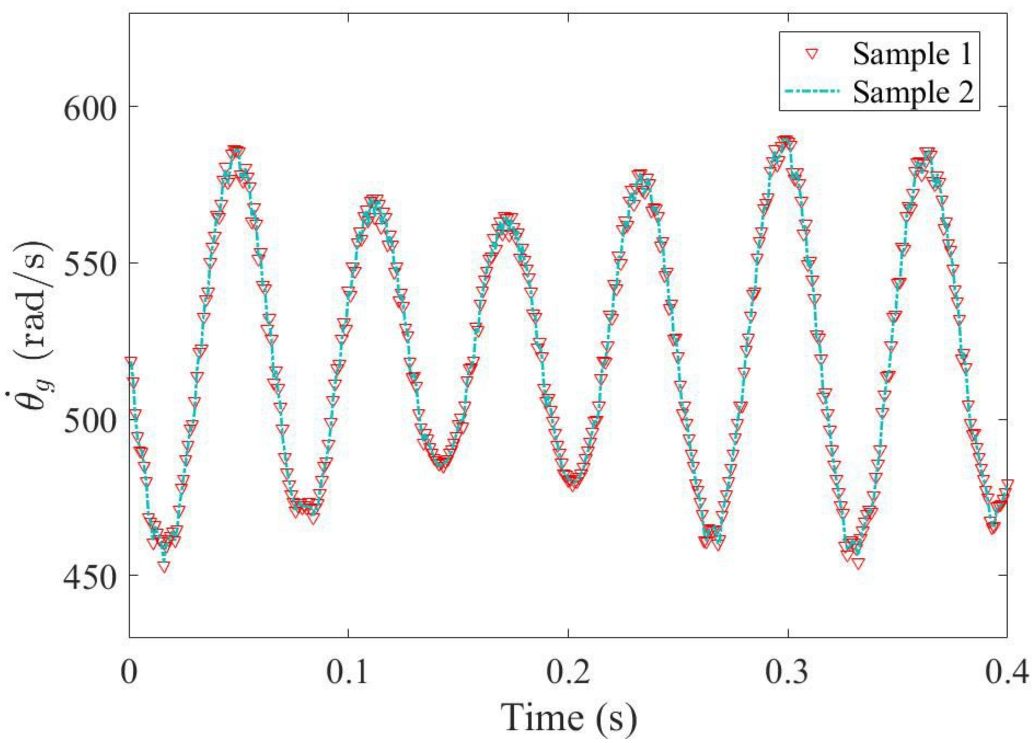

Fig. 3.3: Time history for $\dot{\theta}_g$ with $\lambda_1 = 1$

The responses described in Fig. 3.2 are deterministic, which means δ has a unique value at arbitrary time point. We know that the responses of a gear model become random due to the stochastic load. Fig. 3.3 and Fig. 3.4 show two realizations of $\dot{\theta}_g$ and δ with $\lambda_1 = 1$, respectively. From Fig. 3.3, the rotation speed

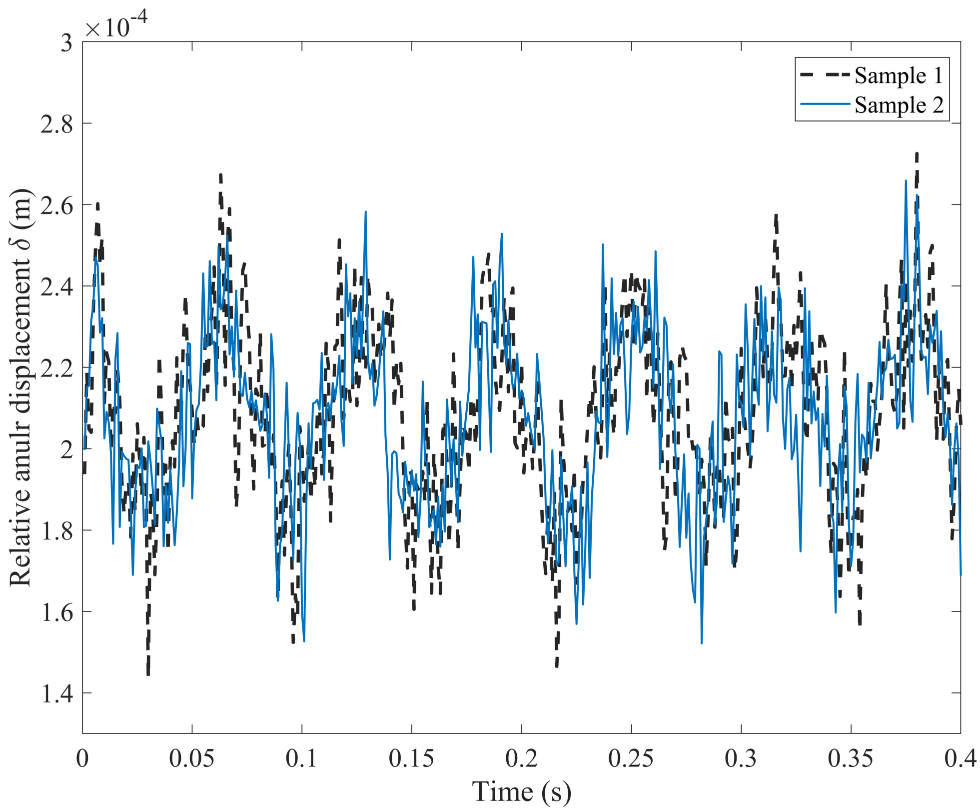

Fig. 3.4: Time history for δ with $\lambda_1 = 1$

$\dot{\theta}_g$ has significant periodicity. The modulated sinusoidal waves are not smooth and contain disturbance. But the difference between the two realizations is very small.

In Fig. 3.4, the relative displacement δ shows its quasi sinusoidal property. However, the disturbances are much greater than that in $\dot{\theta}_g$. The difference in the amplitude of δ among the two curves is easy to find which is only caused by the stochastic load.

Probability method is the most common approach to study the uncertainty. Other approaches include interval method, fuzzy method and so on [2] [102]. To obtain the responses of a gear model under stochastic load by the probability methods, researchers usually focus on getting the statistical characteristics of the responses, such as, mean, variance, and PDF [103] [104]. In some applications, such as fatigue prediction and reliability, actual PDF is needed [105].

Enough samples are obtained through MC method to obtain a reasonable

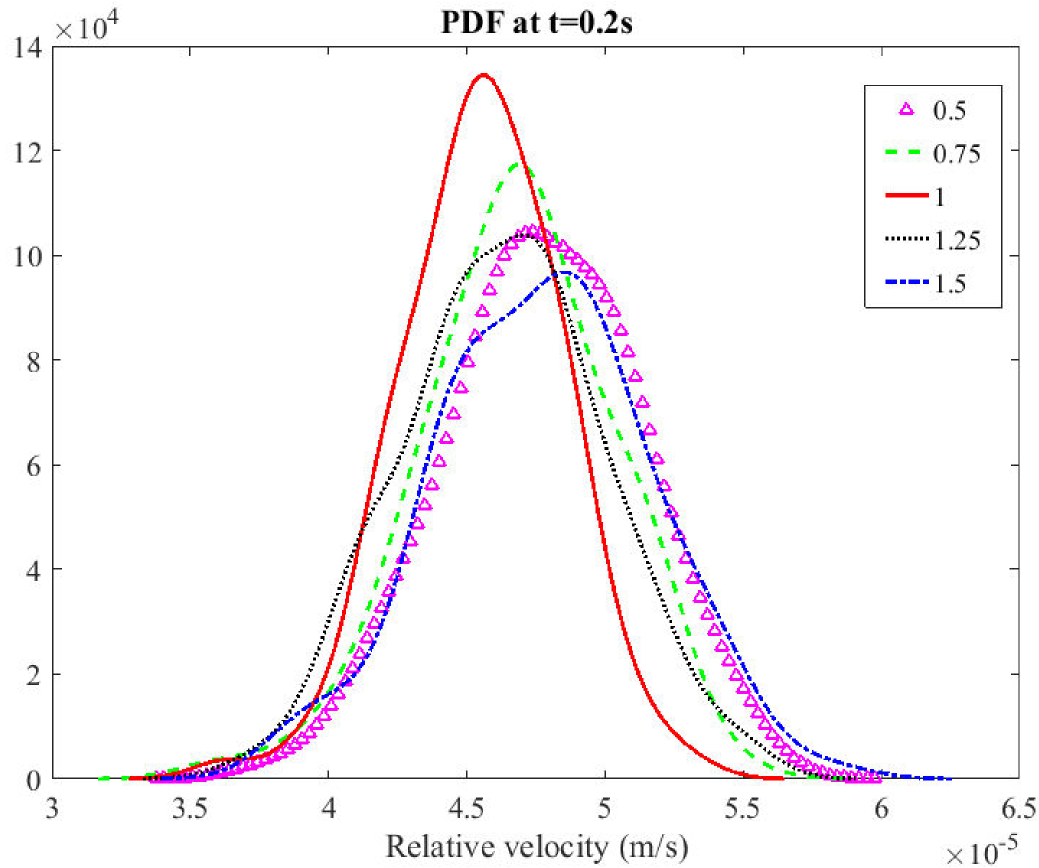

Fig. 3.5: PDFs of $\dot{\delta}$ at 0.2 s in five cases of λ_1

accuracy. According to the statistical analysis on responses of five cases of λ_1 ($\lambda_1 \in \{0.5, 0.75, 1, 1.15, 1.5\}$), five instantaneous PDFs under different relative velocities are shown in Fig. 3.5. Note that the relative velocity, denoted $\dot{\delta}$, is the first derivation of δ. The standard deviations of the five cases from $\lambda_1 = 0.5$ to $\lambda_1 = 1.5$ are 1.4458×10^{-5}, 1.5137×10^{-5}, 1.2578×10^{-5}, 1.6283×10^{-5}, and 1.5987×10^{-5}, respectively. It is found that, at $t = 0.2$ s, the driving speed with $\lambda_1 = 1$ leads to the lowest dispersion in responses among the five cases. Thus, the variation of amplitude in $\dot{\theta}_p$ affects the dispersion of response.

3.3.3 Dynamic responses under stochastic driving speed and stochastic load

In this section, the stochastic $\dot{\theta}_p$ is considered while $\dot{\theta}_p$ is considered as deterministic in the previous section. This assumption might be suitable on some occasions, for example, the crankshaft of engine has deflection [106] or fouled spark plugs have excessive carbon deposits [60].

The load is simulated using Eq. (3.23) and the driving speed is simulated using Eq. (3.17). Thus, $\dot{\theta}_p(t)$ is set in the form of Eq. (3.27) with $r_1 = 25$:

$$\dot{\theta}_p(t) = 800 + 80\cos(100t + \pi/2) + 20\cos(80t + \pi/2) + \xi_1(t) \tag{3.27}$$

Compare Eq. (3.27) with Eq. (3.24) ($\lambda_1 = 1$), the only difference is the random term $\xi_1(t)$. Thus, the gear model is now excited by two stochastic excitations (T and $\dot{\theta}_p(t)$).

Fig. 3.6 presents the two instantaneous PDFs with two profiles of the driving speed at $0.2s$. Keep everything else the same, the two profiles of the driving speed are only distinct in the stochastic term. From Fig. 3.6, the difference of PDFs is only caused by the stochastic term in the driving speed. It is clearly shown that the responses excited by stochastic driving speed has more dispersion than those excited by deterministic driving speed. Although the ratio of the uncertainty ($5/800 = 0.625\%$) is quite small, the variance of responses under the stochastic driving speed case is larger than that under the deterministic driving speed case.

The standard derivations of δ under two driving speed profiles are shown in Fig. 3.7. Fig. 3.7 further illustrates that the large variance caused by the stochastic driving speed is not by accident. During the period (0 to 0.4 s), the standard deviation of δ obtained by stochastic driving speed is always greater (about twice greater) than that obtained by deterministic driving speed.

3.3.4 Load and driving speed coupled effects

In this section, we will focus on the coupled effects of load and driving speed on dynamic characteristics. The two excitations are coupled and some nonlinear factors (e.g., friction) are involved in the gear dynamic modelling. The following paragraphs aim to analyze their coupled effects on the dynamic characteristics from two aspects: parametric sensitivity and chaotic analysis.

First, the parametric sensitivity of load and driving speed on dynamic characteristics worth the effort to explore. Define two sensitivity parameters η_1 and η_2 for

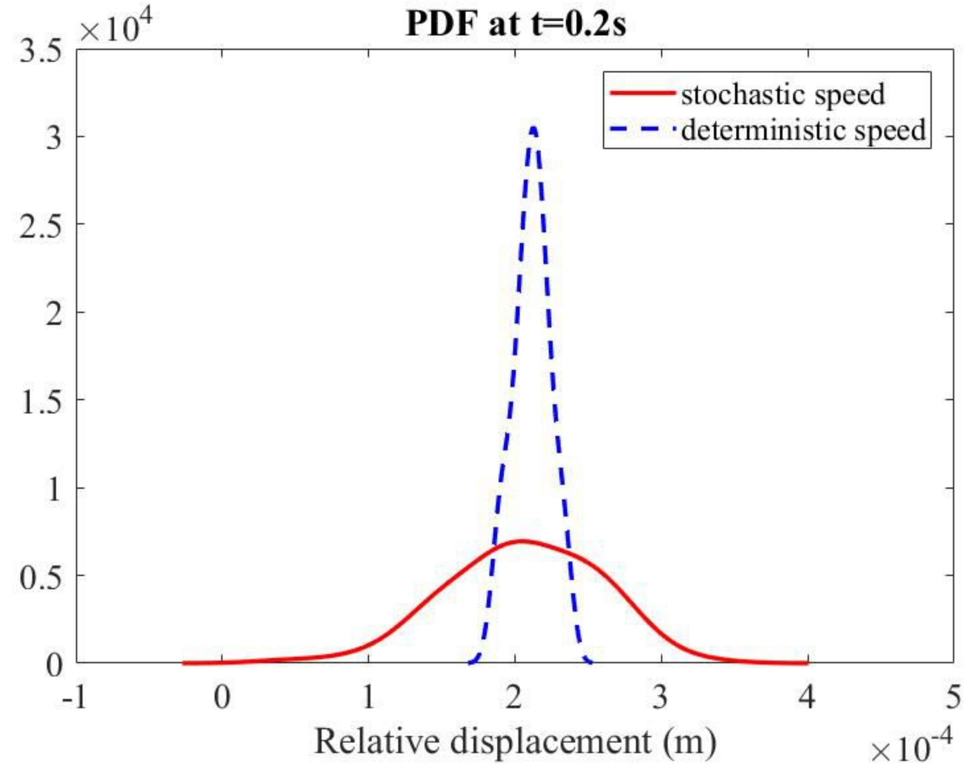

Fig. 3.6: PDF comparison of two cases

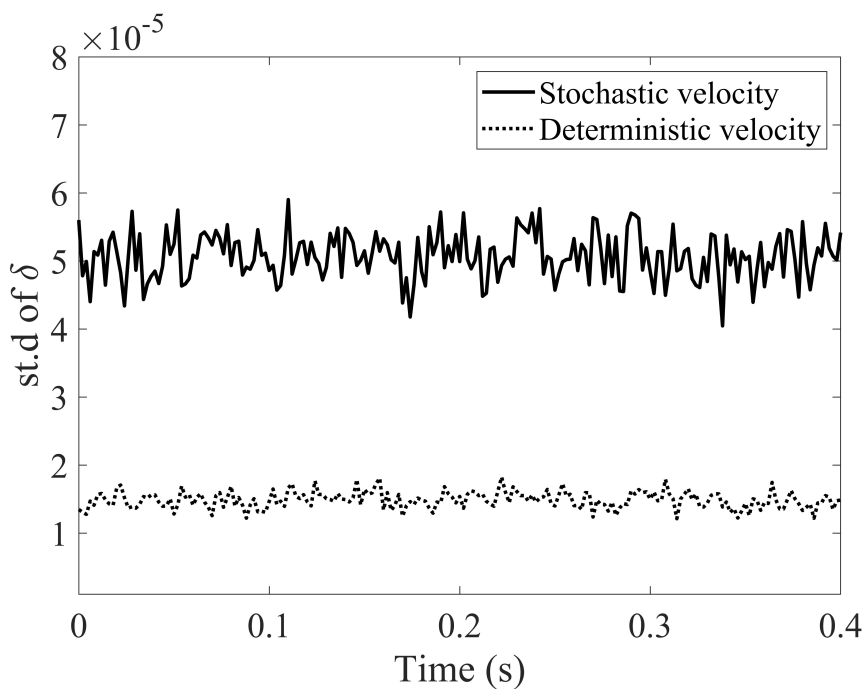

Fig. 3.7: Standard derivation of δ with time variation

driving speed and load, respectively. The expressions of η_1 and η_2 are shown as Eq. (3.28) and Eq. (3.29), respectively. Note that r_1 and r_2 are defined in Eq. (3.16).

$$\eta_1 = \frac{\sqrt{r_1}}{E(\dot{\theta}_p)} \tag{3.28}$$

$$\eta_2 = \frac{\sqrt{r_2}}{E(\mathrm{T})} \tag{3.29}$$

Keep the mean values $E(\dot{\theta}_p)$ and $E(\mathrm{T})$ invariant and adjust the values of r_1 and r_2 to change the values of η_1 and η_2. Table 3.4 summarizes the standard deviation of δ under different η_1 and η_2. According to Table 3.4, the standard deviation of δ increases with the increase of η_1 and η_2. Fig. 3.8 and Fig. 3.9 demonstrate the results of the standard derivation of δ with the varying of η_1 and η_2, respectively. It can be seen that the slope in Fig. 3.8 is greater than that in Fig. 3.9. It is proven that the standard derivation of δ increases more with the variation in η_1. Alternatively, the average increase rates, denoted κ_1 and κ_2, are different (see Eqs. (3.30) (3.31) for definition).

$$\kappa_1 = \frac{1}{6}\sum_{i=1}^{3}\left(\frac{< i, 2 >}{< i, 1 >} + \frac{< i, 3 >}{< i, 2 >}\right) \tag{3.30}$$

$$\kappa_2 = \frac{1}{6}\sum_{i=1}^{3}\left(\frac{< 2, i >}{< 1, i >} + \frac{< 3, i >}{< 2, i >}\right) \tag{3.31}$$

where κ_1 and κ_2 are the average increase rates of the driving speed and load, respectively. $< i, j >$ represents the element in ith row and jth column in Table 3.4 without counting the header.

Table 3.4: Standard derivation of δ under different η_1 and η_2

	η_1		
η_2	0.5%	0.65%	0.8%
0.5%	1.0655×10^{-5}	2.0038×10^{-5}	3.7009×10^{-5}
0.65%	1.0715×10^{-5}	2.1316×10^{-5}	4.3268×10^{-5}
0.8%	1.1444×10^{-5}	2.4168×10^{-5}	4.5109×10^{-5}

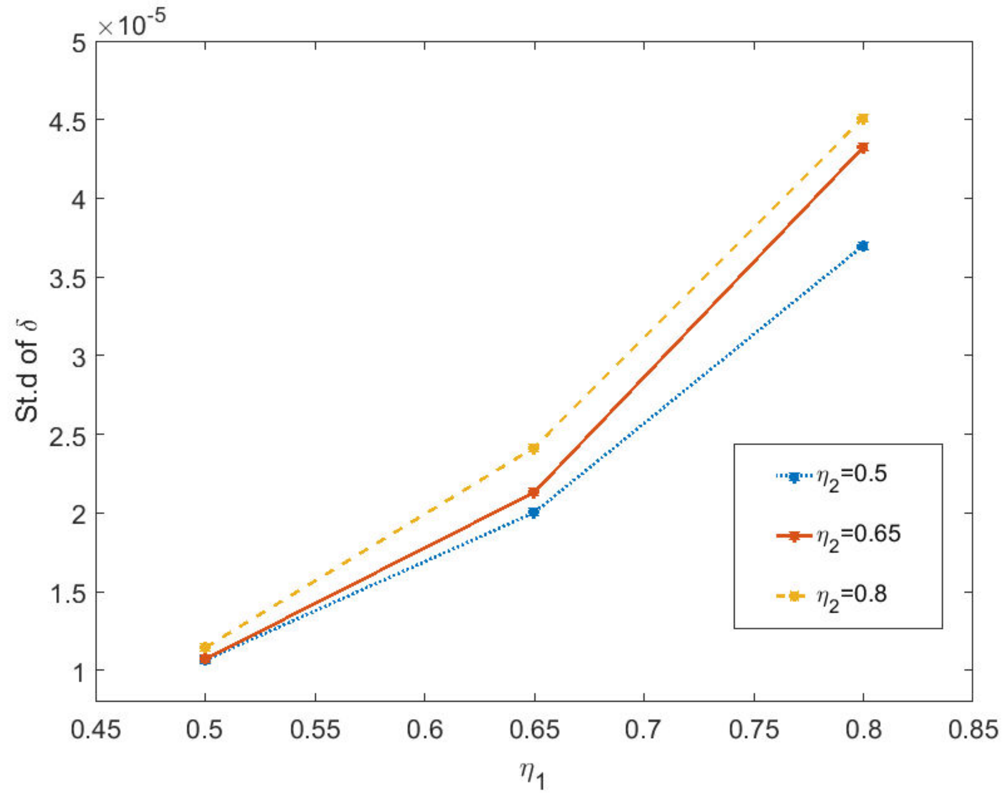

Fig. 3.8: Standard derivation of δ with varying η_1 at the same η_2

Under the same η_1, the average increasing rate κ_2 is 1.09. For the same η_2, the average increase rate κ_1 is 1.97. Thus, the standard deviation of δ is more sensitive to the increasing of η_1. It is concluded that the same increment ratio in the variance of the driving speed causes a larger increase in the variance of responses than that of load. It means that the randomness in the $\dot{\theta}_p(t)$ has a more significant effects on gear systems than that in T. To some degree, the randomness in the $\dot{\theta}_p(t)$ may cause more vibration and failure. The control of its randomness is more important in real applications.

Fig. 3.10 describes the phase diagram ($\delta - \dot{\delta}$ relationship) with the driving speed defined in Eq. (3.27). It should be noticed that δ and $\dot{\delta}$ are the mean value of the total samples. Recalling the phase diagram in Ref. [23], the orbit $\delta - \dot{\delta}$ in the phase portrait is non-smooth and non-periodic with the consideration of the driving speed as an excitation. This chaotic oscillation can be intuitively observed in Fig. 3.10. This phenomenon could be affected by the coupling of the stochastic driving speed and stochastic load.

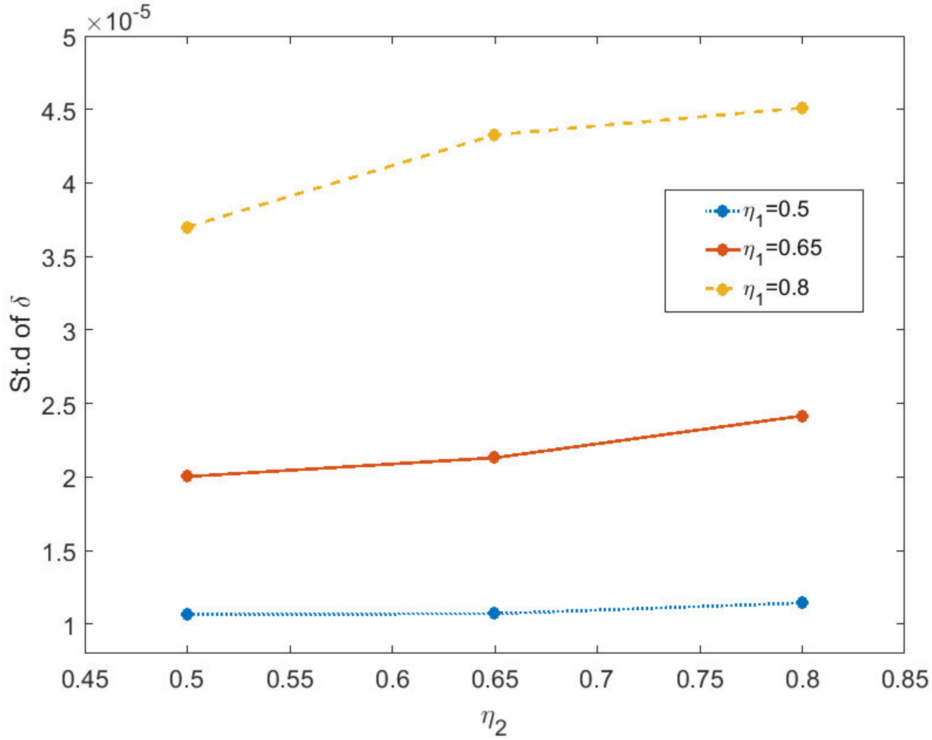

Fig. 3.9: Standard derivation of δ with varying η_2 at the same η_1

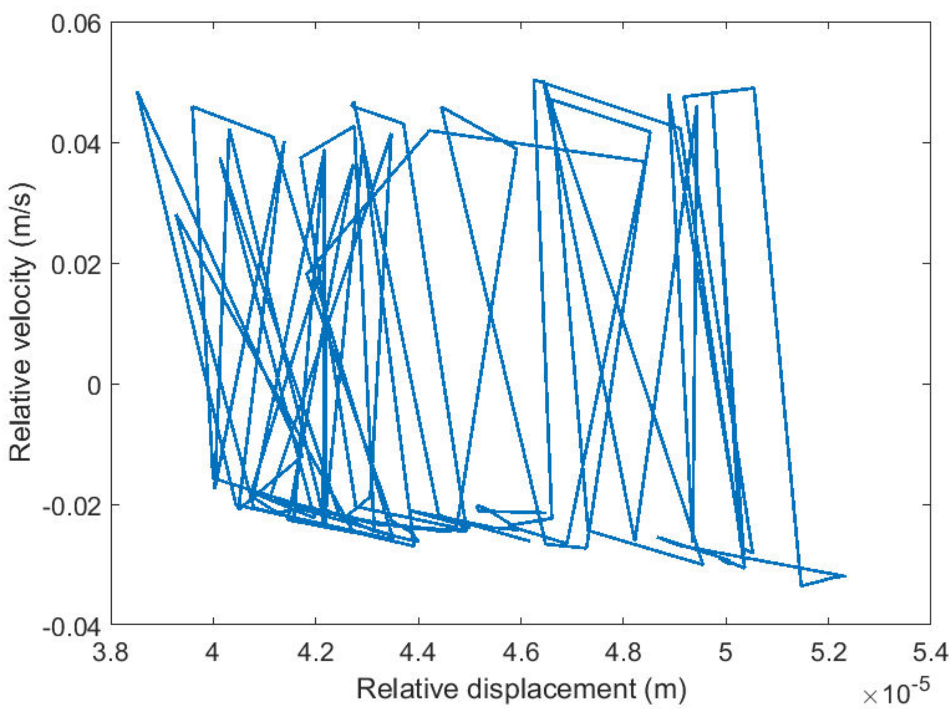

Fig. 3.10: Phase diagram

It is known that dispersion and chaos in dynamic responses cause more noise and failure. Therefore, controlling the randomness in the engine is quite important. Especially, reducing the same ratio of randomness in the driving speed leads to a greater decrease in potential failure than that of load. More attention needs to be paid to the randomness in the driving speed. Furthermore, regular inspection of the engine is expected to reduce the randomness in the load and driving speed.

3.4 Conclusion

In this study, a gear stochastic dynamic model for a spur gear pair considering TVMS, gear mesh damping, backlash, friction, and stochastic load is established. In addition, the driving speed (including deterministic or stochastic) is modeled in the gear dynamic model. The dynamic responses of this model are investigated using numerical simulation and compared with previous work.

Some insightful conclusions are demonstrated as follows:

(a) the established model is more realistic by considering the randomness in the driving speed and load compared with the existing models,

(b) under the same stochastic load, the amplitude of the deterministic driving speed affects the responses' rotational motion, vibration, and dispersion,

(c) under the same stochastic load, a small ratio of randomness in the driving speed will greatly increase the dispersion in responses,

(d) the dispersion in responses is more sensitive to the uncertainty in the driving speed than that of load.

The proposed gear dynamic model and numerical results can be used as a useful tool to investigate the gear random dynamics due to the following reasons.

(a) The proposed gear dynamic model considers TVMS, backlash, sliding friction, driving speed, and stochastic external load. It is more realistic than the existing works (refer to Table 3.1) that did not consider the driving speed as an external stochastic excitation. Thus, the proposed model can be used to investigate the gear random dynamics and gear diagnosis [107] [108],

(b) Our work investigates the effects of stochastic driving speed variation on gear dynamic characteristics under stochastic load for the first time. Thus, our work provides a method how to analyze a gear dynamic model with multiple stochastic elements (e.g., stochastic driving speed and stochastic load). It can be a reference for other researches about gear dynamic model with multiple stochastic elements,

(c) In our work, some insightful conclusions are summarized by simulation results using MC method. These conclusions are important for the gear random dynamics study.

Future works include design lab experiments to validate our numerical findings. The influence on the gear dynamic characteristics from other types of engine (e.g., electric engine) will be modeled and investigated.

In summary, on top of the work reported in Chapter 2, this chapter addressed the additional external factor of driving speed. Under stochastic load, the external driving speed is modeled as a Fourier series combined with Gaussian white noise. Therefore, the stochastic feature of the driving speed can be modeled well. Then, the coupling effects on gear dynamic characteristics from multiple stochastic excitations were studied. By MC simulation, some insightful conclusions can be obtained. As an extension of the work of Chapter 2, the proposed model in this chapter can demonstrate the real gear systems well. This study broadens the way of thinking in gear stochastic dynamics and provides a reference for engineers to choose proper engine together with its controller.

4

Approximate Analytical Solution considering Stochastic Load and a Stochastic Internal Factor

For the previous two chapters, the stochastic internal factor (friction) and external factors (load and driving speed) have been studied in gear dynamic models. To investigate the dynamic characteristics of gear systems, the proposed gear dynamic models are solved by numerical method in Chapter 2 and Chapter 3. However, the calculation cost of the numerical method is large, especially for the models under stochastic excitations. The cost may not be acceptable in reality. In addition, the stochastic behavior of the internal factors may depend on gear velocity and/or displacement, which will cause the dynamic equations to be difficult to solve. Thus, an efficient solving technique is needed to solve such stochastic model. In this chapter[1], we consider the gear dynamic model under stochastic load with treating one of the internal factors as stochastic. Then, an efficient method is proposed in this chapter, and thus, an approximate analytical

[1]The work of this chapter has been accepted or submitted for peer review as follows:
Y. Fang, M. J. Zuo, and Y. Li, "Efficient analytical method to obtain the responses of a gear model with stochastic load and stochastic friction," in *Proceeding of the 6th International Conference on Mechanical Engineering, Materials Science and Civil Engineering (ICMEMSCE)*, Xiamen, China, Dec. 21-22, 2018. 7 pages (USB).
Y. Fang, X. Liang, and M. J. Zuo, "Approximate analytical solution to a spur gear model with stochastic excitations," *Journal of Mechanical Science and Technology*. Submitted on Oct. 28, 2018.

solution can be obtained under the considered gear model. In the proposed method, a transformation of the original dynamic equation is introduced first so that the reported Path integration (PI) method can be adopted to obtain a tentative analytical solution. Then, a modification function obtained by supervised learning method is applied to the tentative analytical solution to obtain the final approximate analytical solution of the formulated dynamic equation. A case study based on the model in Chapter 2 is used to validate the proposed method and demonstrate its efficiency. Compared to Monte Carlo (MC) method, our proposed method can achieve similar accuracy responses of the gear model but with much smaller time complexity.

4.1 Introduction

Due to the unique technique advantages, gears are one of the most widely adopted mechanical parts. The research about dynamics and vibrations of gear systems is significant important to the development of mechanical theory [27]. Models adopted in gear dynamics under deterministic domain have been investigated in decades. However, stochastic load is one of the main sources of gear vibration and noise in reality [24]. Several researchers considered stochastic load in gear system dynamic modeling. The speed-dependent stochastic errors in spur gear pair model was considered in [32]. Theodossiades and Natsiavas [39] introduced a gear model under stochastic load with transmission error, backlash, and periodic gear mesh stiffness. Yang et al. [44] investigated a gear dynamic model with Gaussian white noise under constant mesh stiffness and constant damping coefficient. Wen et al. [5] studied a gear pair under stochastic load with the consideration of backlash, TVMS, and constant damping coefficient. Imaouchen et al. [109] proposed a new way for gear diagnosis when considering the varying of load. In [77], the characteristics of transmission error and vibration of broken tooth contact were investigated with the varying of load.

Based on the well-developed probabilistic theory, statistical methods are mainly used in obtaining the responses of a gear system under stochastic load (i.e. solving the corresponding dynamic equations). They include statistical linearization method [63], stochastic averaging method [64], Runge Kutta-Monte Carlo method, PI method also called cell mapping [66], [67], and statistical Newmark method [68]. For simplicity, we abbreviate Runge Kutta-Monte Carlo method as MC method. To obtain the responses of a gear model under stochastic load by statistical methods, researchers usually focus on getting the statistical characteristics of the responses, such as, mean, variance, and probability density function (PDF) [110]. Wei et al. [2] reviewed the main ideas and statistical characteristics of each statistical method as shown in Table 4.1.

Table 4.1: Statistical methods and their characteristics [2]

Name	Characteristics
Statistical linearization method	It provides the variance of responses by approximating the original nonlinear system to a linear system with the minimum error.
Stochastic averaging method	It derives an approximate analytical solution (i.e., PDF) to small damping nonlinear system by transforming the time varying parameters in a system to time invariant parameters.
MC method	It provides PDF with high accuracy by using numerical simulation to generate a number of response samples.
Path integration method	It gives analytical expression of the PDF by assuming transition PDF within a short time interval as Gaussian distribution.
Statistical Newmark method	It derives mean and variance of responses by utilizing the recursive equation of each discrete time point.

To demonstrate the responses of a gear system, there are two kinds of forms, namely, analytical expression or numerical solutions (i.e., statistical analysis of responses samples) [2]. About the methods in Table 4.1, some methods, such as stochastic averaging method and PI method, are to obtain the analytical expression. However, the methods including MC method and Statistical Newmark method are to obtain the numerical solutions. Obtaining numerical solutions is costly since a great number of samples are required for reasonable accuracy [91]. By contrast, it would save much time if we could get the approximate analytical solution [12]. We focus on obtaining the approximate analytical solution in this work.

Several researchers have explored the analytical solution to a gear dynamic model under stochastic load. Sato [70] studied the analytical solution of a gear system under stochastic load with consideration of transmission error and TVMS. Naess et al. [67] derived the analytical solution to a gear system considering constant stiffness, constant damping coefficient, and backlash under the excitation of white noise. Wen et al. [5] obtained the analytical solution to a gear system considering constant damping coefficient, TVMS, and backlash under the combination of deterministic load and white noise. All these models considered the internal factors of a gear system (e.g., backlash, TVMS, and damping) as deterministic while the external load is stochastic.

In reality, many internal factors of a gear system have random variations and they affect the system's dynamic behavior greatly [111]. Lu et al. [45] studied the influence of stochastic perturbations of damping ratio and backlash on dynamic behaviors of gear systems. Handschuh [46] and Inalpolat et at. [47] investigated the impact of random spacing errors on transmission error and root stresses of a spur gear pair. Friction, as a main cause of vibration on gear system's transient state, was first introduced to a gear pair model under stochastic load in [23] [112]. Therefore, stochastic internal factor should be considered when modeling gear systems.

Current methods can solve a gear model with deterministic internal factors (e.g., TVMS, backlash, damping ratio, etc.) under stochastic load. However, a gear model with one of the internal factors dependent on gear velocity and/or displacement under stochastic load cannot be solved by these methods [74]. Since the load is stochastic, the gear velocity and/or displacement is stochastic and so does this internal factor. The commonly used numerical algorithms, such as the MC method, require a large amount of calculation time to solve such a gear model. Thus, it is desirable to develop a method to derive analytical solutions to such a model if possible.

In this work, we propose a method to derive an approximate analytical solution for a gear dynamic model under stochastic load with treating one of the internal factors as stochastic. The major contributions of this work are summarized as follows.

1. The gear dynamic model under stochastic load with treating one of the internal factors as stochastic is considered. In addition, the stochastic internal factor may dependent on gear velocity and/or displacement. Under this

model, the corresponding dynamic equations are derived.

2. A method is proposed to derive an approximate analytical solution of the dynamic equations. In the proposed method, a transformation of the original dynamic equations is introduced first so that PI method can be adopted to obtain a tentative analytical solution. Then, a modification function which is obtained by supervised learning method is applied to the tentative analytical solution to obtain the final approximate analytical solution of the formulated dynamic equation.

3. A case study is presented to validate the proposed method. The simulation results show that our proposed method can achieve similar accuracy responses of the gear model compared with MC method. In addition, the efficiency analysis is conducted. It shows that our proposed method cost much less time compared with MC method.

The remaining parts of this chapter are organized as follows. The general gear model considering an internal stochastic factor and stochastic load is introduced in Section 4.2. Section 4.3 gives the procedure of obtaining the approximate analytical solution by the proposed method. The proposed approximate analytical solution is validated by MC simulation and the evaluation of accuracy and efficiency for the proposed method are investigated in Section 4.4. Section 4.5 draws conclusions.

4.2 Problem description

The objectives of this section are to present a gear model and describe the challenges of solving such a model. An existing gear model which could be solved by the current PI method is introduced in Section 4.2.1. All the internal factors including TVMS, backlash, and damping coefficient in this model are deterministic. In Section 4.2.2, we give a more general gear model under stochastic load with one of the internal factors being stochastic. This kind of model considering a stochastic internal factor is more realistic than the existing model in Section 4.2.1.

4.2.1 An existing gear model

A classic gear model for a spur gear pair is reported in [5] and shown in Fig. 1.9. Note that only the torsional motion of gears is considered. Its dynamic model is formulated in Eq. (4.1).

$$\ddot{x} + c\dot{x} + kg(x) = f(t) \tag{4.1}$$

where x, $\dot{x}$, and $\ddot{x}$ represent the relative angular displacement, the relative angular velocity, and the relative angular acceleration, respectively, k denotes the equivalent TVMS as shown in Fig. 2.1, c denotes the damping coefficient which is considered as a constant, and $g(x)$ is the function of backlash (see Fig. 2.3). In addition, we have

$$x = \theta_1 R_{b1} - \theta_2 R_{b2} \tag{4.2}$$

where θ_i and R_{bi} are the angular displacement and the base circle radius of gear $i \in \{1, 2\}$, respectively.

The external load $f(t)$ is modeled as a combination of a constant deterministic part f_0, a periodical deterministic part $f_1 \cos(\varphi t)$, and a random part $\xi(t)$ [5]. About the random part, it is generally set to a Gaussian white noise. Therefore, the expressions of the external load are given as follows.

$$f(t) = f_0 + f_1 \cos(\varphi t) + \xi(t) \tag{4.3}$$

$$E(\xi(t)) = 0 \tag{4.4}$$

$$E[\xi(t)\xi(t+\tau)] = r\Theta(\tau) \tag{4.5}$$

where φ is a constant frequency, t denotes time, r is the variance of the random part $\xi(t)$, and $\Theta(\tau)$ is the Dirac Delta function.

4.2.2 A more general gear model

Except for stochastic load, we consider an internal stochastic factor in our gear system model. This work focuses on the case that this stochastic internal factor is dependent on gear velocity and/or displacement. The general model is defined as:

$$\ddot{x} + G_1(x, \dot{x}, t)\dot{x} + G_2(x, \dot{x}, t)x = f(t) \tag{4.6}$$

where $G_1(x, \dot{x}, t)$ and $G_2(x, \dot{x}, t)$ are the coefficients of the velocity term and the displacement term, respectively, and $f(t)$ is defined in Eq. (4.3). One thing worthy to mention is that $G_1(x, \dot{x}, t)$ and $G_1(x, \dot{x}, t)$ depend on x and/or $\dot{x}$. The dependency of the coefficients on the velocity term and/or displacement term makes Eq. (4.6) hard to solve. In this study, we will propose an approach to deal with the following three scenarios:

1. Stochastic $G_1(x, \dot{x}, t)$ and deterministic $G_2(t)$, e.g., damping coefficient is stochastic in Eq. (4.1).

2. Stochastic $G_2(x, \dot{x}, t)$ and deterministic $G_1(t)$, e.g., gear mesh stiffness or backlash is stochastic in Eq. (4.1).

3. Stochastic $G_1(x, \dot{x}, t)$ and stochastic $G_1(x, \dot{x}, t)$, where $G_1(x, \dot{x}, t) = CG_2(x, \dot{x}, t)$ and C is deterministic, e.g., the model considers stochastic friction. This case will be explained as an example in Section 4.4.

There is no doubt that our proposed method can solve models with stochastic parametric excitations, namely, G_1 and G_2 are independent of x and $\dot{x}$. The proposed method does not restrict the type of randomness involved in the gear systems. For example, this stochastic internal factor can follow the Normal distribution or another distribution.

4.3 The proposed method

For lots of applications (e.g., fatigue prediction, reliability analysis, etc.) an accurate PDF (i.e., tentative analytical solution) of the dynamic model is needed [36] [105]. In this work, we focus on the solving methods to obtain the approximate analytical solution of the stochastic differential equation (SDE) Eq. (4.6). PI method, which can obtain the analytical solution of the differential equation Eq. (4.1), is the foundation of our proposed method. Other techniques including probability density evolution method (PDEM) [113] and Wiener path integral technique [114] can also be adopted to obtain the analytical solution of Eq. (4.1). However, these methods would not be considered in this work due to the following reasons. First, from Eq. (4.6), the coefficients G_1 and G_2 depend on x and $\dot{x}$ in our model, and thus, these methods are not feasible to solve Eq. (4.6) directly. Second, compared to the PI method, these methods are more complicated.

The objective of this section is to give the details of the proposed method. The basic idea of the proposed method contains the following two steps:

1. **Obtain tentative analytical solution.**

   We first introduce a method to transform the SDE Eq. (4.6) into a form that can be solved by PI method. Then, we derive a tentative analytical solution using PI method.

2. **Adjust results by adding a modification function.**

   Due to the previous transformation, errors may be brought into the tentative analytical solution, and thus, a modification function is applied to adjust the tentative analytical solution. Supervised learning is used to obtain the modification function.

Section 4.3.1 introduces the processes of deriving the tentative analytical solution by PI method. The modification function which is used to adjust the tentative analytical solution is given in Section 4.3.2. In Sections 3.3, we summarize the whole procedure of the proposed method.

4.3.1 Tentative analytical solution

The objective of this section is to derive the tentative analytical solution of the SDE Eq. (4.6) by PI method. The main idea of PI method is introduced in Section 4.3.1.1. In Section 4.3.1.2, we propose the method to transform Eq. (4.6) to a form which can be solve by PI method. Section 4.3.1.3 gives the general tentative analytical solution obtained by PI method.

4.3.1.1 Main idea of PI method

PI method is a practical method to capture the PDF evolution in time. PI method can give an analytical solution to the differential equation Eq. (4.1). Several researchers have explored the PI method. Sun and Hsu [73] assumed that the transition process within a short time interval was a Gaussian diffusion process. Naess et al. [66] studied response statistics of nonlinear oscillators excited by white noise using PI method. Kylolu et al. [72] applied PI method to study a single degree of freedom (SDOF) oscillator subject to Gaussian and Poisson random excitations. Kougioumtzoglou et al. [115] developed an improved PI method to obtain the failure probability of nonlinear SDOF dynamic systems.

Assuming that the transition process follows the Gaussian distribution, the PDF of the differential equation's response can be calculated by doing integration in a finite phase plane space [36]. The equation of x and $\dot{x}$ can be expressed as $\mathrm{It\hat{o}'s}$ form in a matrix format, which is given as

$$d\mathbf{X}(t) = A[\mathbf{X}, t]dt + B[\mathbf{X}, t]d\mathbf{W}(t) \tag{4.7}$$

where $\mathbf{X}$ represents the 2-element vector $[x, \dot{x}]$ at each time point t, $A[\mathbf{X}, t]$ denotes the 2-element drift vector at each time point t, $B[\mathbf{X}, t]$ is the diffusion matrix with dimension 2×2, and $\mathbf{W}(t)$ is the 2-element vector of standard Wiener vector process [5].

Based on the basic idea of PI method, the corresponding PDF (i.e., analytical solution) of $\mathbf{X}_i = [x_{t_i}, \dot{x}_{t_i}]$ is derived [116]:

$$p(\mathbf{X}_i, t_i) = \int_R q(\mathbf{X}_i, t_i|\mathbf{X}_{i-1}, t_{i-1}) \times p(\mathbf{X}_{i-1}, t_{i-1}) d\mathbf{X}_{i-1} \tag{4.8}$$

where $p(\mathbf{X}_i, t_i)$ denotes the PDF of $\mathbf{X}_i$ at time t_i, i represents the ith discrete time point, R is the integration region, and $q(\mathbf{X}_i, t_i|\mathbf{X}_{i-1}, t_{i-1})$ denotes the transit PDF from $\mathbf{X}_{i-1}$ to $\mathbf{X}_i$. The expression of $q(\mathbf{X}_i, t_i|\mathbf{X}_{i-1}, t_{i-1})$ is given in Eq. (4.9).

$$q(\mathbf{X}_i, t_i|\mathbf{X}_{i-1}, t_{i-1}) = \frac{1}{2\pi\sigma_{1,t_i}\sigma_{2,t_i}\sqrt{1-{\rho_i}^2}} e^{\frac{-z_i}{2(1-{\rho_i}^2)}} \tag{4.9}$$

where

$$z_i = \frac{(x-\mu_{1,t_i})^2}{\sigma_{1,t_i}^2} - \frac{(x_{t_i}-\mu_{1,t_i})(\dot{x}_{t_i}-\mu_{2,t_i})}{\sigma_{1,t_i}\sigma_{2,t_i}} + \frac{(\dot{x}_{t_i}-\mu_{2,t_i})^2}{\sigma_{2,t_i}^2} \tag{4.10}$$

$$\rho_i = \frac{\sigma_{12,t_i}}{\sigma_{1,t_i}\sigma_{2,t_i}} \tag{4.11}$$

where ρ_i represents the correlation between x_{t_i} and $\dot{x}_{t_i}$, μ_{1,t_i} and σ_{1,t_i} are the mean and the standard deviation (st.d) of x_{t_i}, respectively, μ_{2,t_i} and σ_{2,t_i} are the mean and the standard deviation (st.d) of $\dot{x}_{t_i}$, respectively, and σ_{12,t_i} denotes the covariance of x_{t_i} and $\dot{x}_{t_i}$. In addition, we have

$$p(\mathbf{X}_0, t_0) = \frac{1}{2\pi\sigma_{1,t_0}\sigma_{2,t_0}} \exp\left\{-\frac{(x_{t_0}-\mu_{1,t_0})^2}{2\sigma_{1,t_0}} - \frac{(\dot{x}_{t_0}-\mu_{2,t_0})^2}{2\sigma_{2,t_0}}\right\} \tag{4.12}$$

where $p(\mathbf{X}_0, t_0)$ represents the PDF of $\mathbf{X}_0$ at initial time t_0.

Starting from this point, we omit the subscript t_i in x_{t_i}, $\dot{x}_{t_i}$, μ_{j,t_i}, and σ_{j,t_i} for simplicity. We need to keep in mind that x, $\dot{x}$, μ_1, μ_2, σ_1, σ_2, and σ_{12} have the implicit information with regard to time.

4.3.1.2 Transformation of the gear dynamic equation

Since the SDE Eq. (4.6) cannot be solved by PI method directly, a transformation method is proposed in this section. In PI method, it requires all the coefficients in the left hand of the differential equation to be deterministic. Thus, the key problem is to transform the stochastic coefficients of Eq. (4.6) to be deterministic. The details of the transformation are given as follows.

According to the superposition principle, it is assumed that the deterministic part of load, denoted $\hat{f}(t) = f_0 + f_1 \cos(\varphi t)$, excites the deterministic part of $x(t)$ and $\dot{x}(t)$, while the stochastic part of the load, denoted $\xi(t)$, excites the stochastic part of $x(t)$ and $\dot{x}(t)$. To solve Eq. (4.6), we first consider:

$$x(t) = \mu_1(t) + \tilde{\mu}_1(t) \tag{4.13}$$

$$\dot{x}(t) = \mu_2(t) + \tilde{\mu}_2(t) \tag{4.14}$$

$$G_1(x, \dot{x}, t) = \lambda_{G_1}(t) + \tilde{G}_1(t) \tag{4.15}$$

$$G_2(x, \dot{x}, t) = \lambda_{G_2}(t) + \tilde{G}_2(t) \tag{4.16}$$

where $\mu_1(t)$ and $\mu_2(t)$ are the deterministic part of $x(t)$ and $\dot{x}(t)$, respectively, $\tilde{\mu}_1(t)$ and $\tilde{\mu}_2(t)$ are the stochastic part of $x(t)$ and $\dot{x}(t)$, respectively, $\lambda_{G_1}(t)$ and $\lambda_{G_2}(t)$ are the deterministic part of $G_1(x, \dot{x}, t)$ and $G_2(x, \dot{x}, t)$, respectively, $\tilde{G}_1(t)$ and $\tilde{G}_2(t)$ are the stochastic part of $G_1(x, \dot{x}, t)$ and $G_2(x, \dot{x}, t)$, respectively.

If we do not consider the stochastic part of the load, we can get Eq. (4.17).

$$\ddot{x} + G_1(x, \dot{x}, t)\dot{x} + G_2(x, \dot{x}, t)x = \hat{f}(t) \tag{4.17}$$

Then, we can obtain $x(t)$ and $\dot{x}(t)$ (denotes as $\mu_1(t)$ and $\mu_2(t)$) by solving Eq. (4.17), which are deterministic. Therefore, $G_1(\mu_1(t), \mu_2(t))$ and $G_2(\mu_1(t), \mu_2(t))$ can be obtained. In this case, $\lambda_{G_1}(t)$ and $\lambda_{G_2}(t)$ can be obtained as $\lambda_{G_1}(t) = G_1(\mu_1(t), \mu_2(t))$ and $\lambda_{G_2}(t) = G_2(\mu_1(t), \mu_2(t))$.

Utilizing $G_1(\mu_1, \mu_2)$ and $G_2(\mu_1, \mu_2)$ to replace $G_1(x, \dot{x}, t)$ and $G_2(x, \dot{x}, t)$, respectively, an approximated equation of Eq. (4.6) is given as,

$$\ddot{x} + \lambda_{G_1}(t)\dot{x} + \lambda_{G_2}(t)x = f(t) \tag{4.18}$$

In Eq. (4.18), the coefficients are deterministic except for the load, and thus, it can be solved by the PI method according to the description and the limitations of the PI method (refer to Section 4.3.1.1). The solution of Eq. (4.18) is our tentative analytical solution. We call it tentative analytical solution because we ignored $\tilde{G}_1(t)$ and $\tilde{G}_2(t)$ in Eq. (4.6). The tentative analytical solution will be further adjusted to be more accurate later.

In the next section, the method to derive the tentative analytical solution will be given. In addition, a case study to obtain the tentative analytical solution will be given in Section 4.4.1

4.3.1.3 Derivation of the tentative analytical solution

The objective of this section is to show the procedure of obtaining the tentative analytical solution by PI method.

In order to obtain $p(\mathbf{X}_i, t_i)$, we need to solve Eqs. (4.9-4.11) first. Correspondingly, we need to obtain the expressions for μ_1, μ_2, σ_1, σ_2, and σ_{12}. Since the mean of the stochastic term of $f(t)$ is zero, the solution of Eq. (4.17) could be obtained as μ_1 and μ_2. Then, the remaining problem is to obtain σ_1, σ_2, and σ_{12}.

Due to the existence of backlash, the obtained σ_1, σ_2, and σ_{12} can be classified into two categories, namely, with tooth contact or not. If the backlash value (i.e., $g(x)$) equals to zero in Fig. 2.3, there is no tooth contact. Otherwise, there is a tooth contact. Therefore, we will talk about the derivation process of σ_1, σ_2, and σ_{12} according to the two categories. Here, σ_1, σ_2, and σ_{12} describe the uncertainties in the gear dynamic responses. Recalling Eq. (4.17), we know that these uncertainties are caused by the random term $\xi(t)$ in $f(t)$.

(1) with tooth contact ($G_2 \neq 0$)

In this part, the approximate analytical solution is for the case $g(x) \neq 0$.

We suppose that $f(t)$ in Eq. (4.18) is equal to $\Theta(t)$, where $\Theta(t)$ is the Dirac Delta function. Under the excitation of $\Theta(t)$, there is an impulse function $h_x(t)$ which satisfies Eq. (4.19).

$$\frac{d^2h_x(t)}{dt^2} + \lambda_{G_1}\frac{dh_x(t)}{dt} + \lambda_{G_2} = 0 \tag{4.19}$$

For $t > 0$, we suppose that the initial condition is $h_x'(0^+) = v$ and $h_x(0^+) = 0$, where $v = R_{b1}v_0^{(1)} - R_{b2}v_0^{(2)}$ is the relative initial velocity and $v_0^{(i)}, i \in \{1, 2\}$ is the initial mean velocity of gear i. Note that R_{b1} and R_{b2} are defined in Eq. (4.2). The mean of the gear initial relative angular displacement is 0. Then, the general solution of the homogeneous equation Eq. (4.19) can be obtained as

$$h_x(t) = \frac{v}{\beta}e^{\alpha t}\sin(\beta t) \tag{4.20}$$

where

$$\alpha = -\frac{\lambda_{G_1}}{2} \tag{4.21}$$

$$\beta = \frac{\sqrt{4\lambda_{G_2} - \lambda_{G_2}^2}}{2} \tag{4.22}$$

Then, the autocorrelation function of $f(t)$, denoted $\phi_{ff}(t,s)$, is derived as

$$\begin{aligned} &\phi_{ff}(t,s) \\ &= E[f(t)f(s)] \\ &= f_0^2 + f_0 f_1(\cos(\varphi s) + \cos(\varphi t)) + f_1^2 \cos^2(\varphi t) + G_0 \Theta(t-s) \end{aligned} \tag{4.23}$$

where $G_0 = 2\pi r$. The auto covariance function of $f(t)$, denoted $K_{ff}(t,s)$, is derived as

$$K_{ff}(t,s) = \phi_{ff}(t,s) - E[f(t)]E[f(s)] = G_0 \Theta(t-s) \tag{4.24}$$

The auto covariance function of the relative displacement x, denoted $K_{xx}(t_1,t_2)$, is derived as

$$K_{xx}(t_1,t_2) = \int_{-\infty}^{\infty}\int_{-\infty}^{\infty} K_{ff}(s_1,s_2) h_x(t_1-s_1) h_x(t_2-s_2) ds_1 ds_2 \tag{4.25}$$

According to the expression of $K_{ff}(t,s)$ and $h_x(s)$, The following equation is obtained.

$$\begin{aligned} &K_{xx}(t_1,t_2) = \tfrac{G_0 v^2}{4\beta^2(\alpha^2+\beta^2)} \{ e^{\alpha|t_1-t_2|} \{ -\tfrac{\beta^2}{\alpha} \cos[\beta(t_1-t_2)] + \beta \sin[\beta|t_1-t_2|] \} \\ &-e^{\alpha(t_1+t_2)} \{ -\tfrac{\alpha^2+\beta^2}{\alpha} \cos[\beta(t_1-t_2)] + \alpha \cos[\beta(t_1+t_2)] + \beta \sin[\beta(t_1+t_2)] \} \end{aligned} \tag{4.26}$$

Let $K_{x\dot{x}}(t_1,t_2)$ denote the auto covariance function of the relative angular displacement x and the relative angular velocity $\dot{x}$. Due to $K_{x\dot{x}}(t_1,t_2) = \frac{\partial K_{xx}(t_1,t_2)}{\partial t_2}$, $K_{x\dot{x}}(t_1,t_2)$ can be derived as

$$\begin{aligned} &K_{x\dot{x}}(t_1,t_2) \\ &= \tfrac{G_0 v^2}{4\beta^2} \{ -e^{\alpha|t_1-t_2|} \tfrac{\beta}{\alpha} \sin[\beta|t_1-t_2|] \\ &\quad -e^{\alpha(t_1+t_2)} \{ -\tfrac{\beta}{\alpha} \sin[\beta(t_1-t_2)] - \cos[\beta(t_1-t_2)] + \cos[\beta(t_1+t_2)] \} \} \end{aligned} \tag{4.27}$$

Let $K_{\dot{x}\dot{x}}(t_1,t_2)$ denote the auto covariance function of the relative angular velocity $\dot{x}$. Due to $K_{\dot{x}\dot{x}}(t_1,t_2) = \frac{\partial^2 K_{xx}(t_1,t_2)}{\partial t_1 \partial t_2}$, $K_{\dot{x}\dot{x}}(t_1,t_2)$ can be derived as

$$\begin{aligned} &K_{\dot{x}\dot{x}}(t_1,t_2) \\ &= \tfrac{G_0 v^2}{4\alpha\beta^2} \{ -e^{\alpha|t_1-t_2|} \alpha\beta \sin[\beta|t_1-t_2|] \\ &\quad -e^{\alpha|t_1-t_2|} \beta^2 \cos[\beta|t_1-t_2|] \\ &\quad -e^{\alpha(t_1+t_2)} \{ -(\alpha^2+\beta^2) \cos[\beta(t_1-t_2)] \\ &\quad -\alpha\beta \sin[\beta(t_1+t_2)] + \alpha^2 \cos[\beta(t_1+t_2)] \} \} \end{aligned} \tag{4.28}$$

Let $t_1 = t_2 = \Delta t$, and then, we can obtain the corresponding variances:

$$\sigma_1^2 = \frac{G_0 v^2}{4\beta^2(\alpha^2+\beta^2)}(-\frac{\beta^2}{\alpha} - e^{2\alpha\Delta t}(-\frac{\alpha^2+\beta^2}{\alpha} + \alpha\cos(2\beta\Delta t) + \beta\sin(2\beta\Delta t))) \tag{4.29}$$

$$\sigma_{12} = \frac{G_0 v^2}{4\beta^2} e^{2\alpha\Delta t}\left[1 - \cos(2\beta\Delta t)\right] \tag{4.30}$$

$$\sigma_2^2 = -\frac{G_0 v^2}{4\alpha\beta^2}\{\beta^2 - e^{2\alpha\Delta t} \times [\alpha^2 + \beta^2 + \alpha\beta\sin(2\beta\Delta t) - \alpha^2\cos(2\beta\Delta t)]\} \tag{4.31}$$

Note that σ_1^2 and σ_2^2 are the variances of x and $\dot{x}$, respectively, and σ_{12} is the covariance of x and $\dot{x}$.

(2) without tooth contact ($G_2 = 0$)

In this part, the approximate analytical solution is for the case $g(x) = 0$. Therefore, the differential equation is given as:

$$\ddot{x} + G_1\dot{x} = f(t) \tag{4.32}$$

By eliminating the stochastic term of $f(t)$, we can obtain the following equation.

$$\ddot{x} + G_1\dot{x} = \hat{f}(t) \tag{4.33}$$

Then, $\tilde{\lambda}_{G_1}$ is obtained by solving Eq. (4.33).

The following equation is obtained by replacing G_1 with $\tilde{\lambda}_{G_1}$ in Eq. (4.32)

$$\ddot{x} + \tilde{\lambda}_{G_1}\dot{x} = f(t) \tag{4.34}$$

Similar to solving Eq. (4.19), the general solution of the homogeneous equation Eq. (4.34), denoted $h_x^{(2)}(t)$, can be derived as

$$h_x^{(2)}(t) = \frac{v}{a_2}\left(1 - e^{a_2 t}\right) \tag{4.35}$$

where $a_2 = c\tilde{\lambda}_L$ and v is the mean of initial velocity.

Similar to the procedures of the case with tooth contact, we can obtain the corresponding variances:

$$\sigma_1^2 = \frac{G_0 v^2}{a_2^2}\left(\Delta t - \frac{1}{a_2}\left(\frac{3}{2} - 2e^{-a_2\Delta t} + \frac{1}{2}e^{-a_2\Delta t})\right)\right) \tag{4.36}$$

$$\sigma_{12} = \frac{G_0 v^2}{a_2^2}\left[\frac{1}{2} - e^{-a_2\Delta t} + \frac{1}{2}e^{-2a_2\Delta t}\right] \tag{4.37}$$

$$\sigma_2^2 = \frac{G_0 v^2}{2a_2}\left(1 - e^{-2a_2\Delta t}\right) \tag{4.38}$$

4.3.2 Updated approximate analytical solution

Due to the transformation in Section 4.3.1.2, the obtained tentative analytical solution is not the accurate solution of Eq. (4.6). Therefore, the objective of this section is to derive the modification function and then apply it to the tentative analytical solution to obtain the approximate solution of Eq. (4.6). A case study to obtain the modification function will be given in Section 4.4.1.

Generally, the exact analytical solution of Eq. (4.6) is hard to derive. However, numerical responses (i.e., samples) can be obtained by MC method. Then, we can also generate samples by the obtained tentative analytical solution. Therefore, we can find a modification function to demonstrate the rule of errors according to the samples obtained by MC method and the tentative analytical solution. A supervised learning algorithm is applied to obtain the modification function. Finally, we adjust the tentative analytical solution by the modification function and then obtain the final PDF. The obtained final PDF is called the approximate analytical solution (i.e., PDF) of the SDE Eq. (4.6).

To obtain the responses of x and $\dot{x}$, the procedure of conducting MC method can be summarized as:

1. Generate N_{MC} (number of samples) load profiles using Eq. (4.3). Note that the value of N_{MC} is obtained based on the following rule. With the increase of the number of samples, the PDF will become steady. Thus, the number of samples N_{MC} is selected such that the PDF becomes stable.

2. Substitute each load to Eq. (4.6) and solve it using differential equation solver (ode15s) in Matlab (Runge-Kutta).

3. Obtain N_{MC} samples of responses corresponding to the N_{MC} load profiles.

Supervised learning is used to find a mapping between a set of input samples and the corresponding output and this mapping is then applied to predict the outputs under other input data [117]. The samples obtained by the tentative analytical solution would be the input samples (also called PI results) and the samples obtained by MC method would be the corresponding output (also called MC results). We define the input samples and the corresponding output as $\chi(t)$ and $\zeta(t)$, respectively. Then, we try to seek a function $\eta(t) : \chi(t) \rightarrow \zeta(t)$. Note that $\eta(t)$ is a t-correlation function. To evaluate $\eta(t)$, the risk function ε is defined as [118]:

$$\varepsilon = \int_{t_1}^{t_2} \left| \frac{\zeta\left(t\right) - \eta\left(t\right)\chi\left(t\right)}{\zeta\left(t\right)} \right| dt \tag{4.39}$$

To get a proper $\eta(t)$, the value of ε should be minimized. There are two basic methods for getting the expression of $\eta(t)$, empirical risk minimization [119] and structural risk minimization [120]. Empirical risk minimization method has the disadvantage of overfitting when the training data set is not sufficiently large. For structural risk minimization, the algorithm tries to avoid overfitting by introducing a regularization penalty. It prefers to find a simpler $\eta(t)$ over a complex one to prevent overfitting [121]. In this work, the structural risk minimization method is adopted as the number of training data is limited.

Hence, the learning algorithm is to find $\eta(t)$ that minimizes $\varepsilon + \kappa Q\left(\eta\right)$, where κ could control the bias-variance tradeoff and $Q\left(\eta\right)$ is the regularization penalty which is used to avoid overfitting. The appropriate κ can be obtained by cross validation. The detailed information about the learning algorithm can be found in [122].

There are many supervised learning algorithms, including support vector machines [123]- [125], linear regression [126], nonlinear regression [127], neural networks [128] and so on. In this study, we choose nonlinear regression.

Therefore, the procedure of obtaining $\eta(t)$ is summarized as follows [129]

1. Define the average error function
2. Find the type of $\eta(t)$ by analyzing the properties between the input samples and corresponding output
3. Define $\eta(t)$ and the regularization penalty $Q(\eta)$
4. Choose the bias-variance tradeoff κ
5. Minimize $\varepsilon + \kappa Q\left(\eta\right)$ using the steepest descent method [130]

According to the obtained modification function $\eta(t)$, the modified PI results can be obtained:

$$\tilde{\sigma}_1(t) = \sigma_1(t)\eta_1(t) \tag{4.40}$$

$$\tilde{\sigma}_2(t) = \sigma_2(t)\eta_2(t) \tag{4.41}$$

$$\tilde{\sigma}_{12}(t) = \sigma_{12}(t)\eta_{12}(t) \tag{4.42}$$

where $\tilde{\sigma}_1(t)$, $\tilde{\sigma}_2(t)$, and $\tilde{\sigma}_{12}(t)$ are the modified values of $\sigma_1(t)$, $\sigma_2(t)$, and $\sigma_{12}(t)$, respectively, and $\eta_1(t)$, $\eta_2(t)$, and $\eta_{12}(t)$ are the corresponding modification functions. Updating $\sigma_1(t)$, $\sigma_2(t)$, and $\sigma_{12}(t)$ in Eqs. (4.29-4.31) by $\tilde{\sigma}_1(t)$, $\tilde{\sigma}_2(t)$, and $\tilde{\sigma}_{12}(t)$ respectively, the improved PDF expressions of x and $\dot{x}$ with a high accuracy are obtained. Therefore, the improved PDF expressions of x and $\dot{x}$ is called the approximate analytical solution to Eq. (4.6). The validation of this modification will be demonstrated in Section 4.4.

4.3.3 Summary of procedure

We summary the proposed method in Fig. 4.1, which contain the following five steps.

1. Replace the stochastic load in the dynamic equation by deterministic load and then solve the dynamic equations (see Eq. (4.17))
2. Replace $G_1(x, \dot{x}, t)$ and $G_2(x, \dot{x}, t)$ by $\lambda_{G_1}(t)$ and $\lambda_{G_2}(t)$, respectively
3. Derive $\sigma_1(t)$, $\sigma_2(t)$, $\sigma_{12}(t)$ by PI method
4. Use MC results as training data and find out a proper $\eta(t)$ by nonlinear regression
5. Update tentative analytical solution by $\eta(t)$ according to Eqs. (4.40)-(4.42)

4.4 Validation and evaluation

In this section, a gear model considering damping, TVMS, backlash, and friction is introduced. In this model, both the load and the friction (i.e., the single stochastic internal factor) are stochastic. In this section, we use this case (i.e. obtaining the approximate analytical solution of the introduced model) as an example to explain our proposed method. This case is the most complex case among the three cases mentioned in Section 4.2.2. Other cases can also follow the same procedure to obtain the approximate analytical solution.

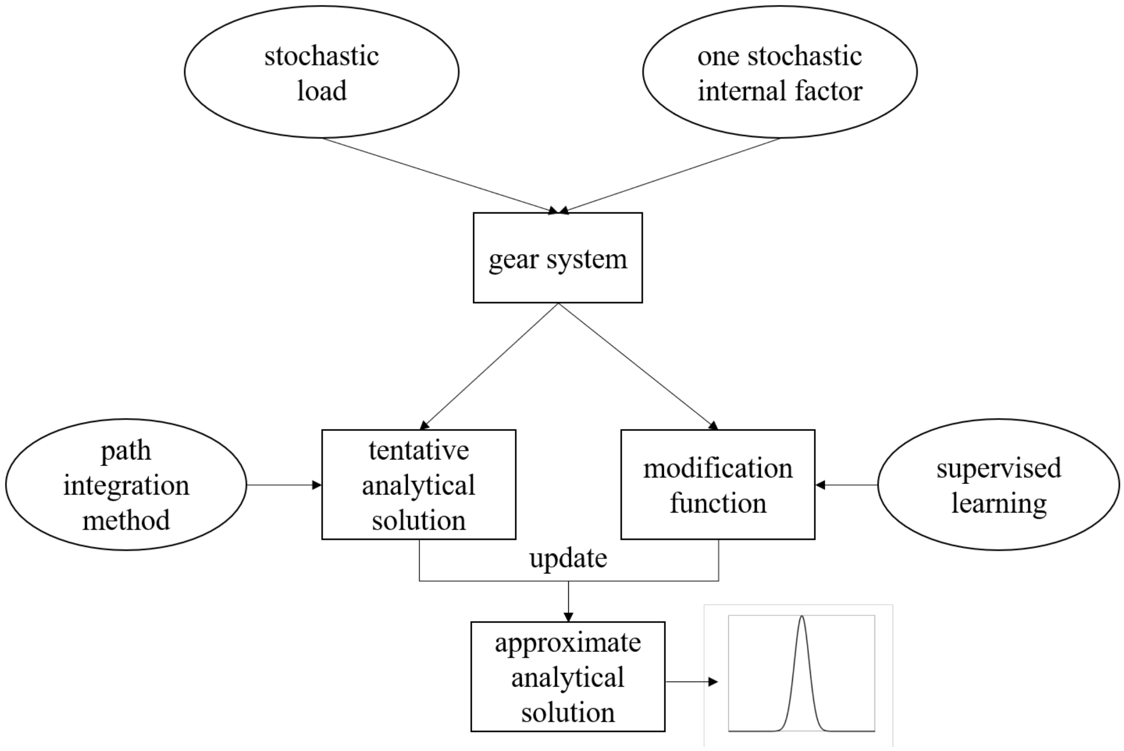

Fig. 4.1: The overview of our proposed method

In order to validate the proposed method, the comparison will be made between the results from the proposed method and the MC method. This validation is performed in Section 4.4.2. Section 4.4.3 evaluates the accuracy and efficiency of the proposed method.

The parameters of the gear system used in this validation are from [75] and friction coefficient μ is set to be a constant 0.04. For the stochastic load in Eq. (4.3), the parameters are set as $f_0 = 2 \times 10^4$, $f_1 = 2 \times 10^3$, $\varphi = 100$, and $r = 2 \times 10^3$.

4.4.1 A gear model used to validate the proposed method

This section contains three parts. First, a gear model used in validation is introduced and the tentative analytical solution of this model is derived. Then, gear parameters are substituted to the gear model, and thus, the modification function is obtained. Finally, the approximate analytical solution is obtained by updating the tentative analytical solution using the modification function.

The considered model in this section is formulated as [23]:

$$J_1\ddot{\theta}_1 = T_1 - FR_{b1} - F_f X_1 \tag{4.43}$$

$$J_2\ddot{\theta}_2 = T_2 + FR_{b2} + F_f X_2 \tag{4.44}$$

where J_i, T_i, X_i, and R_{bi} are the moment of inertia, external torque, arm length of friction, and base circle of gear $i \in \{1,2\}$, respectively, F represents the total force between the contact teeth, F_f is the sliding friction.

Simplify Eq. (4.43, 4.44), and then, a normalized equation is obtained and shown as

$$\ddot{x} + cL(\theta_1, \mu, t)\dot{x} + kL(\theta_1, \mu, t)g(x) = f(t) \tag{4.45}$$

where c and k are defined in Eq. (4.1), θ_1 is defined in Eq. (4.2), μ represents the friction coefficient, and $L(\theta_1, \mu, t)$ is a function which is caused by friction. The expression of $L(\theta_1, \mu, t)$ can be obtained as Eq. (4.46) [23].

$$L(\theta_1, \mu, t) = \chi_1 + \mu\left(\chi_2\theta_1 + \chi_3\right) \tag{4.46}$$

where $\chi_j (j = 1, 2, 3)$ relates to gear design parameters. Note that $\chi_j (j = 1, 2, 3)$ and μ can be considered as constant.

From Eq. (4.46), we can see that $L(\theta_1, \mu, t)$ depends on θ_1. Since θ_1 is stochastic because of $f(t)$ given in Eq. (4.3), $L(\theta_1, \mu, t)$ is also stochastic.

By considering the deterministic part of the load, Eq. (4.47) is obtained.

$$\ddot{x} + cL\dot{x} + kLg(x) = \hat{f}(t) \tag{4.47}$$

Then, x (considered as μ_1) and $\dot{x}$ (considered as μ_2) can be obtained by solving Eq. (4.47). Note that, according to Eq. (4.2), $\hat{\theta}_1$ and $\hat{\theta}_2$ can be obtained according to the obtained x.

After that, we get $\lambda_L(t)$ as expressed in Eq. (4.48) by substituting $\hat{\theta}_1$ to Eq. (4.46).

$$\lambda_L(t) = \chi_1 + \mu\left(\chi_2\hat{\theta}_1 + \chi_3\right) \tag{4.48}$$

Eq. (4.49) is obtained by replacing $L(\theta_1, \mu, t)$ by $\lambda_L(t)$ in Eq. (4.45).

$$\ddot{x} + c\lambda_L(t)\dot{x} + k\lambda_L(t)g(x) = f(t) \tag{4.49}$$

Based on this transformation, all parameters in Eq. (4.49) become deterministic except for load, which could be solved by PI method now.

Backlash is adopted the same as Fig. 2.3, where

$$g(x) = \begin{cases} x - b, & x > b \\ 0, & -b \leq x \leq b \\ x + b, & x < -b \end{cases} \tag{4.50}$$

For the case that $g(x) \neq 0$, the system equation is shown in Eq. (4.49). Under the excitation of $\Theta(t)$, there is an impulse function $h_x(t)$ which satisfies Eq. (4.51).

$$\frac{d^2 h_x(t)}{dt^2} + c\lambda_L(x)\frac{dh_x(t)}{dt} + k\lambda_L(x)h_x(t) = 0 \tag{4.51}$$

The general solution to the homogeneous equation Eq. (4.51) is same as Eq. (4.20), where

$$\alpha = -\frac{c\lambda_L(x)}{2} \tag{4.52}$$

$$\beta = \frac{\sqrt{4k\lambda_L(x) - (c\lambda_L)^2}}{2} \tag{4.53}$$

Then, σ_1, σ_2, and σ_{12} under $g(x) \neq 0$ can be obtained by Eqs. (4.29-4.31).

For the system with $g(x) = 0$, the differential equation is:

$$\ddot{x} + cL(\theta_1, \mu, t)\dot{x} = f(t) \tag{4.54}$$

By eliminating the random term of $f(t)$ in Eq. (4.54), we have

$$\ddot{x} + cL(\theta_1, \mu, t)\dot{x} = \hat{f}(t) \tag{4.55}$$

Then, we can obtain the results by solving Eq. (4.55). By substituting the obtained results to Eq. (4.48), we can obtain $\tilde{\lambda}_L(x)$. The following equation is obtained by replacing $L(\theta_1, \mu, t)$ to $\tilde{\lambda}_L(x)$ in Eq. (4.54).

$$\ddot{x} + c\tilde{\lambda}_L(x)\dot{x} = f(t) \tag{4.56}$$

The general solution to the homogeneous equation Eq. (4.56) is the same as Eq. (4.35), where $a_2 = c\tilde{\lambda}_L(x)$ and v represents the mean of initial velocity.

In the case of $g(x) = 0$, σ_1, σ_2, and σ_{12} can be obtained by Eq. (4.36-4.38).

Based on Section 4.3.2, a modification to μ_1, μ_2, σ_1, σ_2, and σ_{12} should be taken. The modification function $\eta(t)$ is based on the results of MC method and the tentative analytical solution. For different cases, $\eta(t)$ may have different forms, such as polynomial function, exponential function, and so on. Therefore, it is important to analyze the properties of the responses so that an appropriate form for $\eta(t)$ can be obtained. The gear parameters given at the beginning of Section 4.4 are used for simulation. Fig. 4.2 gives a sample of responses x under stochastic load. From this figure, we can see x fluctuates greatly at the beginning, but the fluctuation amplitude decreases until a stable state. The system is considered as stable when the amplitude of x has a small variation. In this simulation, the system is considered as stable under the applied stochastic load after 2.5s based on Fig. 4.2. The data under the stable state are used in the following calculation.

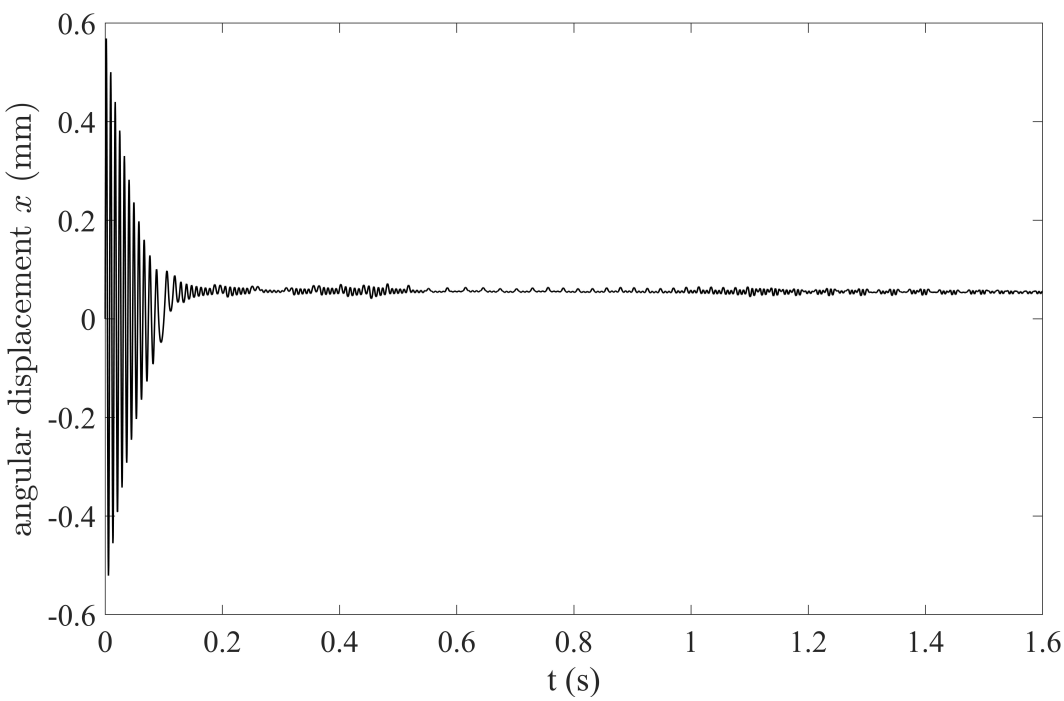

Fig. 4.2: An example of responses x

In Fig. 4.3 (a) and (b), μ_1 and μ_2 between [0.35, 0.4] s are compared, respectively. It is concluded that the mean of responses by PI method is almost the same as the result by MC method. Thus, for the gear parameters used in this work, there is

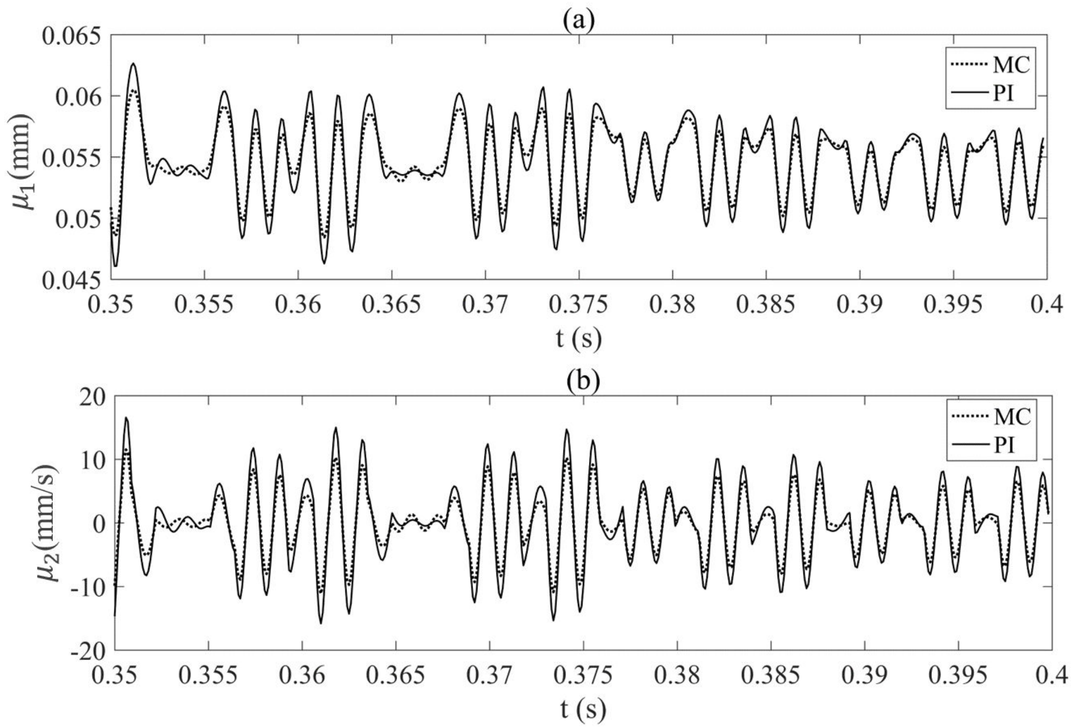

Fig. 4.3: Comparison between PI and MC in mean value of (a) x and (b) $\dot{x}$

no need to adjust the mean values (μ_1 and μ_2) and only σ_1, σ_2, and σ_{12} need to be adjusted.

In the following, σ_2 is used as an example to obtain its modification function using nonlinear regression algorithm (the procedure is similar for σ_1 and σ_{12}). The data obtained between [0.25, 0.3] s is used as the training data as the system is considered as stable in this period. The data of σ_2 obtained by PI method and MC method between [0.25, 0.3] s is given in Fig. 4.4. It is easy to find that the PI results and the MC results of σ_2 have the property of periodicity. Both of them have the same period and the period is T as shown in Fig. 4.5.

Therefore, $\eta(t)$ is also a periodic function and it is defined as

$$\eta(t) = \phi\left(\frac{t}{N}\right), t \in [(N-1)T, NT] \tag{4.57}$$

where N is a positive integer which represents the number of periods and $\phi(t)$ is

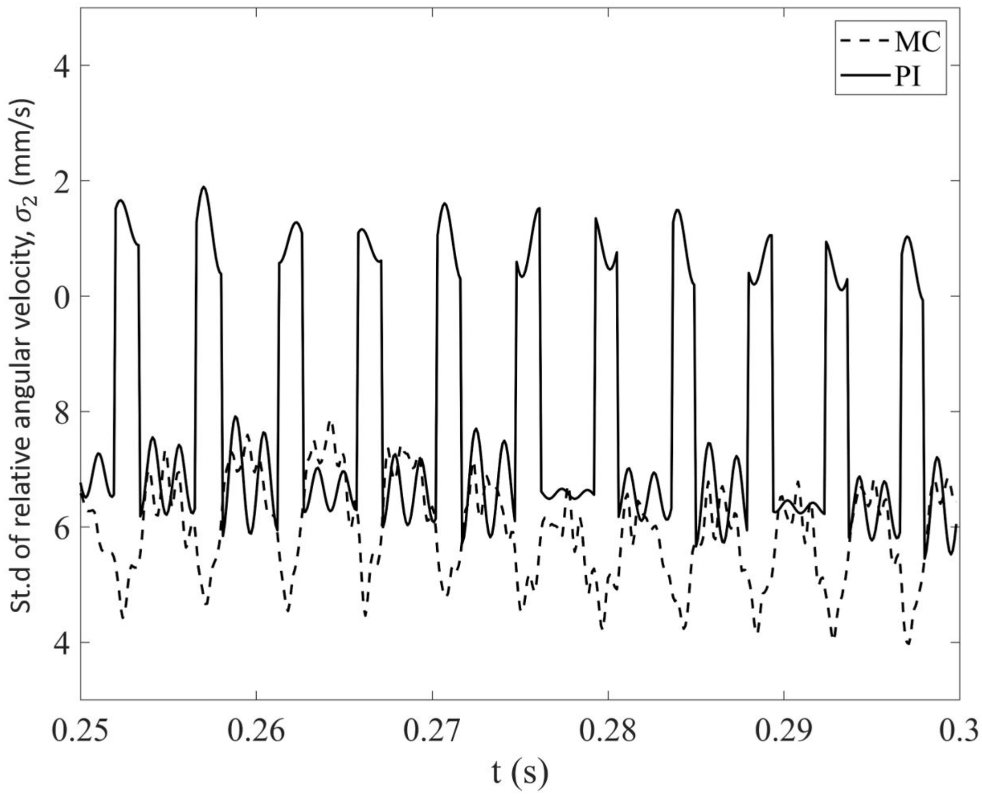

Fig. 4.4: The training data

defined as Eq. (4.58).

$$\phi(t) = \begin{cases} \gamma_1(1+\sin(\varpi t)) & t \in [0, T_m] \\ \gamma_2(1+\sin(\varpi t)) & t \in [T_m, T] \end{cases} \tag{4.58}$$

where γ_1, γ_2, and ϖ are target coefficients, and $T_m = 0.0015s$ is obtained according to Fig. 4.5.

Then, the regularization penalty needs to be obtained. The regularization penalty usually has one of the following forms, L_0 norm which is the number of non-zero γ_i (the weights of $\eta(t)$), L_1 norm which is the absolute-value norm of γ_i, and L_2 norm which is the squared Euclidean norm of γ_i. In this part, L_1 norm is used to define the regularization penalty as did in [120]. It is given as:

$$Q(\eta) = \left| \frac{\gamma_1 T_m + \gamma_2 (T - T_m)}{T} \right| \tag{4.59}$$

By applying the steepest descent method [131], coefficients γ_1, γ_2, and ϖ of $\eta(t)$ are obtained to minimize the error $\varepsilon + \kappa Q(\eta)$ based on the training data. Up

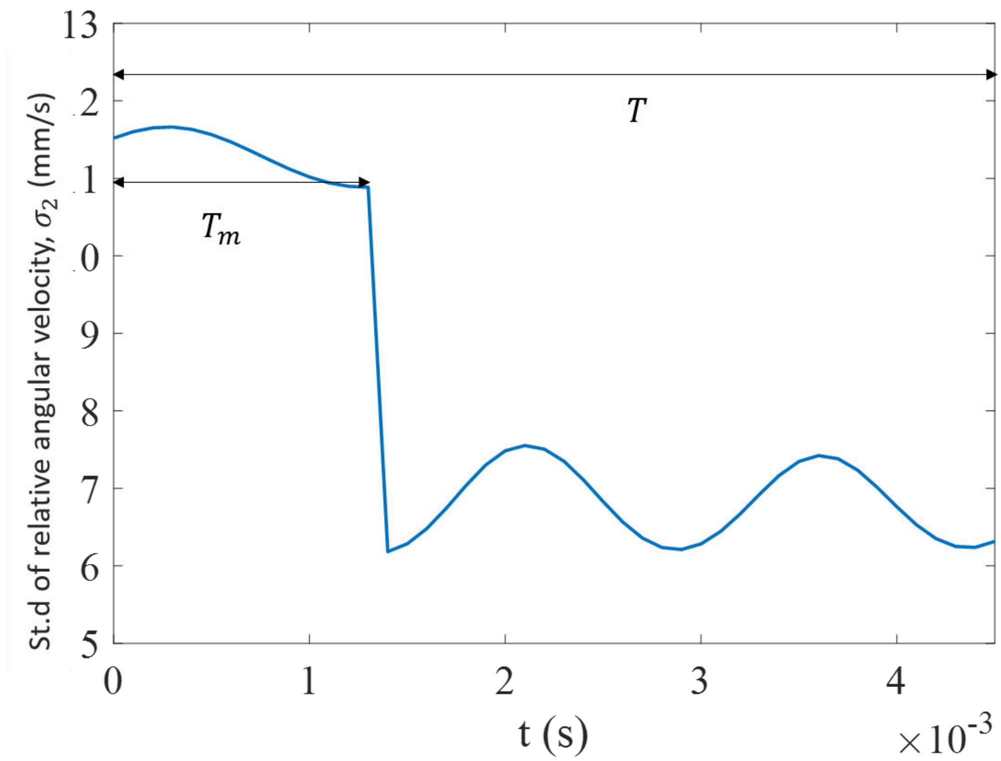

Fig. 4.5: The periodicity of σ_2

to now, the function $\eta(t)$ is obtained. Then, the expression of σ_2 obtained by PI method during [0.35, 0.4] s is adjusted using Eq. (4.41). It means the value of σ_2 using our proposed method can be obtained.

Similarly, the expression of σ_1 and σ_{12} are obtained by obtaining the corresponding $\eta(t)$. After getting the values of σ_1, σ_2, and σ_{12}, solutions in Eqs. (4.8-4.11) are updated.

4.4.2 Validation of the solution

The objective of this section is to validate the solution generated by the proposed method. The gear model described in Section 4.4.1 is used for the validation.

To preliminarily evaluate the performance of our updated solution, σ_2 obtained by MC method and our proposed method during the period [0.35, 0.4] s are compared. The result is shown in Fig. 4.6. Fig. 4.6 shows that the values of σ_2 calculated by the proposed method are very close to the values obtained by MC

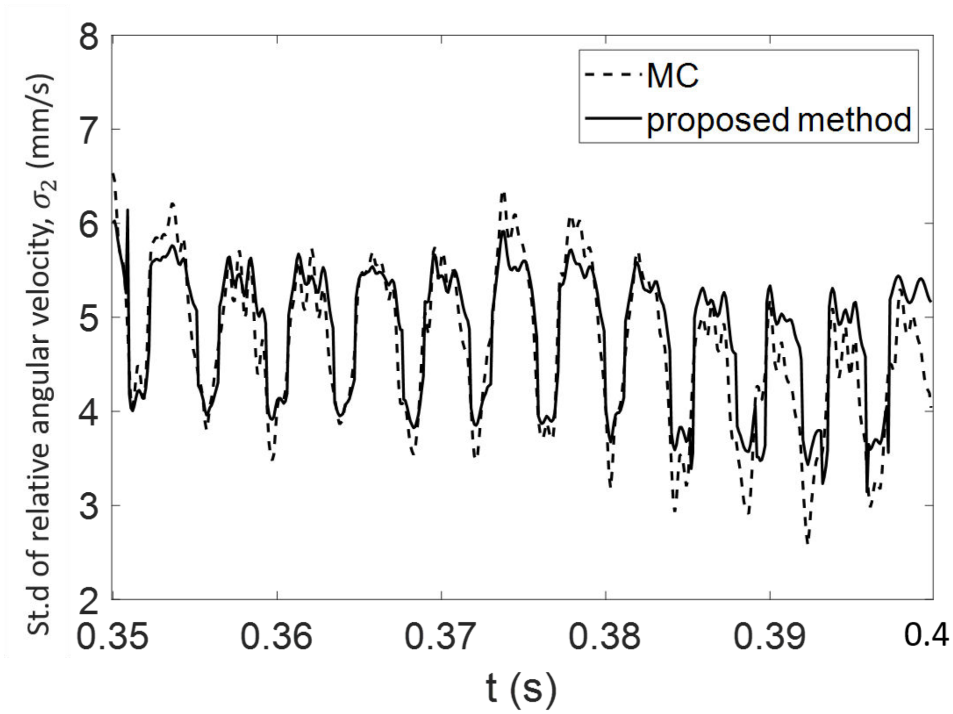

Fig. 4.6: The testing data

method.

The instantaneous marginal PDF of x and $\dot{x}$ at 0.39s are shown in Fig. 4.7. Despite there's a slight distinct in st. d by MC method and the proposed method (shown in Fig. 4.6), the PDFs of the two methods are very close in Fig. 4.7. This agreement validates the approximate analytical solution which is obtained by the proposed method is accurate.

The joint PDFs of x and $\dot{x}$ under different methods are shown in Fig. 4.8. It illustrates the joint PDFs of x and $\dot{x}$ at $t = 0.76s$. It is observed that the joint PDF from the proposed method agrees well with that from the MC method.

4.4.3 Evaluation of the proposed method

In the previous section, we have qualitatively compared our proposed method with MC method. This section will quantitatively assess the performance of the proposed method. Accuracy evaluation will be done in Section 4.4.3.1 and efficiency evaluation will be conducted in Section 4.4.3.2.

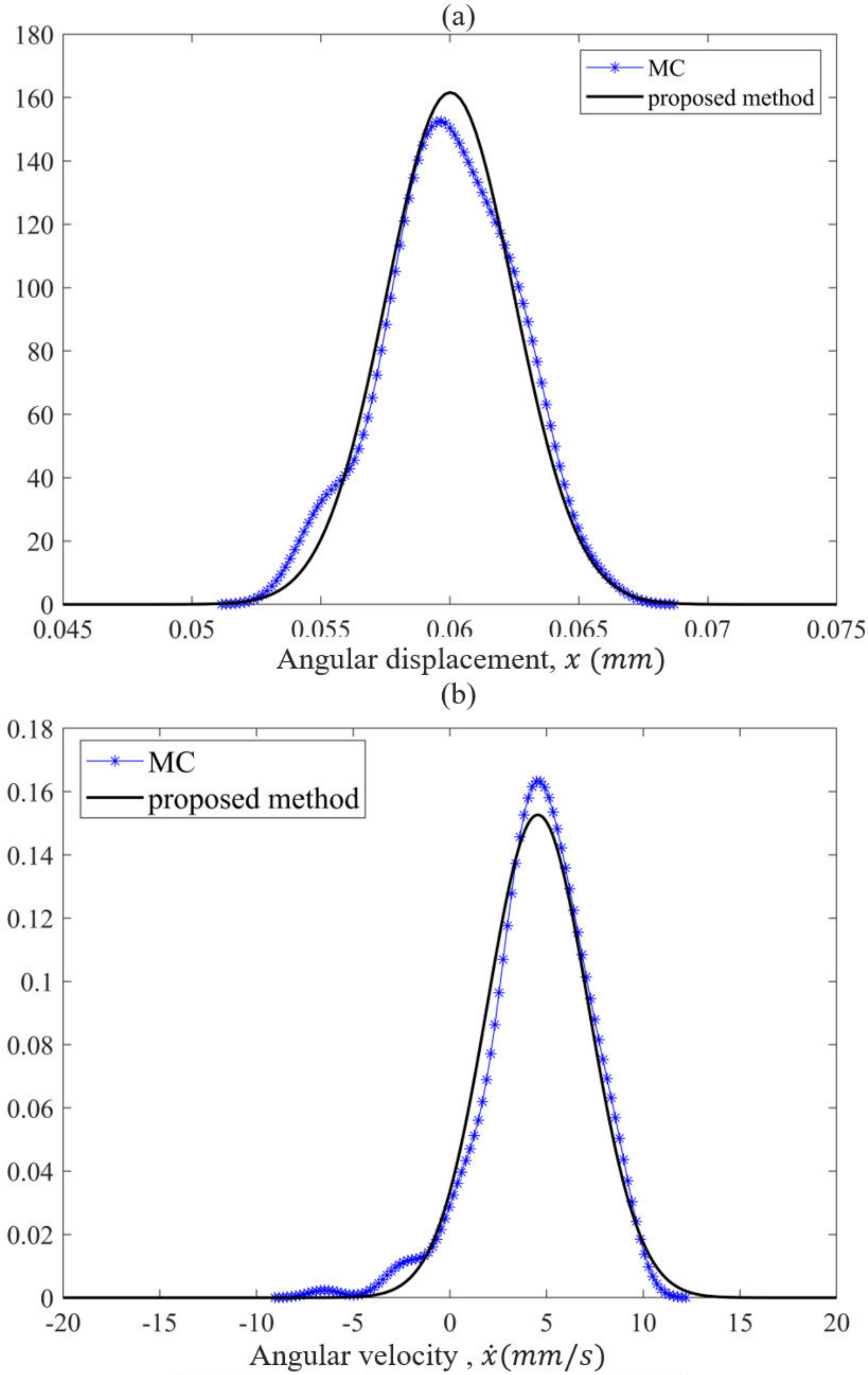

Fig. 4.7: Marginal distribution of (a) x (b) $\dot{x}$ at $t = 0.39s$

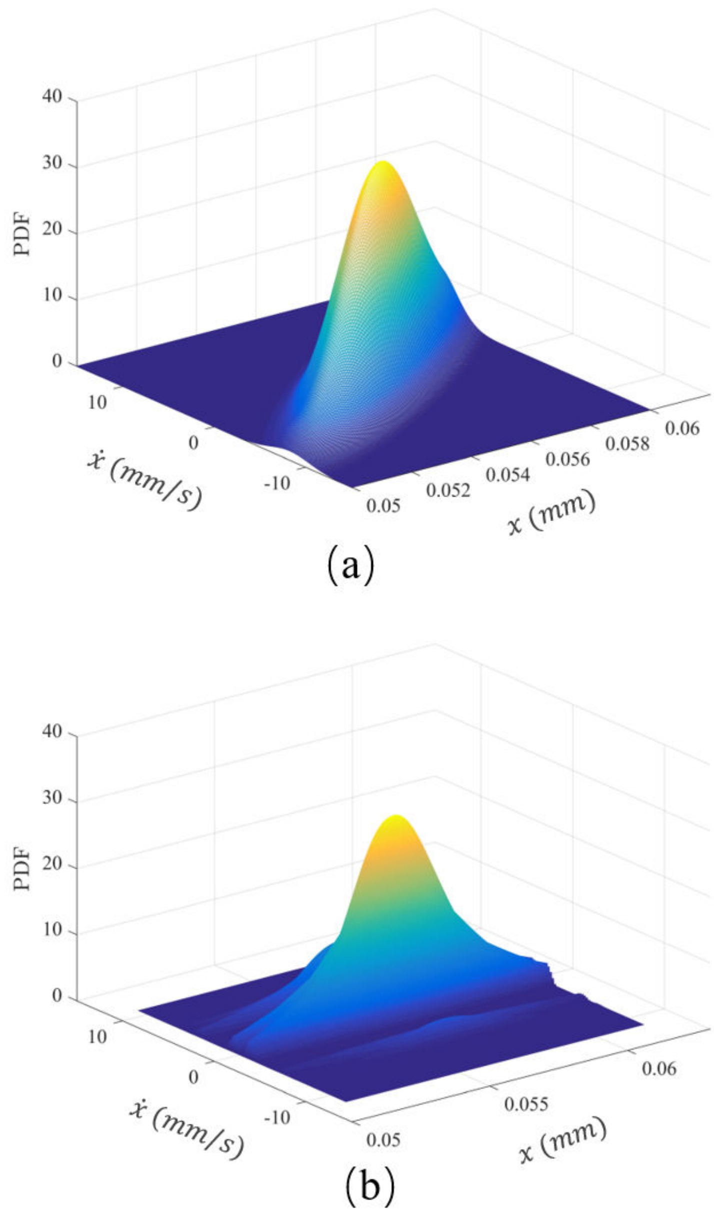

Fig. 4.8: Joint distribution at 0.76 s: (a) proposed method, (b) MC method

4.4.3.1 Accuracy evaluation

Accuracy evaluation aims to quantify the errors generated by the proposed method comparing with MC method. Risk function defined in Eq. (4.39) can be used to quantify the errors, but it is not easy to obtain. In practical, it is common to use the following definition to represent the average error between $\tilde{\sigma}_2$ (st. d of $\dot{x}$ by the proposed method) and σ_2^{MC} (st. d of $\dot{x}$ obtained by MC method).

$$\bar{\varepsilon} = \frac{1}{M} \sum_{i=1}^{N} \frac{\left|\tilde{\sigma}_2(j) - \sigma_2^{MC}(j)\right|}{\sigma_2^{MC}(j)} \times 100\% \tag{4.60}$$

where M is the number of time points and j represents a time point. Eq. (4.60) can be also used to calculate the average error of μ_1, μ_2, and $\tilde{\sigma}_1$.

Using responses in [0.35, 0.4] s as an example, the average errors of μ_1, μ_2, $\tilde{\sigma}_1$, and $\tilde{\sigma}_2$ between two methods are 9.2%, 2.25%, 7.19%, and 5.28%, respectively. These errors are all less than 10%, which is acceptable in some degree.

4.4.3.2 Efficiency evaluation

In this section, the objective is to explain the efficiency gain using the proposed method.

To solve the formulated problem, we propose an improved PI method. It is based on MC simulation. But, only a limited number of samples are needed to be generated by the MC method for our learning procedure, which can greatly save computation time compared with the traditional MC method. The detailed analysis about the efficiency is given as follows.

Suppose H is the total computational cost for single simulation under stochastic load (e.g. generate one sample of $x(t)$ in Fig. 4.2), H_1 is the time cost by solving the equation under deterministic load (obtaining μ_1 and μ_2), H_2 is the time cost by obtaining a learning sample by MC method ($H_2 \ll H$), and N_m denotes the sample number. Table 4.2 gives the total computational cost comparison between MC method and the proposed method. The numbers in Table 4.2 give the time cost for obtaining approximate analytical solution from [0, 1.6] s by the proposed method and MC method (one sample by MC method is shown in Fig. 4.2), respectively. In our simulation, we have $H = 671.368$s, $H_1 = 11.3$s, $H_2 = 125.284$s, and $N_m = 100$.

Table 4.2: The total computational cost comparison

	The computational cost	
MC method	$H \times N_m$	67136.8s
Proposed method	$H_1 + H_2 \times N_m$	12539.7s

From Table 4.2, the proposed method saves 81.3% (i.e., $(1 - 12539.7/67136.8) \times 100\%$) computational cost. We can see the proposed method greatly increases the calculation efficiency compared to MC method. In addition, once the modification function is obtained, it can be applied to the following responses. Therefore, with the increasing of simulation length of gear system, our proposed method could save more time in calculation.

4.5 Conclusion

This work proposes an approximate analytical solution to a spur gear dynamic model with stochastic load and one additional stochastic internal factor. A tentative analytical solution is derived using PI method and then updated using a supervised learning algorithm. A case study taking friction as an example of the additional stochastic element is used to validate our proposed method. The dynamic responses of this model are investigated using our proposed method and then compared with MC results. The analysis results demonstrate that (a) the proposed method can deal with the gear model with stochastic load and a stochastic internal factor. Especially, the proposed method can handle the internal factor that is dependent on gear velocity and/or displacement. (b) although the proposed method loses a bit accuracy comparing with MC method, it greatly increases the calculation efficiency. Future works may consider the method to obtain a more accuracy modification function. Therefore, the proposed method in this chapter can obtain a more accuracy solution.

In summary, to investigate the dynamic characteristics of gear systems, the time cost is large when obtaining the simulation results in Chapter 2 and Chapter 3. It is because the large time complexity of numerical methods, which are adopted to solve gear dynamic models under stochastic excitations. To address this problem, this chapter proposed an efficient method to obtain approximate analytical solution to a gear model under stochastic load with one stochastic internal factor. The model in Chapter 2 was also taken as an example to demonstrate the efficiency and accuracy of the proposed method. Focusing on the two main aspects of this thesis (i.e., modeling and solving), this chapter proposed an efficient method to solve gear dynamic models under stochastic excitations which made this thesis more complete in the study of gear dynamics.

5 Summary and Future work

This chapter summarizes the contributions of this thesis and describes some problems that remain to be addressed.

5.1 Contributions of Thesis

Lumped parameter modeling (LPM) has been widely used in the dynamic modeling of gear systems. The understanding of dynamic characteristics of a gear system considering stochastic internal and external excitations helps the development in the design and effective tools of condition monitoring of a gear system. This study aims to simulate and investigate the dynamic characteristics of a gear system, which are affected by stochastic internal and external excitations. The contributions of this thesis are summarized in three categories, which are given in the next three sections.

5.1.1 Effects of friction on gear dynamic characteristics

The main objective of this topic as documented in Chapter 2 is to investigate the effects of friction and stochastic load on gear systems' transient characteristics.

In this thesis, a single degree of freedom (SDOF) nonlinear dynamic model of a spur gear pair is developed based on the model reported in [5]. TVMS, backlash, sliding friction, and stochastic load are considered in our model. Friction is the first time introduced to a gear dynamic model under stochastic load. The validation is done by comparing with the result reported in [50], which considered the model of a spur gear pair under deterministic load considering TVMS and backlash.

To analyze the dynamic characteristics of the proposed model, this topic gives the numerical simulation results. Six cases of the friction coefficient values are used and responses are compared with one another. The dynamic model of gear systems is solved by Runge-Kutta method. The statistical characteristics of gear response are obtained by MC method.

The analysis results demonstrate that (a) the established SDOF gear dynamic model is more realistic than reported models which did not consider friction, (b) under the same friction coefficient value, the stochastic load generates longer duration in the transient state and higher fluctuation in the steady state compared with those under deterministic load, (c) under stochastic load, the gear system has different transient stability under different friction coefficients. The case with friction generates higher dispersion of relative angular displacement in the transient state and lower dispersion in the steady state compared with those of the case without friction.

This analysis gives us better understanding on the effects of stochastic load and friction on the gear dynamic characteristics. The proposed gear dynamic model and numerical results can be used as a reliable tool to investigate the gear random dynamics.

In summary, a gear stochastic dynamic model for a spur gear pair is established in this topic. Friction is introduced in the model under stochastic load for the first time. Therefore, the proposed model is more realistic than reported models. The model proposed in this topic is then improved by the work in Chapter 3. In addition, considering the model in this chapter, an efficient method is proposed in Chapter 4 to solve this model. This topic, as the pioneer of the whole thesis, explores the history of the development of gear dynamics and laid a firm foundation of the following studies.

5.1.2 Effects of driving speed on gear dynamic characteristics

In this topic, as documented in chapter 3, a stochastic nonlinear gear dynamic model is presented. Due to manufacturing error, energy loss, possible change of the engine status, and variation of operating environment, the driving speed and external load are not deterministic in the future. Thus, under the presented model, the effects of the driving speed variation (including deterministic or stochastic driving speed) on gear dynamic characteristics under stochastic load are investigated for the first time. MC method is applied to analyze the dynamic characteristics focusing on the effects caused by driving speed coupled with stochastic load.

Some insightful conclusions are obtained based on the simulation results. It shows that the random element of the driving speed affects the gear response a lot which should not be ignored. Under the stochastic load, a small ratio of randomness in driving speed greatly increases the dispersion in responses. In addition, the dispersion in responses is more sensitive to the uncertainty of the driving speed than that of the load.

In summary, an improved gear model based on the model in Chapter 2 is proposed in this topic. It explores one more external excitation (i.e., driving speed), which is an improvement in gear dynamic modeling. Therefore, the stochastic features of real gear systems can be well modelled by our proposed gear model. Considering the two main aspects of this thesis (i.e., modeling and solving of gear systems), the works in Chapter 2 and Chapter 3 make the dynamic modeling of gear systems more realistic.

5.1.3 Approximate analytical solution to a gear model with treating one internal factor as stochastic

Researchers have considered stochastic load and deterministic internal factors such as damping and TVMS in gear system dynamic models. In this topic, as documented in Chapter 4, we treat one of the internal factors as stochastic which is more realistic. The stochastic behavior of this internal factor may depend on gear velocity and/or displacement, which will cause the dynamic equations to be difficult to solve. The main objective of this topic is to propose a method to obtain the approximate analytical solution for a gear pair model under stochastic load considering one stochastic internal factor.

A transformation of the original dynamic equation is introduced so that the reported PI method can be used to obtain a tentative analytical solution. Then, we propose a method to improve the accuracy of the tentative analytical solution as follows. It is based on MC simulation. However, only a limited number of samples are needed to be generated by the MC simulation. A supervised learning algorithm is then used to establish the relationship between the tentative analytical solution obtained by PI method and the responses obtained by MC method in order to obtain a modification function. The modification function is applied to the tentative analytical solution to obtain more accurate solution of the system dynamic equations considering the load and an internal factor as stochastic. A case study is presented to validate the proposed approach and demonstrate its efficiency. Compared to the numerical methods, our proposed method can achieve similar accuracy responses of the gear model but with much smaller time complexity.

In summary, different from the works in Chapter 2 and Chapter 3, this topic focuses on the other aspect of this thesis (i.e., the solving techniques of gear models). When dealing with the proposed dynamic models in Chapter 2 and Chapter 3, the simulation takes a lot of time due to the large time complexity of numerical methods, which are adopted to solve gear models under stochastic excitations. Thus, this work proposes an efficient method to solve gear dynamic models with stochastic excitations involved. By the proposed method, an approximate analytical solution of the considered dynamic gear model can be derived. This method can be used but not limited to solve the gear dynamic model in Chapter 2. It can be widely adopted for gear dynamic models under stochastic load with one additional stochastic internal excitation.

5.2 Directions for Future Work

Although this thesis improves the modeling and solving techniques of gear models, there are still some problems that need to be further addressed. Based on the scope of this dissertation, the following three perspectives are suggested for future consideration.

These three perspectives are corresponding to the contents in Section 1.2 which are modeling, solution, and dynamic characteristics, respectively. The following three sections are listed as potential topics regarding to the three perspectives. The exploring of the gear stochastic and nonlinear dynamics are not only limited to these three listed examples.

5.2.1 Modeling and influence analysis of a chaotic load on gear dynamics

The assumption of external load to be Gaussian white noise maybe not proper in some machines, e.g. ships, mining machines, wind turbines, etc.. Under these machines, the load profile is quite complicated and the load varies greatly [132]-[135]. For wind turbines, their driven chain loads are generated by wind speed. The relationship between the load and wind speed is positive correlation, but has no fixed pattern [136]. The generated load cannot be expressed as analytical expression using probabilistic method. Thus, it is necessary to develop a reliable non-probabilistic load model to represent the load profiles of wind turbines.

A chaotic load model will be first introduced to a gear dynamic model. A SDOF nonlinear dynamic model of a spur gear pair is developed based on the model reported in [49]. TVMS, backlash, sliding friction, and chaotic load are considered in our model. This model is the same as Chapter 2 except load. The main objective of this topic is to investigate a chaotic load model and its effects on system's dynamic characteristics.

A generator of variable load of wind turbines will be proposed according to Ref. [136]. The procedures of this topic are stated as:

1. The model for generation of wind speed is designed by the Weierstrass function.
2. The rotational speed of the main shaft is proposed as a function of the wind speed value. The function depends on a few parameters that are fitted by using a genetic algorithm.
3. The model of the torque of the main shaft is introduced. Chaotic load will be generated by a multi-layer artificial neural network [63] and an open source wind speed and energy data will be adopted for validation.

4. The dynamic model of gear systems is solved by Runge-Kutta method. The chaotic characteristics of gear response are analyzed by Poincaré map.

This way of generating load can be extended other realistic cases by using different study samples. The proposed chaotic load model and numerical results can improve the gear condition monitoring and fault diagnosis [137].

5.2.2 Gear dynamic modelling considering variable mass

Several studies have shown the great effects of the stochastic internal excitations on the dynamic characteristics of gear systems [138]. Guerine et al. [135] considered mass and moment of inertia as random variables with Gaussian white noise on a one stage gear system. Abo et al. [139] investigated the variability in gear design parameters and operational conditions. Therefore, it is necessary to take the uncertainties of internal excitations into account. Variable moment of the inertia (or variable mass) will be considered with friction and stochastic load.

Stochastic averaging method, which is an efficient tool for obtaining stationary responses of ODEs, is used in some literature. When the PDF of the dynamic system's responses varies within a certain small range of time, the response is called stationary response and the system is in steady state. The response before reaching the steady state is called transient response. Qiao et al. [140] studied a variable-mass duffing oscillator with mass disturbance, which is modeled as Gaussian white noise.

Although stochastic averaging method can deal with stochastic variable-mass systems, the coupling of stochastic mass and friction is still a big problem. Proper treatment on the friction is the key to solve this problem.

5.2.3 Stability analysis using Lyapunov exponent

There are several versions of stability definitions [141], among which the asymptotic stability with probability one is widely adopted. In recent years, based on the Oseledec multiplicative ergodic theorem [142], there is a trend to analyze the asymptotic Lyapunov stability with probability one through evaluating the largest Lyapunov exponent of the system. Therefore, it is possible for us to study the effects of stochastic internal and external excitations on the asymptotic stability.

It has been known that the stability shows a great effects on actual situations, and the consequence will be disastrous once the stability of a system is destroyed. Hence, stochastic stability, as one of the most fundamental characteristics of nonlinear stochastic dynamics, has been extensively studied.

Here, the stability refers to the stability of the solutions, where the solutions denote the mean and standard deviation of displacement or velocity in my work. If the solutions under a certain initial condition stay near the equilibrium point forever, then it is called stable (or Lyapunov stable). If the solutions under a certain initial condition converge to equilibrium point, then it is called asymptotically stable. Fig. 5.1 shows the solutions of a dynamic system under different initial conditions [143]. Fig. 5.1(a) approaches to an equilibrium point while Fig. 5.1(b) does not.

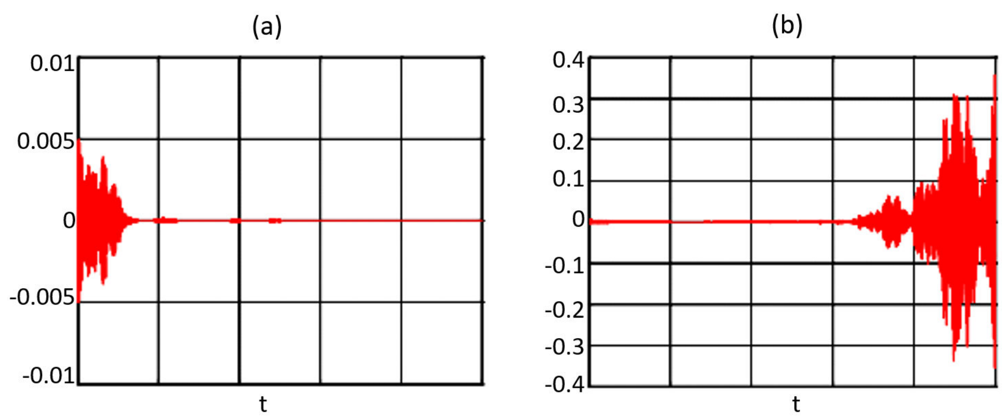

Fig. 5.1: Sample of solutions with different initial condition a) stable b) unstable

Thus, it is necessary to investigate the stability of a spur gear model considering variable moment of inertia and friction under stochastic load. Stochastic averaging method will be applied to a such model and an adjustment will be done. Stochastic stability will be studied by Lyapunov exponent [143].

With the future extension, we envision that these advanced models can be used to the gear health diagnosis area. With the better understanding of the mechanism in gear dynamics, engineers can have better strategies in gear design phase. This will bring more benefits in the extension of gear systems' potential useful life.

Bibliography

[1] F. Liu, H. Jiang, S. Liu, and X. Yu, "Dynamic behavior analysis of spur gears with constant & variable excitations considering sliding friction influence," *Journal of Mechanical Science and Technology*, vol. 30, no. 12, pp. 5363–5370, 2016.

[2] S. Wei, Q. Han, and F. Chu, "Review on research of uncertain dynamics for gear system," *Journal of Mechanical Engineering*, vol. 1, pp. 1–19, 2016.

[3] Z. Levai, "Structure and analysis of planetary gear trains," *Journal of mechanisms*, vol. 3, no. 3, pp. 131–148, 1968.

[4] M. Lias, R. TVVLN, M. Awang, and M. Khan, "The stress distribution of gear tooth due to axial misalignment condition," *Journal of Applied Sciences*, vol. 12, no. 23, pp. 2404–2410, 2012.

[5] Y. Wen, J. Yang, and S. Wang, "Random dynamics of a nonlinear spur gear pair in probabilistic domain," *Journal of Sound and Vibration*, vol. 333, no. 20, pp. 5030–5041, 2014.

[6] F. D. Jones and H. H. Ryffel, *Gear design simplified*. Industrial Press Inc., 1961.

[7] J. Wang, R. Li, and X. Peng, "Survey of nonlinear vibration of gear transmission systems," *Applied Mechanics Reviews*, vol. 56, no. 3, pp. 309–329, 2003.

[8] B. Alonzo, H.-K. Ringkjob, B. Jourdier, P. Drobinski, R. Plougonven, and P. Tankov, "Modelling the variability of the wind energy resource on monthly and seasonal timescales," *Renewable Energy*, vol. 113, pp. 1434–1446, 2017.

[9] A. L. Kapelevich and R. E. Kleiss, "Direct gear design for spur and helical involute gears." *Gear Technology*, vol. 19, no. 5, pp. 29–35, 2002.

[10] Y. Cai, "Simulation on the rotational vibration of helical gears in consideration of the tooth separation phenomenon (a new stiffness function of helical involute tooth pair)," *Journal of Mechanical Design*, vol. 117, no. 3, pp. 460–469, 1995.

[11] F. Pfeiffer, *Mechanical system dynamics*. Springer Science & Business Media, vol. 40, 2008.

[12] X. Liang, M. J. Zuo, and Z. Feng, "Dynamic modeling of gearbox faults: A review," *Mechanical Systems and Signal Processing*, vol. 98, pp. 852–876, 2018.

[13] H. N. Özgüven and D. R. Houser, "Mathematical models used in gear dynamics: a review," *Journal of sound and vibration*, vol. 121, no. 3, pp. 383–411, 1988.

[14] C. W. De Silva, *Modeling and control of engineering systems*. Crc Press, 2009.

[15] Hibbitt, Karlsson, and Sorensen, *ABAQUS/Standard user's manual*. Hibbitt, Karlsson & Sorensen, vol. 1, 2001.

[16] T. Stolarski, Y. Nakasone, and S. Yoshimoto, *Engineering analysis with ANSYS software*. Butterworth-Heinemann, 2018.

[17] X. Liang, M. J. Zuo, and T. H. Patel, "Evaluating the time-varying mesh stiffness of a planetary gear set using the potential energy method," *Proceedings of the Institution of Mechanical Engineers, Part C: Journal of Mechanical Engineering Science*, vol. 228, no. 3, pp. 535–547, 2014.

[18] S. Li and A. Kahraman, "A spur gear mesh interface damping model based on elastohydrodynamic contact behaviour," *International Journal of Powertrains*, vol. 1, no. 1, pp. 4–21, 2011.

[19] F. Li, Y. Qin, L. Ge, Z. Pang, S. Liu, and D. Lin, "Influences of planetary gear parameters on the dynamic characteristics-a review," *Journal of Vibroengineering*, vol. 17, no. 2, pp. 574–586, 2015.

[20] Y. Zhang, Q. Liu, and B. Wen, "Practical reliability-based design of gear pairs," *Mechanism and Machine Theory*, vol. 38, no. 12, pp. 1363–1370, 2003.

[21] A. Patil and A. Thosar, "Steady state and transient stability analysis of wind energy system," in *Control, Instrumentation, Energy & Communication (CIEC), 2016 2nd International Conference*. IEEE, pp. 250–254, 2016.

[22] R. Drago, "The effect of start-up load conditions on gearbox performance and life failure analysis, with supporting case study," in *American Gear Manufacturers Association Fall Technical Meeting*, 2009.

[23] Y. Fang, X. Liang, and M. J. Zuo, "Effects of friction and stochastic load on transient characteristics of a spur gear pair," *Nonliear Dynamics*, vol. 93, no. 2, pp. 599–609, 2018.

[24] M. Khabou, N. Bouchaala, F. Chaari, T. Fakhfakh, and M. Haddar, "Study of a spur gear dynamic behavior in transient regime," *Mechanical Systems and Signal Processing*, vol. 25, no. 8, pp. 3089–3101, 2011.

[25] J. Wang, T. C. Lim, and M. Li, "Dynamics of a hypoid gear pair considering the effects of time-varying mesh parameters and backlash nonlinearity," *Journal of Sound and Vibration*, vol. 308, no. 1-2, pp. 302–329, 2007.

[26] F. Liu, L. Zhang, and X. Yu, "Stability investigation of velocity-modulated gear system using a new computational algorithm," *Nonlinear Dynamics*, vol. 89, no. 2, pp. 1111–1128, 2017.

[27] Y. Shao and Z. Chen, "Dynamic features of planetary gear set with tooth plastic inclination deformation due to tooth root crack," *Nonlinear dynamics*, vol. 74, no. 4, pp. 1253–1266, 2013.

[28] A. Guerine, A. El Hami, L. Walha, T. Fakhfakh, and M. Haddar, "Dynamic response of wind turbine gear system with uncertain-but-bounded parameters using interval analysis method," *Renewable Energy*, vol. 113, pp. 679–687, 2017.

[29] M. Hashemi and M. Saeed Safizadeh, "Design of a fuzzy model based on vibration signal analysis to auto-detect the gear faults," *Industrial Lubrication and Tribology*, vol. 65, no. 3, pp. 194–201, 2013.

[30] M. Utagawa and T. Harada, "Dynamic loads on spur gear teeth having pitch errors at high speed," *Bulletin of JSME*, vol. 5, no. 18, pp. 374–381, 1962.

[31] T. Tobe and K. Sato, "Statistical analysis of dynamic loads on spur gear teeth," *Bulletin of JSME*, vol. 20, no. 145, pp. 882–889, 1977.

[32] Y. Wang and W. Zhang, "Stochastic vibration model of gear transmission systems considering speed-dependent random errors," *Nonlinear dynamics*, vol. 17, no. 2, pp. 187–203, 1998.

[33] B. Liu, J. Xu, and X. Zhao, "Parameter estimation for load-sharing systems with degrading components," in *2016 IEEE International Conference on Industrial Engineering and Engineering Management*. IEEE, pp. 1310–1314, 2016.

[34] J. C. Butcher, *The numerical analysis of ordinary differential equations: Runge-Kutta and general linear methods*. John Wiley & Sons Inc, 1987.

[35] E. Hairer, C. Lubich, and M. Roche, *The numerical solution of differential-algebraic systems by Runge-Kutta methods*. Springer, vol. 1409, 2006.

[36] J. Yang and P. Yang, "Random gear dynamics based on path integration method," in *ASME 2012 International Mechanical Engineering Congress and Exposition*. American Society of Mechanical Engineers, pp. 879–887, 2012.

[37] T. Tobe, K. Sato, and N. Takatsu, "Statistical analysis of dynamic loads on spur gear teeth: experimental study," *Bulletin of JSME*, vol. 20, no. 148, pp. 1315–1320, 1977.

[38] L. Wang, T. Shen, C. Chen, and H. Chen, "Dynamic reliability analysis of gear transmission system of wind turbine in consideration of randomness of loadings and parameters," *Mathematical Problems in Engineering*, vol. 2014, 2014.

[39] S. Theodossiades and S. Natsiavas, "Non-linear dynamics of gear-pair systems with periodic stiffness and backlash," *Journal of Sound and Vibration*, vol. 229, no. 2, pp. 287–310, 2000.

[40] M. Benton and A. Seireg, "Simulation of resonances and instability conditions in pinion-gear systems," *Journal of Mechanical Design*, vol. 100, no. 1, pp. 26–32, 1978.

[41] H. Vinayak, R. Singh, and C. Padmanabhan, "Linear dynamic analysis of multi-mesh transmissions containing external, rigid gears," *Journal of Sound and Vibration*, vol. 185, no. 1, pp. 1–32, 1995.

[42] A. Kahraman and R. Singh, "Non-linear dynamics of a geared rotor-bearing system with multiple clearances," *Journal of sound and vibration*, vol. 144, no. 3, pp. 469–506, 1991.

[43] A. Kahraman and R. Singh, "Non-linear dynamics of a spur gear pair," *Journal of sound and vibration*, vol. 142, no. 1, pp. 49–75, 1990.

[44] J. Yang, "Vibration analysis on multi-mesh gear-trains under combined deterministic and random excitations," *Mechanism and Machine Theory*, vol. 59, pp. 20–33, 2013.

[45] J. Lu, F. Zeng, J. Xin, E. Miao, and M. Liu, "Influences of stochastic perturbation of parameters on dynamic behavior of gear system," *Journal of mechanical science and technology*, vol. 25, no. 7, p. 1667, 2011.

[46] M. J. Handschuh, "An investigation into the impact of random spacing errors on static transmission error and root stresses of spur gear pairs," Ph.D. dissertation, The Ohio State University, 2013.

[47] M. Inalpolat, M. Handschuh, and A. Kahraman, "Influence of indexing errors on dynamic response of spur gear pairs," *Mechanical Systems and Signal Processing*, vol. 60, pp. 391–405, 2015.

[48] Z. Li and K. Mao, "Frictional effects on gear tooth contact analysis," *Advances in Tribology*, vol. 2013, 2013.

[49] K. Martin, "A review of friction predictions in gear teeth," *Wear*, vol. 49, no. 2, pp. 201–238, 1978.

[50] D. Yang and J. Lin, "Hertzian damping, tooth friction and bending elasticity in gear impact dynamics," *Journal of mechanisms, transmissions, and automation in design*, vol. 109, no. 2, pp. 189–196, 1987.

[51] H. Iida, A. Tamaura, and Y. Yamada, "Vibrational characteristics of friction between gear teeth," *Bulletin of JSME*, vol. 28, no. 241, pp. 1512–1519, 1985.

[52] I. Krupka, M. Hartl, and P. Svoboda, "Effect of surface topography on mixed lubrication film under transient conditions," in *ASME/STLE 2009 International Joint Tribology Conference*. American Society of Mechanical Engineers, pp. 481–482, 2009.

[53] S. He, S. Cho, and R. Singh, "Prediction of dynamic friction forces in spur gears using alternate sliding friction formulations," *Journal of Sound and Vibration*, vol. 309, no. 3-5, pp. 843–851, 2008.

[54] R. Guilbault, S. Lalonde, and M. Thomas, "Nonlinear damping calculation in cylindrical gear dynamic modeling," *Journal of Sound and Vibration*, vol. 331, no. 9, pp. 2110–2128, 2012.

[55] T. M. Ericson and R. G. Parker, "Experimental measurement of the effects of torque on the dynamic behavior and system parameters of planetary gears," *Mechanism and Machine Theory*, vol. 74, pp. 370–389, 2014.

[56] G. Sika and P. Velex, "Instability analysis in oscillators with velocity-modulated time-varying stiffnessapplications to gears submitted to engine speed fluctuations," *Journal of Sound and Vibration*, vol. 318, no. 1-2, pp. 166–175, 2008.

[57] I. S. Al-Tubi and H. Long, "Prediction of wind turbine gear micropitting under variable load and speed conditions using iso/tr 15144-1: 2010," *Proceedings of the Institution of Mechanical Engineers, Part C: Journal of Mechanical Engineering Science*, vol. 227, no. 9, pp. 1898–1914, 2013.

[58] X. Qiu, Q. Han, and F. Chu, "Analytical investigation on unstable vibrations of single-mesh gear systems with velocity-modulated time-varying stiffness," *Journal of Sound and Vibration*, vol. 333, no. 20, pp. 5130–5140, 2014.

[59] W. Tutak and A. Jamrozik, "Characteristics of the flow field in the combustion chamber of the internal combustion test engine," *Chemical and Process Engineering*, vol. 32, no. 3, pp. 203–214, 2011.

[60] L. Pruvost, Q. Leclere, and E. Parizet, "Diesel engine combustion and mechanical noise separation using an improved spectrofilter," *Mechanical systems and signal processing*, vol. 23, no. 7, pp. 2072–2087, 2009.

[61] R. B. Randall, "Basic signal processing techniques," *Vibration-based Condition Monitoring*, pp. 63–141, 2011.

[62] W. Yang, X. Tang, and X. Chen, "Nonlinear modelling and transient dynamics analysis of a hoist equipped with a two-stage planetary gear

transmission system." *Journal of Vibroengineering*, vol. 17, no. 6, pp. 2858–2868, 2015.

[63] A. Kumar, M. Osman, and T. Sankar, "On statistical analysis of gear dynamic loads," *Journal of vibration, acoustics, stress, and reliability in design*, vol. 108, no. 3, pp. 362–368, 1986.

[64] J. Roberts and P. Spanos, "Stochastic averaging: an approximate method of solving random vibration problems," *International Journal of Non-Linear Mechanics*, vol. 21, no. 2, pp. 111–134, 1986.

[65] W. R. Gilks, S. Richardson, and D. Spiegelhalter, *Markov chain Monte Carlo in practice*. CRC press, 1995.

[66] A. Naess and V. Moe, "Efficient path integration methods for nonlinear dynamic systems," *Probabilistic engineering mechanics*, vol. 15, no. 2, pp. 221–231, 2000.

[67] A. Naess, F. Kolnes, and E. Mo, "Stochastic spur gear dynamics by numerical path integration," *Journal of sound and vibration*, vol. 302, no. 4-5, pp. 936–950, 2007.

[68] Y. Park and H. Park, "Dynamic characteristic analysis of mold oscillator including improved gear mesh model and cam profile for eccentric shaft," *Journal of Mechanical Science and Technology*, vol. 28, no. 11, pp. 4465–4473, 2014.

[69] J. Rice, *Mathematical statistics and data analysis*. Nelson Education, 2006.

[70] K. Sato, S. Yamamoto, O. Kamada, and N. Takatsu, "Approximate solution of a gear system subjected to random excitation," *Bulletin of JSME*, vol. 29, no. 251, pp. 1586–1589, 1986.

[71] M. Belhadj and T. Aldemir, "The cell to cell mapping technique and chapman-kolmogorov representation of system dynamics," *Journal of sound and vibration*, vol. 181, no. 4, pp. 687–707, 1995.

[72] H. Köylüolu, S. Nielsen, and A. Çakmak, "Fast cell-to-cell mapping (path integration) for nonlinear white noise and poisson driven systems," *Structural safety*, vol. 17, no. 3, pp. 151–165, 1995.

[73] J. Sun and C. t. Hsu, "The generalized cell mapping method in nonlinear random vibration based upon short-time gaussian approximation," *Journal of applied mechanics*, vol. 57, no. 4, pp. 1018–1025, 1990.

[74] C. S. Hsu, *Cell to cell mapping: a method of global analysis for nonlinear systems*. Springer Science & Business Media, vol. 64, 2013.

[75] D. Yang and Z. Sun, "A rotary model for spur gear dynamics," *Journal of mechanisms, transmissions, and automation in design*, vol. 107, no. 4, pp. 529–535, 1985.

[76] X. Tian, "Dynamic simulation for system response of gearbox including localized gear faults," Master's thesis, University of Alberta, Edmonton, 2004.

[77] D. Lee, K. Moon, and W. Lee, "Characteristics of transmission error and vibration of broken tooth contact," *Journal of Mechanical Science and Technology*, vol. 30, no. 12, pp. 5547–5553, 2016.

[78] R. Munro, "A review of the theory and measurement of gear transmission error," *Gearbox noise and vibration*, pp. 3–10, 1990.

[79] W. Bartelmus, F. Chaari, R. Zimroz, and M. Haddar, "Modelling of gearbox dynamics under time-varying nonstationary load for distributed fault detection and diagnosis," *European Journal of Mechanics - A/Solids*, vol. 29, pp. 637–646, 2010.

[80] S. He, R. Gunda, and R. Singh, "Effect of sliding friction on the dynamics of spur gear pair with realistic time-varying stiffness," *Journal of Sound and Vibration*, vol. 301, no. 3-5, pp. 927–949, 2007.

[81] R. Guilbault, S. Lalonde, and M. Thomas, "Modeling and monitoring of tooth fillet crack growth in dynamic simulation of spur gear set," *Journal of Sound and Vibration*, vol. 343, pp. 144–165, 2015.

[82] K. Itô, P. Henry Jr *et al.*, *Diffusion processes and their sample paths*. Springer Science & Business Media, 2012.

[83] R. Durrett, *Probability: theory and examples*. Cambridge university press, 2010.

[84] E. Simoen, G. De Roeck, and G. Lombaert, "Dealing with uncertainty in model updating for damage assessment: A review," *Mechanical Systems and Signal Processing*, vol. 56, pp. 123–149, 2015.

[85] G. Benedict and B. Kelley, "Instantaneous coefficients of gear tooth friction," *ASLE transactions*, vol. 4, no. 1, pp. 59–70, 1961.

[86] T. Huang, L. Dai, and H. Zhang, "An approach combining periodicity ratio and secondary poincaré map for characteristics diagnosis of nonlinear oscillatory systems," *Nonlinear Dynamics*, vol. 84, no. 2, pp. 959–975, 2016.

[87] T. Fang and E. Dowell, "Numerical simulations of periodic and chaotic responses in a stable duffing system," *International Journal of Non-Linear Mechanics*, vol. 22, no. 5, pp. 401–425, 1987.

[88] P. Kundur, N. J. Balu, and M. G. Lauby, *Power system stability and control*. McGraw-hill New York, vol. 7, 1994.

[89] R. E. Barlow and F. Proschan, "Statistical theory of reliability and life testing: probability models," Florida State Univ Tallahassee, Tech. Rep., 1975.

[90] P. Hu, J. Lu, and Y. Zhang, "Analysis of dynamic response and sensitivity of gear systems based on stochastic perturbation theory," *Journal of Northeastern University (Natural Science)*, vol. 2, pp. 257–262, 2014.

[91] A. Guerine, A. El Hami, L. Walha, T. Fakhfakh, and M. Haddar, "A perturbation approach for the dynamic analysis of one stage gear system with uncertain nnparameters," *Mechanism and Machine Theory*, vol. 92, pp. 113–126, 2015.

[92] D. Zhou, X. Zhang, and Y. Zhang, "Dynamic reliability analysis for planetary gear system in shearer mechanisms," *Mechanism and Machine Theory*, vol. 105, pp. 244–259, 2016.

[93] Z. Chen, W. Zhai, Y. Shao, K. Wang, and G. Sun, "Analytical model for mesh stiffness calculation of spur gear pair with non-uniformly distributed tooth root crack," *Engineering Failure Analysis*, vol. 66, pp. 502–514, 2016.

[94] Y. Wen, J. Yang, and P. Yang, "Random vibration response of a spur gear pair with periodic stiffness and backlash," in *ASME 2013 International Mechanical*

Engineering Congress and Exposition. American Society of Mechanical Engineers, 2013, pp. V04BT04A012–V04BT04A012.

[95] W. Bartelmus and R. Zimroz, "Vibration condition monitoring of planetary gearbox under varying external load," *Mechanical Systems and Signal Processing*, vol. 23, no. 1, pp. 246–257, 2009.

[96] D. Qin, Z. Zhou, J. Yang, and H. Chen, "Time-dependent reliability analysis of gear transmission system of wind turbine under stochastic wind load," *Jixie Gongcheng Xuebao(Chinese Journal of Mechanical Engineering)*, vol. 48, no. 3, pp. 1–8, 2012.

[97] F. Chaari, W. Bartelmus, R. Zimroz, T. Fakhfakh, and M. Haddar, "Effect of load shape in cyclic load variation on dynamic behavior of spur gear system," in *Key Engineering Materials*, vol. 518, pp. 119–126, 2012.

[98] K. Ito, *Foundations of stochastic differential equations in infinite dimensional spaces*. Siam, vol. 47, 1984.

[99] D. Talay, *Numerical solution of stochastic differential equations*. Taylor & Francis, 1994.

[100] L. Arnold, "Stochastic differential equations," *New York*, 1974.

[101] A. Rößler, "Runge–kutta methods for the strong approximation of solutions of stochastic differential equations," *SIAM Journal on Numerical Analysis*, vol. 48, no. 3, pp. 922–952, 2010.

[102] F. Zhao, Z. Tian, and Y. Zeng, "Uncertainty quantification in gear remaining useful life prediction through an integrated prognostics method," *IEEE Transactions on Reliability*, vol. 62, no. 1, pp. 146–159, 2013.

[103] M. H. DeGroot and M. J. Schervish, *Probability and statistics*. Pearson Education, 2012.

[104] A. Papoulis and S. U. Pillai, *Probability, random variables, and stochastic processes*. Tata McGraw-Hill Education, 2002.

[105] C. Jiang, T. Fang, Z. Wang, X. Wei, and Z. Huang, "A general solution framework for time-variant reliability based design optimization," *Computer Methods in Applied Mechanics and Engineering*, vol. 323, pp. 330–352, 2017.

[106] H. Hiroyasu, “Diesel engine combustion and its modeling,” in *COMODIA*, vol. 85, pp. 53–75, 1985.

[107] M. Kedadouche, M. Thomas, and A. Tahan, “A hybrid method combining teager kaiser energy operator, empirical mode decomposition and minimum entropy deconvolution for monitoring gears damages,” *Mechanics & Industry*, vol. 16, no. 6, p. 610, 2015.

[108] M. Kedadouche, M. Thomas, A. Tahan, and R. Guilbault, “Nonlinear parameters for monitoring gear: comparison between lempel-ziv, approximate entropy, and sample entropy complexity,” *Shock and Vibration*, vol. 2015, 2015.

[109] Y. Imaouchen, R. Alkama, and M. Thomas, “Complexity based on synchrosqueezing analysis in gear diagnosis,” *Mechanics & Industry*, vol. 16, no. 5, pp. 387–401, 2015.

[110] J. A. Rice, *Mathematical statistics and data analysis*. China machine press Beijing, 2003.

[111] Y. Shen, S. Yang, and X. Liu, “Nonlinear dynamics of a spur gear pair with time-varying stiffness and backlash based on incremental harmonic balance method,” *International journal of mechanical sciences*, vol. 48, no. 11, pp. 1256–1263, 2006.

[112] Y. Fang, X. Liang, and M. J. Zuo, “Effect of sliding friction on transient characteristics of a gear transmission under random loading,” in *Proceedings of 2017 IEEE International Conference on Systems, Man, and Cybernetics (SMC)*. IEEE, Banff, Canada, pp. 2551–2555, 2017.

[113] J. Li and J. Chen, *Stochastic dynamics of structures*. John Wiley & Sons, 2009.

[114] I. Kougioumtzoglou and P. Spanos, “An analytical wiener path integral technique for non-stationary response determination of nonlinear oscillators,” *Probabilistic Engineering Mechanics*, vol. 28, pp. 125–131, 2012.

[115] I. A. Kougioumtzoglou, A. Di Matteo, P. D. Spanos, A. Pirrotta, and M. Di Paola, “An efficient wiener path integral technique formulation for stochastic response determination of nonlinear mdof systems,” *Journal of Applied Mechanics*, vol. 82, no. 10, pp. 1–7, 2015.

[116] J. Yu and Y. Lin, "Numerical path integration of a non-homogeneous markov process," *International Journal of Non-Linear Mechanics*, vol. 39, no. 9, pp. 1493–1500, 2004.

[117] M. Cord and P. Cunningham, *Machine learning techniques for multimedia: case studies on organization and retrieval*. Springer Science & Business Media, 2008.

[118] E. Alpaydin, *Introduction to machine learning*. MIT press, 2014.

[119] R. Caruana and A. Niculescu-Mizil, "An empirical comparison of supervised learning algorithms," in *Proceedings of the 23rd international conference on Machine learning*. ACM, pp. 161–168, 2006.

[120] V. Vapnik, "Principles of risk minimization for learning theory," in *Advances in neural information processing systems*, pp. 831–838, 1992.

[121] G. M. James, "Variance and bias for general loss functions," *Machine Learning*, vol. 51, no. 2, pp. 115–135, 2003.

[122] H. J. Motulsky and R. E. Brown, "Detecting outliers when fitting data with nonlinear regression–a new method based on robust nonlinear regression and the false discovery rate," *BMC bioinformatics*, vol. 7, no. 1, pp. 1–20, 2006.

[123] Z. Xuegong, "Introduction to statistical learning theory and support vector machines," *Acta Automatica Sinica*, vol. 26, no. 1, pp. 32–42, 2000.

[124] B. Samanta, "Gear fault detection using artificial neural networks and support vector machines with genetic algorithms," *Mechanical Systems and Signal Processing*, vol. 18, no. 3, pp. 625–644, 2004.

[125] D. Bordoloi and R. Tiwari, "Health monitoring of gears based on vibrations by support vector machine algorithms," in *ASME 2012 Gas Turbine India Conference*. American Society of Mechanical Engineers, pp. 639–648, 2012.

[126] J. Neter, M. H. Kutner, C. J. Nachtsheim, and W. Wasserman, *Applied linear statistical models*. Irwin Chicago, vol. 4, 1996.

[127] R. E. Kass, "Nonlinear regression analysis and its applications," *Journal of the American Statistical Association*, vol. 85, no. 410, pp. 594–596, 1990.

[128] D. Chen and W. Wang, “Classification of wavelet map patterns using multi-layer neural networks for gear fault detection,” *Mechanical systems and signal processing*, vol. 16, no. 4, pp. 695–704, 2002.

[129] J. Hampton and A. Doostan, “Coherence motivated sampling and convergence analysis of least squares polynomial chaos regression,” *Computer Methods in Applied Mechanics and Engineering*, vol. 290, pp. 73–97, 2015.

[130] R. Fletcher and M. J. Powell, “A rapidly convergent descent method for minimization,” *The computer journal*, vol. 6, no. 2, pp. 163–168, 1963.

[131] P. Pedregal, *Introduction to optimization*. Springer Science & Business Media, vol. 46, 2006.

[132] D. Hanumanna, S. Narayanan, and S. Krishnamurthy, “Prediction of fatigue life of gear subjected to varying loads,” *Defence Science Journal*, vol. 48, no. 3, pp. 277–285, 1998.

[133] N. Baydar and A. Ball, “Detection of gear deterioration under varying load conditions by using the instantaneous power spectrum,” *Mechanical Systems and Signal Processing*, vol. 14, no. 6, pp. 907–921, 2000.

[134] M. Feki, F. Chaari, M. Abbes, F. Viadero, A. F. del Rincon, and M. Haddar, “Dynamic analysis of planetary gear transmission under time varying loading conditions,” in *New Trends in Mechanism and Machine Science*. Springer, pp. 311–318, 2013.

[135] A. Guerine, A. El Hami, L. Walha, T. Fakhfakh, and M. Haddar, “Dynamic response of a spur gear system with uncertain parameters,” *Journal of Theoretical and Applied Mechanics*, vol. 54, no. 3, pp. 1039–1049, 2016.

[136] Y. Qiao, W. Xu, W. Jia, and W. Liu, “Stochastic stability of variable-mass duffing oscillator with mass disturbance modeled as gaussian white noise,” *Nonlinear Dynamics*, vol. 89, no. 1, pp. 607–616, 2017.

[137] Y. Lei, J. Lin, M. J. Zuo, and Z. He, “Condition monitoring and fault diagnosis of planetary gearboxes: A review,” *Measurement*, vol. 48, pp. 292–305, 2014.

[138] A. Guerine and A. El Hami, “A polynomial chaos method for the analysis of the dynamic response of a gear friction system,” in *International Conference Design and Modeling of Mechanical Systems*. Springer, pp. 893–898, 2017.

[139] A. A. Al-Kheer, A. El-Hami, M. G. Kharmanda, and A. M. Mouazen, "Reliability-based design for soil tillage machines," *Journal of Terramechanics*, vol. 48, no. 1, pp. 57–64, 2011.

[140] Y. Qiao, W. Xu, W. Jia, and Q. Han, "Stochastic stationary response of a variable-mass system with mass disturbance described by poisson white noise," *Physica A: Statistical Mechanics and its Applications*, vol. 473, pp. 122–134, 2017.

[141] F. Kozin, "A survey of stability of stochastic systems," *Automatica*, vol. 5, no. 1, pp. 95–112, 1969.

[142] V. I. Oseledec, "A multiplicative ergodic theorem. liapunov characteristic number for dynamical systems," *Transaction of the Moscow Mathematical Society*, vol. 19, pp. 197–231, 1968.

[143] P. Landa and R. Stratonovich, "Theory of stochastic transitions of various systems between different states," *Proceedings of Moscow University, Series III, Vestinik, MGU*, pp. 33–45, 1962.